

AD/A-007 152

PAVEMENT FUNCTIONAL CONDITION  
INDICATORS

Mohamed Y. Shahin, et al

Army Construction Engineering Research  
Laboratory  
Champaign, Illinois

February 1975

DISTRIBUTED BY:

**NTIS**

National Technical Information Service  
U. S. DEPARTMENT OF COMMERCE

REPORT DOCUMENTATION PAGE		READ INSTRUCTIONS BEFORE COMPLETING FORM
1. REPORT NUMBER TECHNICAL REPORT C-15	2. GOVT ACCESSION NO.	3. RECIPIENT'S CATALOG NUMBER <b>AD/A-007152</b>
4. TITLE (and Subtitle) PAVEMENT FUNCTIONAL CONDITION INDICATORS		5. TYPE OF REPORT & PERIOD COVERED Final Report
		6. PERFORMING ORG. REPORT NUMBER
7. AUTHOR(s) Mohamed Y. Shahin Michael I. Darter		8. CONTRACT OR GRANT NUMBER(s)
9. PERFORMING ORGANIZATION NAME AND ADDRESS CONSTRUCTION ENGINEERING RESEARCH LABORATORY P.O. Box 4005 Champaign, Illinois 61820		10. PROGRAM ELEMENT, PROJECT, TASK AREA & WORK UNIT NUMBERS 4A664717D895-04-010
11. CONTROLLING OFFICE NAME AND ADDRESS		12. REPORT DATE February 1975
		13. NUMBER OF PAGES 96
14. MONITORING AGENCY NAME & ADDRESS (if different from Controlling Office)		15. SECURITY CLASS. (of this report) UNCLASSIFIED
		15a. DECLASSIFICATION/DOWNGRADING SCHEDULE
16. DISTRIBUTION STATEMENT (of this Report)  Approved for public release; distribution unlimited.		
17. DISTRIBUTION STATEMENT (of the abstract entered in Block 20, if different from Report)		
18. SUPPLEMENTARY NOTES  Reproduced by NATIONAL TECHNICAL INFORMATION SERVICE U.S. Department of Commerce Springfield VA 22151		
19. KEY WORDS (Continue on reverse side if necessary and identify by block number)  pavement evaluation airfield pavement pavement condition		
20. ABSTRACT (Continue on reverse side if necessary and identify by block number)  Functional performance is defined as the trend of the level of service provided to the pavement users through the initial life of the pavement and between major rehabilitations. The information presented in this report includes: (1) identification of pavement functional condition indicators, (2) state of the art of measuring and evaluating the most significant functional indicators (roughness and skid resistance).		

and (3) preliminary concepts for incorporating functional consideration into pavement life-cycle analysis.

The report covers pavements in general, with special consideration given to airfields. Sources of information used in developing this report come from existing literature and on-going research projects of various agencies.

1a

UNCLASSIFIED

## FOREWORD

This work was conducted for the Directorate of Military Construction, Office of the Chief of Engineers (OCE), as part of the FY 1974 RDT&E Army Program 6.47-17A, Project 4A664717D895, "Military Construction Systems Development," Task 04, "Military Airfield Facilities," Work Unit 010, "Condition Indicators for Military Pavements." The OCE Technical Monitor was A. F. Muller, DAEN-MCE-D. The principal investigator was Dr. E. L. Marvin, U.S. Army Construction Engineering Research Laboratory (CERL).

The findings were reported and documented by Drs. M. Y. Shahin and M. I. Darter of the Facilities Engineering Branch, Facilities Engineering and Construction Division, CERL. During this research, R. L. Larson was Branch Chief and E. A. Lotz was Division Chief.

Appreciation is expressed to the Air Force Weapons Laboratory (AFWL) for providing information about its on-going research in pavement roughness and skid resistance and to the U.S. Army Waterways Experiment Station (WES) for its information about pavement functional performance.

COL M. D. Remus is Commander/Director of CERL and Dr. L. R. Shaffer is Deputy Director.

## CONTENTS

DD FORM 1473 .....	1
FOREWORD .....	3
LIST OF TABLES AND FIGURES .....	6
 1 INTRODUCTION .....	 11
Objective .....	11
Background .....	11
Approach .....	11
 2 FUNCTIONAL CONDITION INDICATORS .....	 11
 3 ROUGHNESS EVALUATION AND MEASUREMENT:	
STATE OF THE ART .....	12
Factors Influencing Roughness .....	12
Construction Effects .....	12
Traffic and Environmental Effects .....	12
Characterization of Roughness .....	13
Roughness Index .....	13
Slope Variance .....	14
Wavelength/Amplitude Characteristics .....	16
Acceleration .....	21
Absorbed Power .....	25
Human Evaluation .....	27
Roughness Measurement Equipment .....	32
Profile Measuring Equipment .....	32
Vehicle Axle/Body Displacement Measuring Equipment .....	40
Acceleration/Absorbed Power Measurement .....	42
Slope Variance Measurement .....	45
Roughness Summary .....	45
 4 SKID RESISTANCE EVALUATION AND MEASUREMENT	
STATE OF THE ART .....	46
Introduction .....	46
Methods for Measuring Skid Resistance .....	48
Trailer Methods .....	48
Automobile Methods .....	53
Portable Field and Laboratory Methods .....	54
Texture Identification Methods .....	54
Effect of Individual Variables on Skid Resistance .....	54
Traffic and Seasonal Variations .....	54
Vehicle Factors .....	57
Pavement Factors .....	58
Correlation Between Friction Measurements .....	64
Mu-Meter vs Skid Trailer .....	64
Automobile Method vs Skid Trailers .....	64
Automobile Method vs Mu-Meter .....	64
Trailers and Automobiles vs Portable Field .....	70
and Laboratory Methods .....	
Automobile vs Actual Aircraft .....	70
Skid Resistance Summary .....	75

<b>5</b>	<b>FUNCTIONAL PERFORMANCE AS PART OF PAVEMENT</b>	
	<b>LIFE-CYCLE ANALYSIS</b> .....	<b>76</b>
	Introduction	76
	Pavement Management	76
	Present Status of Management System Being Developed by CERL	77
	Preliminary Concepts for Incorporating Functional Performance	78
	Into Pavement Life-Cycle Analysis	
<b>6</b>	<b>SUMMARY, CONCLUSIONS, AND RECOMMENDATIONS</b> .....	<b>83</b>
	Summary	83
	Roughness Indicators	83
	Skid Resistance Indicators	83
	Conclusions	84
	Recommendations	84
	<b>APPENDIX: Introduction to Power Spectral Density</b> .....	<b>85</b>
	<b>REFERENCES</b> .....	<b>90</b>
	<b>DISTRIBUTION</b>	

## TABLES

Number	Page
1 Summary of Major "Roughness" Measurement Equipment	32
2 Comparison of Road Roughness Devices	43
3 Tentative Recommendations for Use of Roughness Indicators	46
4 Tentative Recommendations of Roughness Indicators and Equipment for Determining Maintenance Needs	47
5 Tentative Recommendations for Skid Measurement of Different Pavement Types	72
6 Mu-Meter Aircraft Pavement Rating	76
7 Stopping Distance Ratio/ Airfield Pavement Rating	76

## FIGURES

1 Histogram of Initial Roughness Index Values for 177 Newly Constructed Flexible and Rigid Pavements	13
2 Profilometer Measurement of Roughness Index (RI)	14
3 Roughometer Measurement of Roughness Index (RI)	14
4 Examples of Roughness Indexes for Various Pavements Determined by a Profilometer-type Device	15
5 Schematic of Profilometer Used to Determine Slope at AASHO Road Test	16
6 Typical Profile Record of Slope	16
7 Power Spectral Density Versus Frequency Illustrative Plot	17
8 Wavelength Versus Average Vertical Rise ( $2\lambda$ )	18
9 Effect of Wavelength and Mean Power on Subjective Serviceability Ratings for Highway Pavement (Speed = 50 mph)	20
10 Illustration of the AFD Technique of Characterizing Profile Amplitude/ Wavelength Distribution	21
11 Illustration of Effect of Digital Filtering of a Profile	22
12 Simulated and Measured Acceleration Time Histories of a 400,000-lb B-52 During a 40-Knot Taxi Over the U-TAPAO Runway 18 Profile	24
13 Human Tolerance Vibration Criteria	25

## FIGURES (cont'd)

Number	Page
14 Absorbed Power and Vertical Accelerations Determined in the Cockpit of B-727 on a Runway at a Major U.S. Airport	26
15 Serviceability Rating Form Used at the AASHO Road Test	27
16 Performance Rating Form Used by the Canadian Good Roads Association	27
17 Pilot's Subjective Roughness Rating Form	30
18 Pilot's Subjective Roughness Rating Instruction Sheet	31
19 Pilot's Rating Data for Take-off on Runway 31R, Love Field, Dallas	32
20 Surface Dynamics Profilometer Measurement System Used by Texas Highway Department	33
21 Detailed Diagram of SDP Measurement System of Texas Highway Department	34
22 View of Profilometer Vehicle and Lasar Setup for Horizontal Control	36
23 View of Profilometer Road-following Wheel	36
24 Lasar and Lasar-leveling Assembly in Lasar Vehicle	37
25 Lasar System Tacking Vehicle	38
26 General View of AFWL Lasar System Profilometer	38
27 Rolling Straightedge-type Profilometer	39
28 Ontario's RRL-type Profilometer	40
29 Bureau of Public Roads Roughometer	41
30 Schematic Illustration of PCA Roadometer	41
31 Typical Rainhart MRM Measurement Record	44
32 Kentucky DOT Automatic Acceleration Measuring System	44
33 Reported U.S.A.F. Hydroplaning Accidents	46
34 Generalized Representation of Coefficient of Friction Between a Steel Sphere and Rubber as a Function of Sliding Speed	48
35 Typical Road Friction Testers	49



## **FIGURES (cont'd)**

<b>Number</b>	<b>Page</b>
36 Friction Factor as Function of Slip	49
37 Ratio of Maximum and Locked-wheel Friction Factors at 40 mph on Various Wet Surfaces	50
38 Runway Friction Tester with Adjustable Slip	50
39 Typical Sideway Friction Factor vs Yaw Angle Relationships for Two Wet Pavements	50
40a Diagrammatic Layout of Mu-Meter	51
40b Mu-Meter Used by U.S.A.F.	51
41 Sideways-Force Coefficient Routine Investigation Machine	52
42 Braking System for NASA Diagonal-braked Test Vehicle	53
43 Diagonally Braked Vehicle (DBV) Used by U.S.A.F.	53
44 Keystone MARK IV Skid Resistance Tester	55
45 California Portable Skid Tester	55
46 British Road Research Laboratory's Pendulum Friction Tester (British Portable Tester)	56
47 Components of Surface Texture as Identified by Schonfeld	57
48 Seasonal Change of Skid Resistance	57
49 Deterioration of Skid Resistance with Exposure to Traffic	57
50 Loss of Skid Resistance of Two Pavements as a Function of Traffic Exposure	57
51 Friction Values on New Portland Cement Concrete and in Heavy Oil Slick on Old Portland Cement	59
52 Friction Values on a Dense-graded Plant-mix Asphaltic Surface Constructed with Partly Crushed Gravel Aggregate	59
53 Friction Values on Asphalt Seal-coat Surface with Excess Asphalt Contributing to Bleeding in Hot Weather	59
54 Comparison of Friction Coefficient for Two Types of Pressure on Wet Surface and One Type of Pressure on Dry Surface, Portland Cement Concrete Runway	60

## FIGURES (cont'd)

Number	Page
55 Effect of Wheel Load on Skid Resistance of Wet Portland Cement Concrete and Plant Mix Asphalt Surfaces	60
56 Tire-tread Effects on Wet and Puddled Runways for Twin-tandem Bogie Arrangements	60
57 Landing Research Runway at Wallops Station, VA	61
58 Comparison of Braking Friction Coefficients on Wet and Puddled Runways Obtained from 990A Aircraft	62
59 Effect of Runway Groove Configuration on C-141A Aircraft Braking on Landing Research Runway at NASA Wallops Station	63
60 Comparison of Friction-wear Relationship: Portland Cement Concrete, and Asphaltic Concrete with Gravel and Limestone Aggregates	63
61a Effect of Time After Surface-wetting on Side Friction Coefficient as Measured by Mu-Meter	65
61b Effect of Time-after-surface-wetting on Wet - Dry Stopping Distance Ratio as Measured by Diagonal-Braked Vehicle (DBV)	66
62 Correlation Between Mu-Meter and Texas Highway Department Locked-wheel Trailer	67
63 Correlation Between Skid Number Obtained from Car Stopping Distance from 40 mph and Virginia Skid Trailer at 40 mph	68
64 Sideway Friction Measured by Mu-Meter vs Wet - Dry Stopping Distance Ratio Measured by the Diagonal-Braked Vehicle	69
65 Correlation of California Skid Tester and Pennsylvania State Drag Skid Tester	70
66 Correlation Between the Wet - Dry Stopping Distance Ratio Obtained by the C-141A Aircraft and NASA Diagonal-Braked Vehicle (DBV) with Vehicle Brakes Applied at 60 mph	71
67 Correlation Between the Wet - Dry Stopping Distance Ratio Obtained by C-141A Aircraft and Runway Condition Reading (RCR) Vehicle with Vehicle Brakes Applied at 20 mph	73
68 Coordination of Maintenance and Repair Activities in Pavement Management System	78
69 Coordination of Corrective Measures for Pavement Skid Resistance and Structural Deterioration	79

## FIGURES (cont'd)

Number	Page
70 Coordination of Corrective Measures for Pavement Roughness and Structural Deterioration	79
71a Coordination of Structural Deterioration Roughness, and Slipperiness During Pavement Life-cycle: Design Alternative 1	80
71b Design Alternative 2	81
71c Design Alternative 3	81
72 Example Calculation of Average Rideability Factor (ARF) for Two Design Alternatives	82
73 Primary and Secondary Roads That Have the Same Rideability Factor (ARF) But Different Roughness Index Limiting Values	82
74 Consideration of Functional Performance in Pavement Life-cycle Analysis	82
A1 Schematic Representation of a Random Process as an Ensemble of Sample Functions $x_i(p, x)$	85
A2 A Schematic Diagram of the Normalized Autocorrelation Function for Different $\tau$ Values	87
A3 Experimental Determination of Power Spectral Density of a Sample Function $x(x)$	89
A4 A Schematic Diagram of Power Spectral Density vs Frequency	89
A5 Mean Square of a Sine Function $x(x)$ in Terms of Its Amplitude	90

## PAVEMENT FUNCTIONAL CONDITION INDICATORS

### 1 INTRODUCTION

#### Objective

The purpose of this report is to identify the significant indicators of pavement functional performance, to summarize the state of the art of measuring and evaluating these indicators, and to develop preliminary concepts for incorporating functional considerations into the life-cycle pavement systems program (LIFE) developed by the U. S. Army Construction Engineering Research Laboratory (CERL).

#### Background

The functional requirements of pavements include providing a comfortable and safe ride to pavement users throughout the pavement's initial life and between repairs (overlays). (The term *users* refers to the aircraft flight crew and passengers for airfields, and to automobile drivers and passengers for highways.)

Life-cycle design analysis of military pavements is not totally effective unless functional performance and related economic effects are considered in addition to the structural integrity analysis. The major indicators of functional performance—roughness and skid resistance—are described in detail herein. Pavement maintenance and repair are also functions of both structural integrity and functional performance; hence both must be considered if one is to provide optimum life-cycle strategies.

#### Approach

Sources of information used in developing this report were the authors' experience; references provided by the Highway Research Information Service (HRS), Defense Documentation Center (DDC), National Aeronautics and Space Administration (NASA), National Technical Information Service

(NTIS); and additional published information. Ongoing research projects of various agencies were also reviewed.

### 2 FUNCTIONAL CONDITION INDICATORS

The major purpose of a pavement is to provide a surface that meets the functional needs of its users over a specific time period. *Functional performance* is defined as the trend of the level of service provided to the pavement users throughout the initial life of the pavement and between repairs (overlays).

Functional requirements of users include such factors as speed, comfort, safety, appearance, and convenience. Thus a functional pavement is one that, for a specified (or desired) range in speed, provides a *safe* and *comfortable* ride. The functional performance of a pavement is clearly a user-oriented consideration in contrast to the structural, distress-oriented consideration. Some relationships do exist, of course, between functional and structural performance. For example a crack, which is a form of structural distress, may form in a pavement surface but may not affect functional performance until it causes roughness which the user can "feel" or which creates an unsafe condition.

The factors of maintenance and repair also enter into the broad functional requirements, in that a pavement under maintenance or repair may be either partially or completely out of service for a time, and hence not providing service to the user. User delay and increased vehicle operating costs due to maintenance or repair operations are major problems for both runways and high-volume highways.

Because of the increased performance level of operating vehicles, functional condition indicators are becoming increasingly important to the pavement engineer. He must identify functional condition indicators for two reasons:

1. To evaluate the functional condition of in-service pavements to determine existing and future maintenance and repair needs.
2. To accurately compare various pavement designs in an initial analysis of their life-cycle costs.

Functional condition indicators measure the user requirements previously listed. The most significant indicators that have been identified are:

1. Roughness

<sup>1</sup>J. Willmer, P. McManus, and E. Marvin, *User Manual for LIFE Computer Program*, Technical Report S-28 (U.S. Army Construction Engineering Research Laboratory [CERL], 1974).

<sup>2</sup>E. L. Marvin and P. McManus, *Life Cycle Analysis of an Airfield Pavement Facility*, Unpublished Report (CERL, 1973).

2. Skid resistance and hydroplaning
3. Appearance
4. Maintenance and rehabilitation expenditures\*
5. Foreign objects on surface.

This list does not include all possible functional condition indicators. For instance, rutting in the wheel path can be a safety hazard during heavy rain, since it increases water depth in the wheel path, which may lead to hydroplaning. Another type of pavement deterioration that may be considered a functional indicator is disintegration. Although surface disintegration can cause roughness, the resulting loose material can also be a significant safety hazard and a source of excessive maintenance to aircraft engines.

Due to the limited nature of this project, only the two most significant functional performance indicators—roughness and skid resistance—are considered in detail.

### 3 ROUGHNESS EVALUATION AND MEASUREMENT: STATE OF THE ART

*Roughness* is defined as irregularities in the pavement surface that adversely affect ride quality, safety, and vehicle maintenance costs. A state-of-the-art evaluation of pavement roughness related to functional performance is presented. Information is provided for both highway and airfield evaluation. Included in the discussion are factors influencing roughness, methods of roughness characterization, and measurement equipment.

#### Factors Influencing Roughness

Pavement surface irregularities, or "roughness," actually consist of multifrequency random waves with many wavelengths and amplitudes. Pavement roughness occurs from two sources: surface irregularities that are built into a pavement during construction, and surface irregularities that develop after construction due to traffic load and environmental effects (such as swelling subgrade) over the life cycle of the pavement.

\*These are listed as functional condition indicators because the user's taxes are used for maintaining the pavements, and excessive maintenance and rehabilitation activities inconvenience the users by delaying and interrupting traffic.

#### Construction Effects

Newly constructed pavements exhibit varying amounts of roughness even though they usually must meet some type of smoothness criterion (such as less than  $\frac{1}{8}$  in. irregularity in 12 ft). Obviously this type of specification cannot completely control the level of roughness quality needed for high-capacity facilities.

The Kentucky Department of Transportation has measured roughness of newly constructed pavements for several years. The initial roughness of 177 projects as shown in Figure 1 illustrates the point that not all new construction is adequately smooth, and that some projects have a significant degree of built-in roughness.

#### Traffic and Environmental Effects

Since pavement material properties such as resiliency and strength vary greatly along any given project,<sup>3,4,5</sup> overall response under traffic load—such as deflections, rutting, and subgrade consolidation—also shows significant random variation. The greater the variability of materials, density, moisture, etc., the greater the rate of localized failure along a given project—and hence increased roughness.<sup>6</sup> Repeated traffic loads seem to cause primarily relatively short pavement wavelengths. The disintegration of a pavement surface can also contribute to short wavelength roughness.

Environmental effects such as random swelling or shrinking subgrade and frost heaving, as well as consolidation of the subgrade, also contribute to pavement roughness. Environmental factors seem to cause primarily the relatively long pavement wavelengths.

<sup>3</sup>G.B. Sherman, *In Situ Materials Variability*, Special Report 126 (Highway Research Board, 1971).

<sup>4</sup>M.I. Darter and W.R. Hudson, *Application of Probabilistic Concepts to Flexible Pavement System Design*, Research Report 123-18 (Texas Highway Department, 1973).

<sup>5</sup>R.K. Kher and M.I. Darter, *Probabilistic Applications to AASHTO Interim Guide for Design of Rigid Pavement Structures*, HRR 466 (Highway Research Board, 1973).

<sup>6</sup>M.I. Darter, *Probabilistic Application to Rigid Pavement Structures*, Paper presented at ASCE Specialty Conference on Probabilistic Applications in Engineering (Stanford University, 1974).

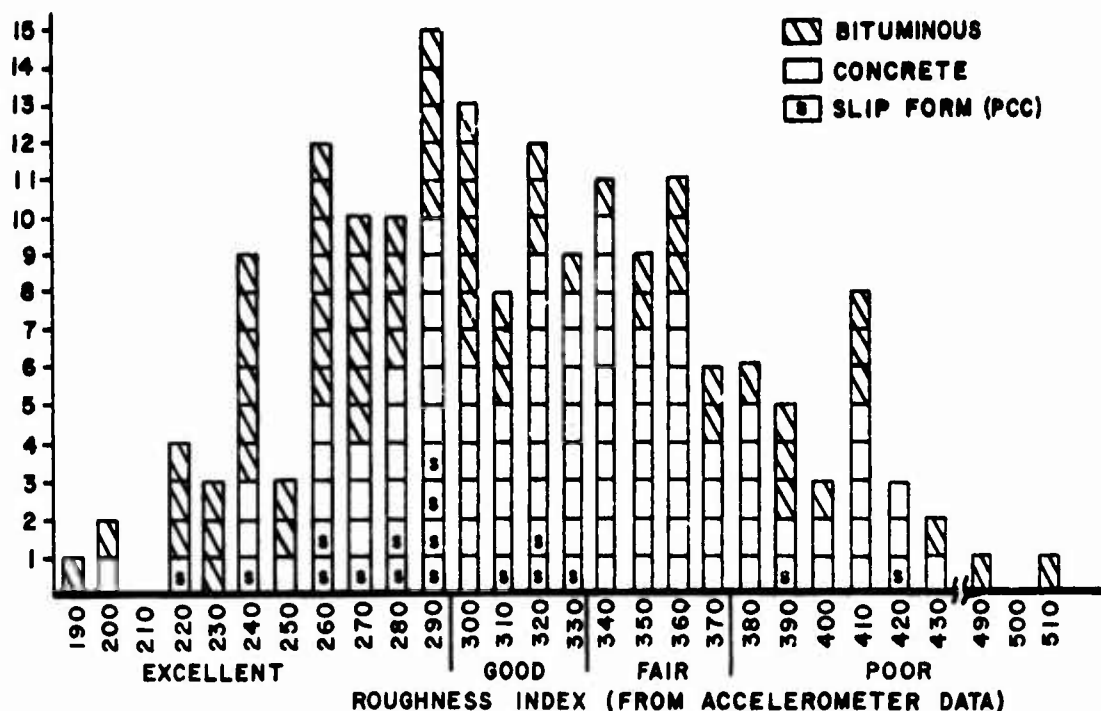


**Figure 1.** Histogram of initial roughness index values for 177 newly constructed flexible and rigid pavements. (From R.L. Rizenbergs et al., *Pavements Roughness: Measurement and Evaluation*, HRR 471 [Highway Research Board, 1973], pp 46-61.)

### Characterization of Roughness

Several indicators have been used to characterize pavement roughness or surface irregularities. Each of these characterization techniques is now described.

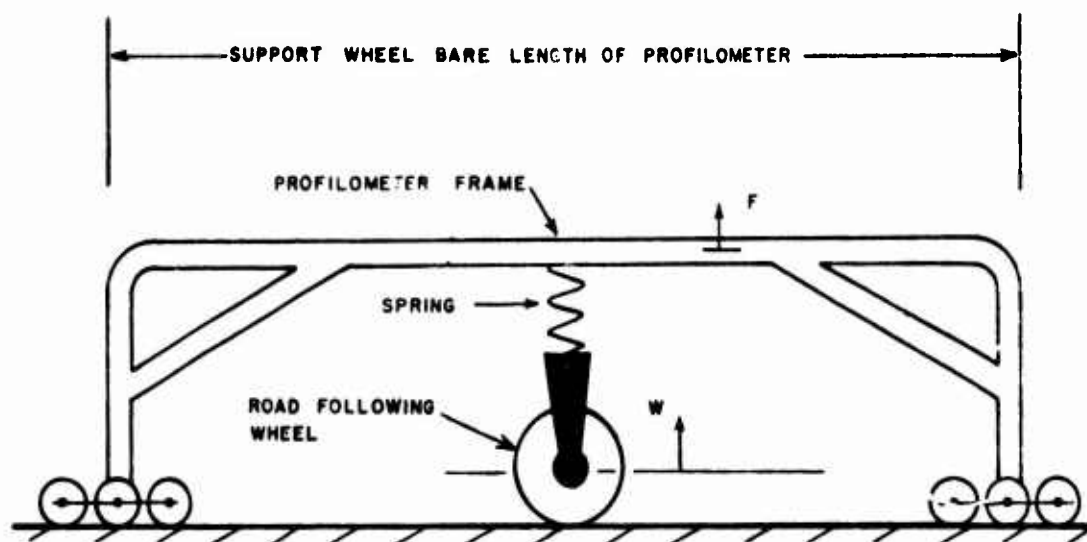
#### Roughness Index

The term *roughness index* has been applied to both the sum of vertical deviations of a pavement surface profile over a specified distance, and the sum of vertical deviations between a vehicle body and axle. It can be measured in units of inches of displacement per mile, or in units of centimeters per kilometer, but gives only a single statistic for roughness characterization of a given pavement. The term has been used rather loosely in the past, and several different types of measuring devices are commercially available. Since these devices actually measure different parameters, each gives a different roughness index for the same pavement profile. One device, the profilometer, measures surface vertical deviation as the difference between the road-following wheel and the profilometer frame, which is supported by widely spaced wheels (see Figure 2).

This displacement can be accumulated to give a "roughness index" over a length of pavement and is influenced somewhat by the spacing and number of the profilometer support wheels. The speed of the profilometer is usually no greater than 3-5 mph, causing few, if any, dynamic vibration effects.

A roughness index also can be determined by a roughometer, as shown conceptually in Figure 3. The displacement measured here, which is the difference between the road-following wheels and the vehicle body, can be accumulated to give a "roughness index." This accumulated displacement, however, depends on factors such as the dynamic spring/damping characteristics and the speed of the vehicle.

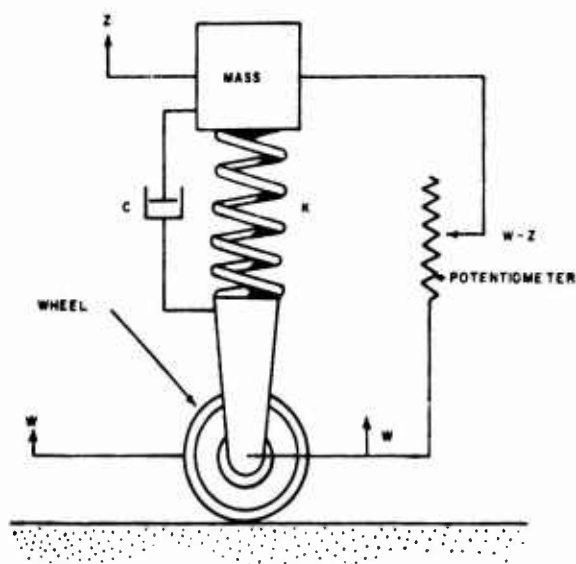
The sum of profile deviation can also be determined if the pavement surface profile is known at closely spaced intervals (i.e., 6 in.). This would give the truest "roughness index" since it would be independent of equipment type, speed, or dynamic characteristics of the test vehicle. Figure 4 shows examples of roughness indexes determined with a profilometer for an asphalt concrete surface and a Portland cement concrete surface. The roughness index values range from 1 in./mile to 225 in./mile for these pavements and equipment.



$X = (F - W) \times$  DIFFERENCE BETWEEN ROAD FOLLOWING WHEEL AND PROFILOMETER FRAME OVER LENGTH OF PAVEMENT

$$RI = \sum X$$

Figure 2. Profilometer measurement of roughness index (RI).



$$RI = \sum (W - Z)$$

Figure 3. Roughometer measurement of roughness index (RI).

### Slope Variance

Pavement slope is defined as the vertical deviation between two points on the surface profile, divided by the distance between the two points. Therefore, if the elevations of consecutive points along a pavement are known, the slopes of the lines between these points can be determined over a length of pavement. Slope variance can be calculated by the following equation:

$$SV = \sum_{i=1}^{i=n} (X_i - \bar{X})^2 / (n - 1) \quad [\text{Eq 1}]$$

where SV = slope variance

$X_i$  = the  $i^{\text{th}}$  slope measurement

$n$  = number of slope measurements

$\bar{X}$  = mean slope measurement,  $(\sum X_i / n)$ .

Slope variance will obviously depend on the spacing between the consecutive points along the pavement.

The slope variance technique was developed at the AASHO Road Test (1958-1960), and equipment is available to measure this indicator. A schematic of the profilometer developed at the AASHO Road Test

# **SAMPLES OF PROFILOGRAMS SHOWING GOOD AND BAD PAVEMENTS**

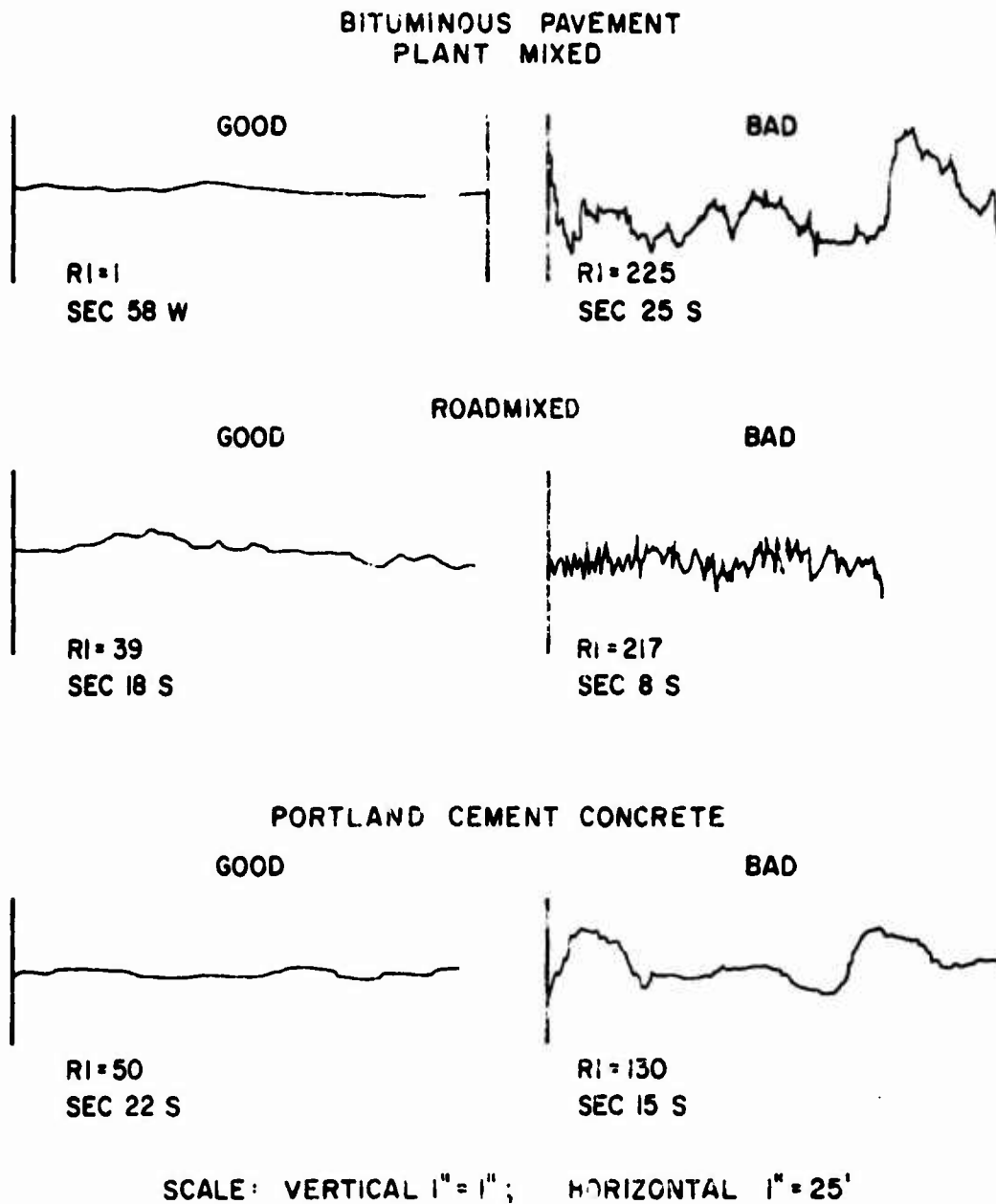


**Figure 4.** Examples of roughness indexes for various pavements determined by a profilometer-type device. (From W.J. Liddle et al., *Evaluation of Pavement Serviceability on Utah Highways*, Interim Report 1969 [Utah Highway Department, 1969].)



is shown in Figure 5. This instrument continuously records the angle (denoted by A) formed by the line of the support wheels (G and H) and the line (CD) that connects the centers of two wheels (E) spaced at 9 in.<sup>7</sup> The slope variance must be calculated from these data. (A typical slope record is shown in Figure 6.) Other equipment that gives a direct read-out of slope variance is described later.

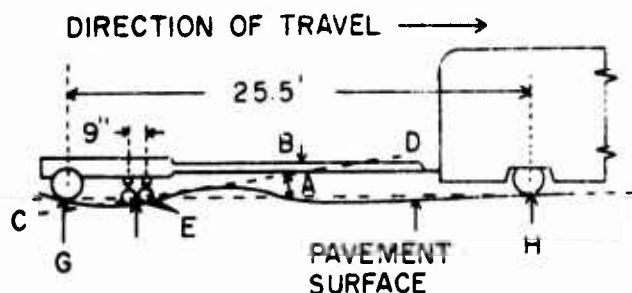


**Figure 5.** Schematic of profilometer used to determine slope at AASHO Road Test. (From *The AASHO Road Test: Report 5—Pavement Research*, Special Report 61-E [Highway Research Board, 1962].)

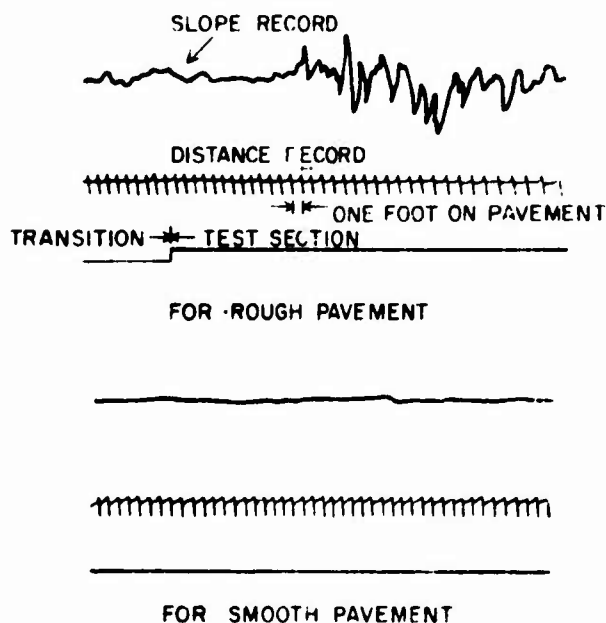


**Figure 6.** Typical profile record of slope. (From *The AASHO Road Test: Report 5—Pavement Research*, Special Report 61-E [Highway Research Board, 1962].)

<sup>7</sup>The AASHO Road Test: Report 5—Pavement Research, Special Report 61-E (Highway Research Board, 1962).

As with the roughness index method, only a single statistic, i.e., slope variance, can be obtained to characterize an entire section of pavement. The slope variance statistic does not include long wavelengths.

#### *Wavelength/Amplitude Characteristics*

The analysis of actual profile wavelength/amplitude characteristics of pavements as an indicator of roughness began in the early 1960's and is currently being studied by several agencies. The development and use of the wavelength/amplitude indicator was initially slow because of the difficulty of obtaining accurate profiles (inadequate equipment), and the complexity of quantitative analysis of the profile. Both difficulties have now been largely overcome with the development of better equipment and computer capability.

At least three techniques have been developed for analyzing profile data. One technique, power spectral analysis, has been used by several investigators to characterize pavement profile wavelengths and amplitudes. The power spectral density (PSD) function of a profile can be calculated from either analog or digital data processing. Figure 7 is a PSD plot for two runway pavements, showing log of power versus log of frequency,  $f$  (reciprocal of wavelength). The PSD (or  $P(f)$ ) ordinate can be thought of as the mean-square amplitude that occurs at a particular frequency or wavelength. Brickman and others<sup>8,9</sup> found that the relationship between  $\log P(f)$  and  $\log$  frequency ( $f$ ) is approximately linear for highway and airport pavements. Therefore, if  $P(f)$  represents the PSD of a particular frequency  $f$  (or wavelength,  $L = 1/f$ ), the average amplitude,  $\bar{A}$ , for this frequency can be calculated as follows:

$$\bar{A} = 2 \sqrt{P(f) \Delta f} \quad [\text{Eq 2}]$$

Therefore, the ordinate of the PSD represents the mean-square height of the pavement roughness (or amplitude) corresponding to specific wavelengths. Figure 8 is a plot of average vertical rise,  $2\bar{A}$ , vs

<sup>8</sup>A.D. Brickman, I.C. Wambold, and J.R. Zimmerman, *An Amplitude-Frequency Description of Road Roughness*, Special Report 116 (Highway Research Board, 1974).

<sup>9</sup>T.L. Coleman and A.W. Hall, *Implications of Recent Investigations on Runway Roughness Criteria*, Paper presented to AGARD, NATO, Paris (1963).

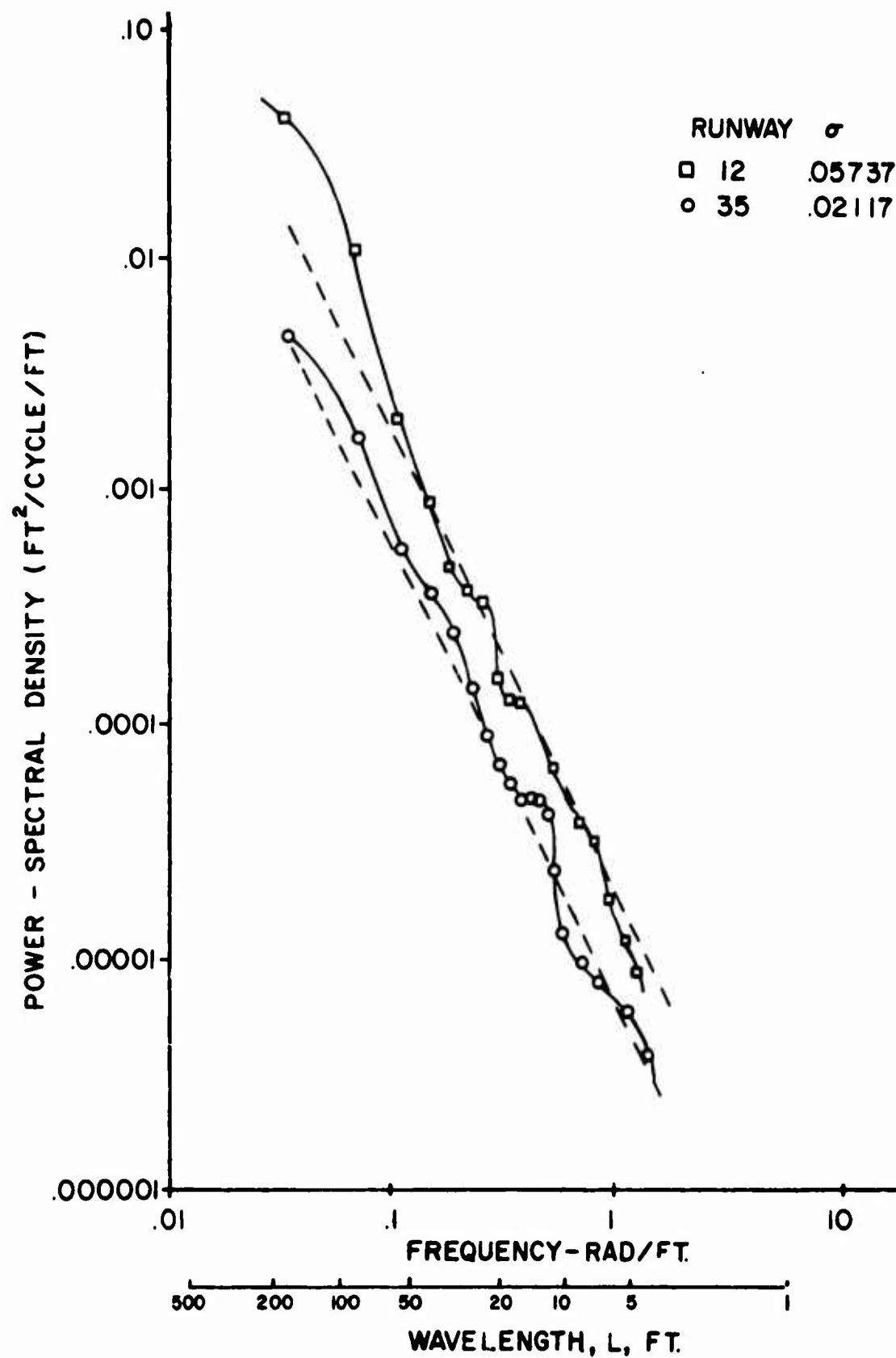


**Figure 7.** Power spectral density versus frequency illustrative plot. For two runways. (From T.L. Coleman and A.W. Hall, *Implications of Recent Investigations on Runway Roughness Criteria*, Paper presented to AGARD, NATO, Paris [1963].)

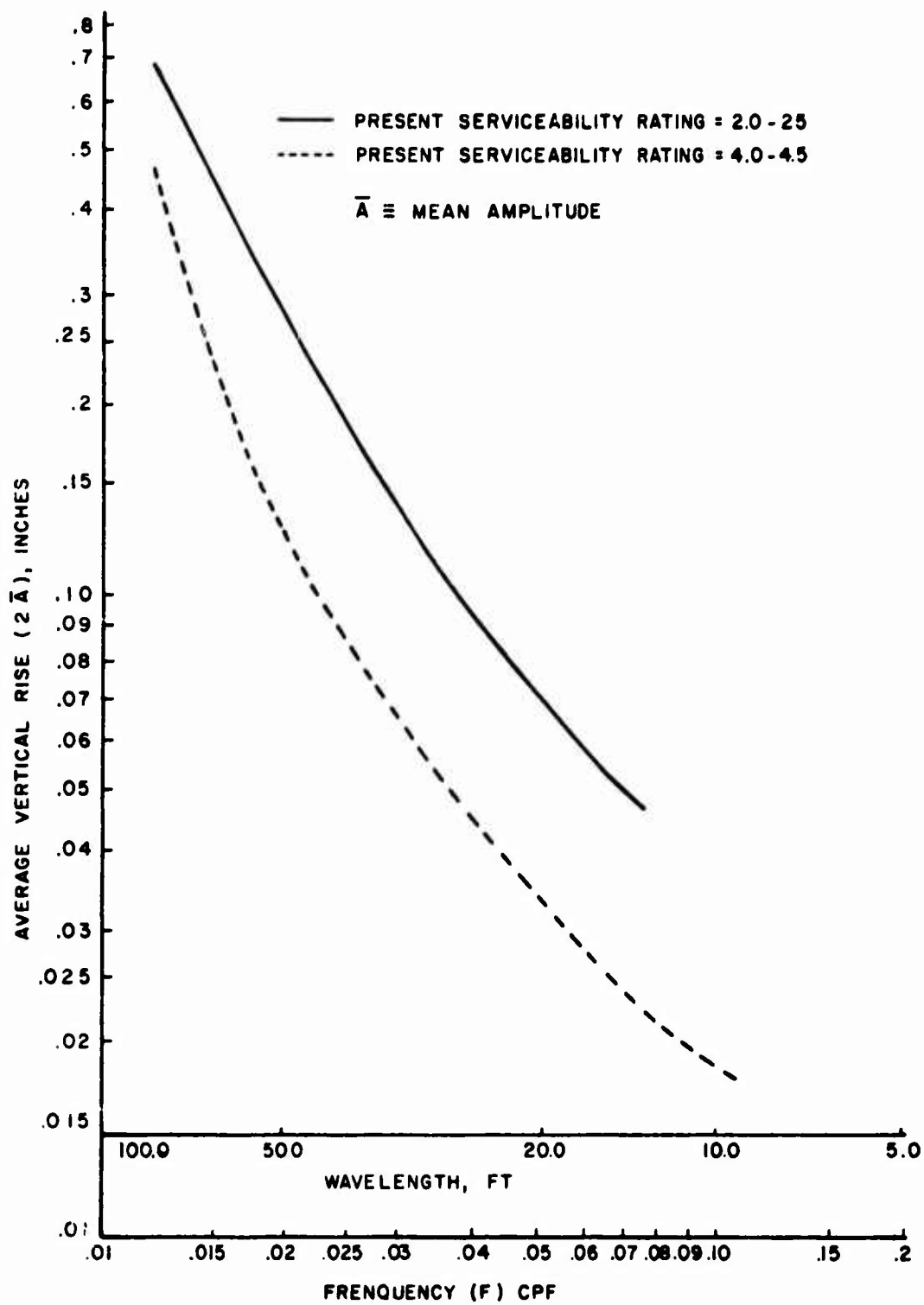


Figure 8. Wavelength versus average vertical rise ( $2\bar{A}$ ).

wavelength,  $1/f$ , obtained by applying Equation 2 to data published in Walker and Hudson.<sup>10</sup> This figure illustrates that a mean amplitude can be calculated for specified wavelengths and that the longer the wavelength, the larger the mean amplitude for this profile. A complete mathematical derivation of the PSD technique and Equation 2 is given in the appendix.

Figure 9 illustrates the effect of wavelength and amplitude on driver subjective response. This plot shows mean PSD versus wavelength for several pavements with serviceabilities ranging from high to low, subjectively rated by a panel. As pavement wavelength increases from 0 to 90 ft, the mean power (or mean amplitude) also increases for any given present serviceability rating (PSR). The PSR values shown here were determined at a speed of 50 mph. Also, for a given wavelength, as the mean power increases, the subjective serviceability rating of the panel decreases. These data clearly show that pavement wavelengths and amplitudes are related to the subjective roughness that a highway driver or passenger experiences.

The PSD technique provides a spectrum of statistics for a given pavement profile. Use of this spectrum of information was found by Walker and Hudson<sup>11</sup> to provide a better indicator of pavement serviceability as judged by the highway user than a single statistic such as slope variance or roughness index. However, it is somewhat difficult to grasp the concept of power and to determine critical limits of PSD. The PSD approach to characterizing roughness has definite shortcomings, as Brickman et al. states:

In determining PSD, for example, an averaging technique is used to establish the power level within a frequency band. If the amplitudes of these frequency components are relatively constant through time, the PSD is a reasonably truthful measure of the random signal. But if, in fact, a few very high amplitude bursts are accompanied by many low level ones, PSD obscures the true situation.<sup>12</sup>

<sup>10</sup>R.S. Walker and W.R. Hudson, *The Use of Spectral Estimates for Pavement Characterization*, Research Report 156-2 (Center for Highway Research, University of Texas at Austin, 1973).

<sup>11</sup>R.S. Walker and W.R. Hudson, *The Use of Spectral Estimates for Pavement Characterization*.

<sup>12</sup>A.D. Brickman et al., *Analysis of Pavement Profile* (Pennsylvania Department of Transportation, 1969), p. 15.

The PSD curve indicates an average roughness amplitude at a particular frequency or wavelength. Therefore, a knowledge of the PSD curve alone is not enough to determine whether the mean amplitude of power is the result of a few large irregularities or many small irregularities. Limiting values for PSD functions were suggested by Coleman.<sup>13</sup> The lower dashed line of Figure 7 indicates a roughness level which he recommends should not be exceeded by new construction, and the upper dashed line represents a level at which runway roughness has become excessive.

Hutchinson also concludes as follows:

The apparent inability of the power spectra to discern between the relative levels of roughness of airport runways is not too surprising, since the power spectral density function represents a general impression of the roughness associated with the various wavelengths over the length of the runway. Thus, it cannot distinguish between roughness due to a few high amplitude distortions, and that due to many low amplitude distortions of the same wavelength.<sup>14</sup>

In light of these limitations, other characterization techniques have been proposed. Brickman et al.<sup>15,16</sup> proposed a method for examining both amplitude and wavelength distribution. The amplitude-frequency distribution, or AFD, is a technique that displays road roughness as a tabular array showing both height and wavelength of surface irregularities (see Figure 10). Specific features of the method are as follows:

1. The AFD tabulation is a method of representing the roughness profile of a road surface in a quantitative way. It not only shows what each wavelength contributes to the overall roughness but also gives the distribution of roughness heights associated with each amplitude.
2. The AFD of a roughness signal can be computed electronically by using standard analog components for filtering, comparing, and counting. The precision of the computed AFD is greatly affected by the shape factor of the filter.

<sup>13</sup>T.L. Coleman and A.W. Hall, *Implications of Recent Investigations on Runway Roughness Criteria*, Paper presented to AGARD, NATO, Paris (1963).

<sup>14</sup>B.G. Hutchinson, *Analysis of Road Roughness Records by Power Spectral Density Techniques*, Final Report No. 101 (Department of Highways, Ontario, Canada, 1965), p. 2(6).

<sup>15</sup>A.D. Brickman et al., *Analysis of Pavement Profile*.

<sup>16</sup>A.D. Brickman, J.C. Wambold, and J.R. Zimmerman, *An Amplitude-Frequency Description of Road Roughness*, Special Report 116 (Highway Research Board, 1974).

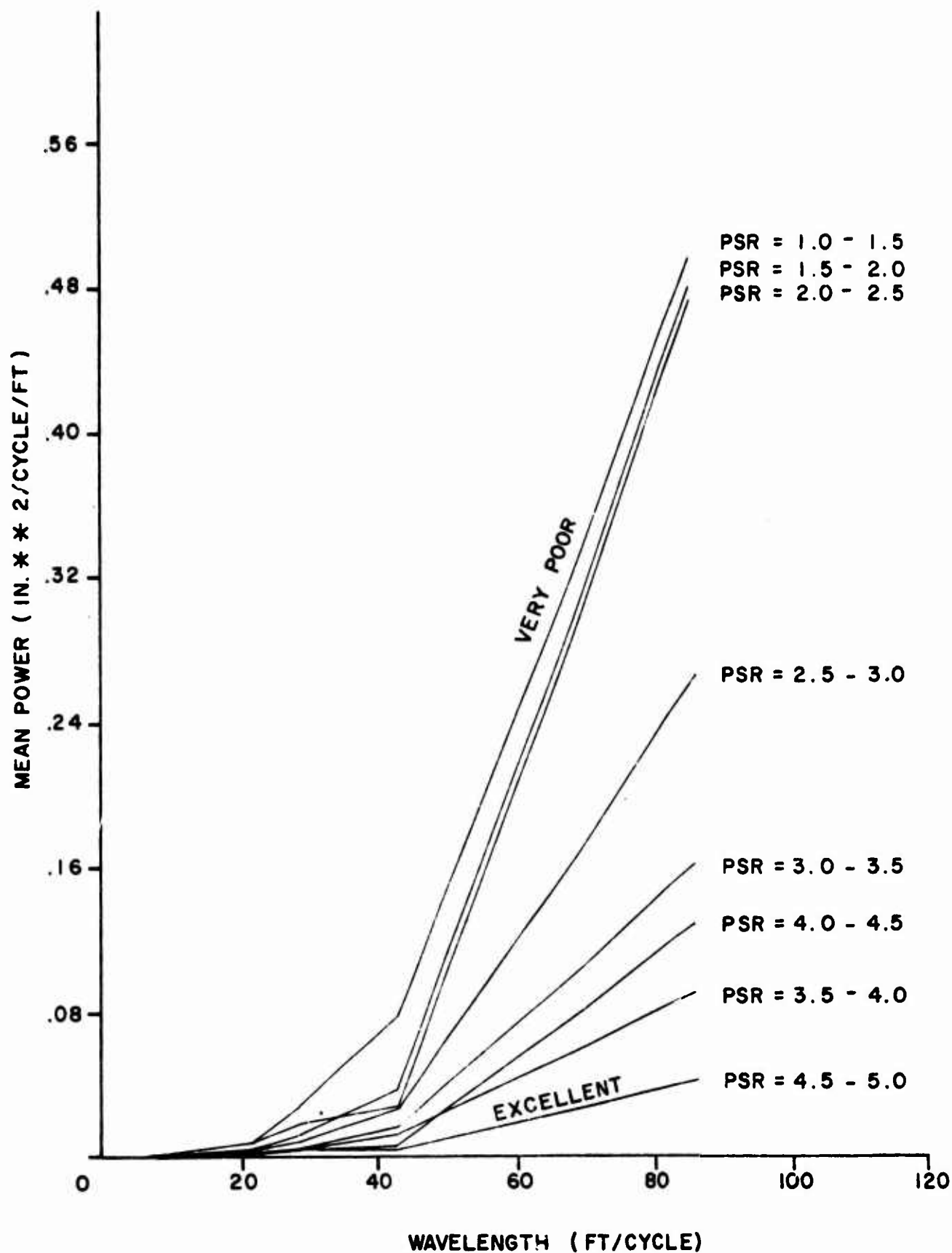


**Figure 9.** Effect of wavelength and mean power on subjective serviceability ratings for highway pavement (speed = 50 mph). (From R.W. Walker and W.R. Hudson, *The Use of Spectral Estimates for Pavement Characterization*. Research Report 156-2 [Center for Highway Research, University of Texas at Austin, 1973].)

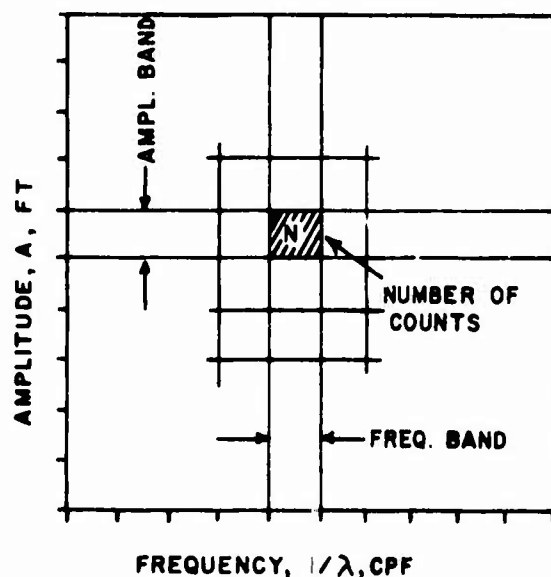
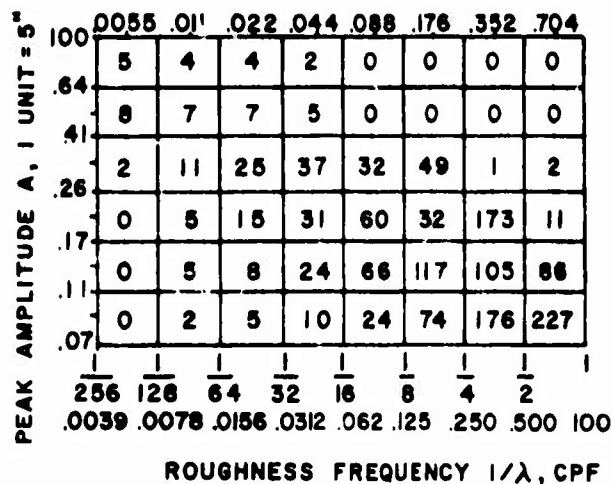


Figure 10. Illustration of the AFD technique of characterizing profile amplitude wavelength distribution. (From A.D. Brickman et al., *Analysis of Pavement Profile* [Pennsylvania Department of Transportation, 1969].)

3. The count values appearing in the AFD tabulation relate theoretically to the PSD of the road profile, and discrete values of roughness PSD can be computed from the AFD counts.

4. By reducing the roughness profile of a road to a table of heights and wavelengths, the AFD table describes the equivalent physical appearance of a road surface in a more understandable way than PSD.<sup>17</sup>

<sup>17</sup>A.D. Brickman, J.C. Wambold, and J.R. Zimmerman, *An Amplitude-Frequency Description of Road Roughness*, Special Report 116 (Highway Research Board, 1974), p. 66.

A method that has been proposed for increasing the usefulness of the power spectral density analysis is the use of digital filtering of the road profile data. Walker and Hudson conclude:

Filtering techniques offer another analysis tool in which the amplitudes of selected wavelength bands can be observed as a function of distance, thus permitting more localized examinations of the true average amplitude variations.<sup>18</sup>

Filtering techniques provide a plot of filtered profile amplitude versus distance. A plot of filtered and nonfiltered profiles is shown in Figure 11.

### Acceleration

Acceleration has been used as an indicator of pavement roughness for both highways and airfields. The occupants of aircraft and automobiles as well as the vehicle itself are subjected to various accelerations (vertical, fore and aft, and side to side) as the vehicle traverses a pavement. Higher accelerations result in greater passenger discomfort, although other factors such as frequency and exposure time also contribute to human discomfort.<sup>19</sup> Accelerations in the body of an automobile or aircraft can also cause structural and vehicle instrumentation damage (to electronic instruments, for example).

Vertical acceleration on highway pavements has been measured by the Kentucky Department of Transportation since the 1950's. Several approaches to the analysis of the acceleration measurements were attempted<sup>20,21,22</sup> by mounting accelerometers on different locations such as the vehicle's seat or the passenger's chest. At present, instrumentation has been developed to automatically sum the vertical

<sup>18</sup>R.S. Walker and W.R. Hudson, *The Use of Spectral Estimates for Pavement Characterization*, Research Report 156-2 (Center for Highway Research, University of Texas, 1973), p. 34.

<sup>19</sup>C.M. Harris and C.F. Crede, *Shock and Vibration Handbook*, 3 Vols (McGraw-Hill Book Company, Inc., 1961).

<sup>20</sup>R.L. Rizenbergs, *Accelerometer Method of Riding—Quality Testing*, Interim Report KYHPR-64-25 (Kentucky Department of Highways, 1965).

<sup>21</sup>R.L. Rizenbergs et al., *Pavement Roughness: Measurement and Evaluation*, HRR 471 (Highway Research Board, 1973), pp. 46-61.

<sup>22</sup>L.E. Gregg and W.S. Foy, *Traxial Acceleration Analyses Applied to the Evaluation of Pavement Riding Qualities*, HRB Proceedings, Vol. 34 (Highway Research Board, 1955), pp. 210-223.

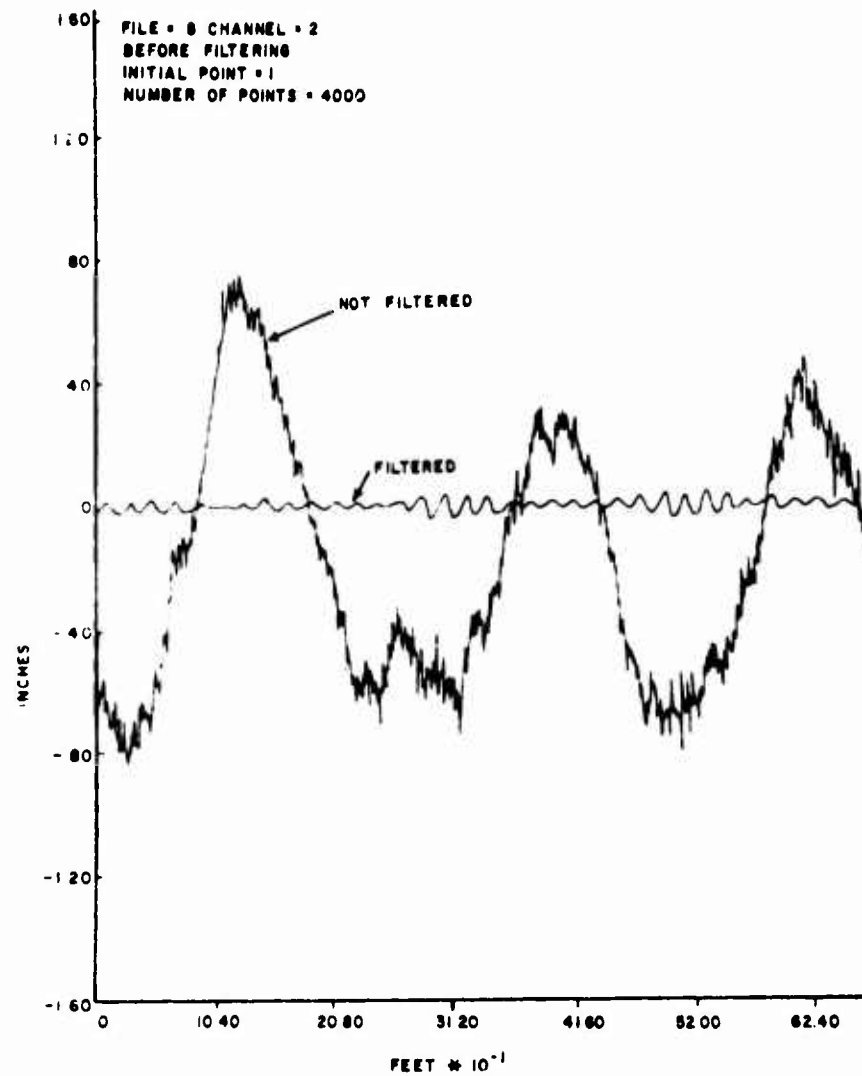


**Figure 11.** Illustration of effect of digital filtering of a profile. (From R.S. Walker and W.R. Hudson, *The Use of Spectral Estimates for Pavement Characterization*, Research Report 156-2 [Center for Highway Research, University of Texas at Austin, 1973].)

accelerations measured over a pavement section. With a typical full-sized passenger automobile traveling at 51.5 mph as the test vehicle, the sum of vertical accelerations and time elapsed during the test are used to compute an index of roughness. Examples of typical oscillographic acceleration outputs for relatively smooth and rough pavements are given by Rizenbergs.<sup>23</sup> To date, Kentucky has obtained acceleration measurements on over 200 pavements, which are being periodically retested. These measurements are used to evaluate quality of construction, to quantify rates of deterioration, and to identify causes of distress.<sup>24</sup> Kentucky has set limits on the various levels of roughness index determined from the acceleration measurements for acceptable and nonacceptable pavements, as shown in Figure 1.

Progress in measuring and predicting vertical accelerations in aircraft traveling on runways and taxiways has been significant. Various aircraft instrumented with accelerometers have taxied over runways while the vertical acceleration was measured at points on the aircraft frame such as the cockpit, center of gravity, and tail.<sup>25,26</sup> Vertical accelerations up to  $\pm 1g$  in the cockpit were found on some runways. Also, computer programs have been developed to model the aircraft runway interaction; this can be used to estimate the vertical acceleration at various points in the aircraft. One program, developed by the Boeing Company in 1967 for a B-52 aircraft, predicted measured acceleration fairly well, but required hours of computer time as well as large amounts of detailed aircraft data.<sup>27</sup> Another program, developed by the Lockheed-Georgia Company in 1970 for simulating the C-141 taxiing over a pavement, required less than one hour of computer time and less aircraft data.<sup>28</sup>

<sup>23</sup>R.L. Rizenbergs, *Accelerometer Method of Riding--Quality Testing*, Interim Report KYHPR-64-25 (Kentucky Department of Highways, 1965).

<sup>24</sup>R.L. Rizenbergs et al., *Pavement Roughness Measurement and Evaluation*, HRR 471 (Highway Research Board, 1973), pp 46-61.

<sup>25</sup>W. Horn, *Private Communication* (Waterways Experiment Station [WES], 1974).

<sup>26</sup>G.B. Hutton, *Uneven Runways Encountered by Subsonic Jet Transport Aircraft During Scheduled Airline Operations*, Technical Report 72095 (Royal Aircraft Establishment, 1972).

<sup>27</sup>D.A. Quade, *Location of Rough Areas of Runways for a B-52 Aircraft*, AFFDL-TR-67-175 (The Boeing Company, 1968).

<sup>28</sup>C.K. Butterworth and D.E. Boozer, *C-141A Computer Code for Runway Roughness Studies*, AFWL-TR-70-71 (AFWL, 1970).

A generalized aircraft runway model capable of simulating any aircraft traversing a runway pavement was recently developed by Gerardi and Lohwasser of the Air Force Flight Dynamics Laboratory. The mathematical model, called the TAXI code, requires less than two minutes on a CDC 6600 computer to simulate a typical aircraft taxi or take-off operation.<sup>29</sup> The program requires several easily obtainable aircraft parameters as input. A comparison of measured and calculated vertical acceleration for three aircraft shows differences of about 50 percent.<sup>30</sup> However, Sonnenburg (CFRE, University of New Mexico), in his work for the Air Force Weapons Laboratory (AFWL), concludes that it is possible to tune the code for specific types of aircraft to obtain better agreement.<sup>31</sup>

An example of measured and computed accelerations is shown in Figure 12. The acceleration versus distance plot along a runway (or highway) can be very useful in locating areas causing excessive accelerations, which can then be smoothed out. Use of the acceleration method can thus be very useful in extending the functional life of a pavement before a major rehabilitation is required. Significant research in this area is being conducted by Sonnenburg under contract with AFWL.<sup>32</sup>

A limiting acceleration of 0.4g has been suggested by Harris and Crede.<sup>33</sup> The curve in Figure 13 shows human tolerance vibration criteria as determined by Harris and Crede as a function of frequency and acceleration. Since the great majority of aircraft vibrations are less than about 12 cps, a single limiting value of 0.4g appears reasonable. Measured accelerations and frequencies in the cockpits of two aircraft on two Air Force bases are also shown on the plot. Gerardi and Lohwasser report that in both these cases the pilots reported excessive crew member discomfort.<sup>34</sup>

<sup>29</sup>A.G. Gerardi and A.K. Lohwasser, "A Digital Computer Program for Aircraft Runway Roughness Studies," *The Shock and Vibration Bulletin*, No. 43 (Part 2) (Naval Research Laboratory, 1973).

<sup>30</sup>C.K. Butterworth and D.E. Boozer.

<sup>31</sup>P.N. Sonnenburg, *Determination of Runway Roughness Criteria*, Interim Report to AFWL (1974).

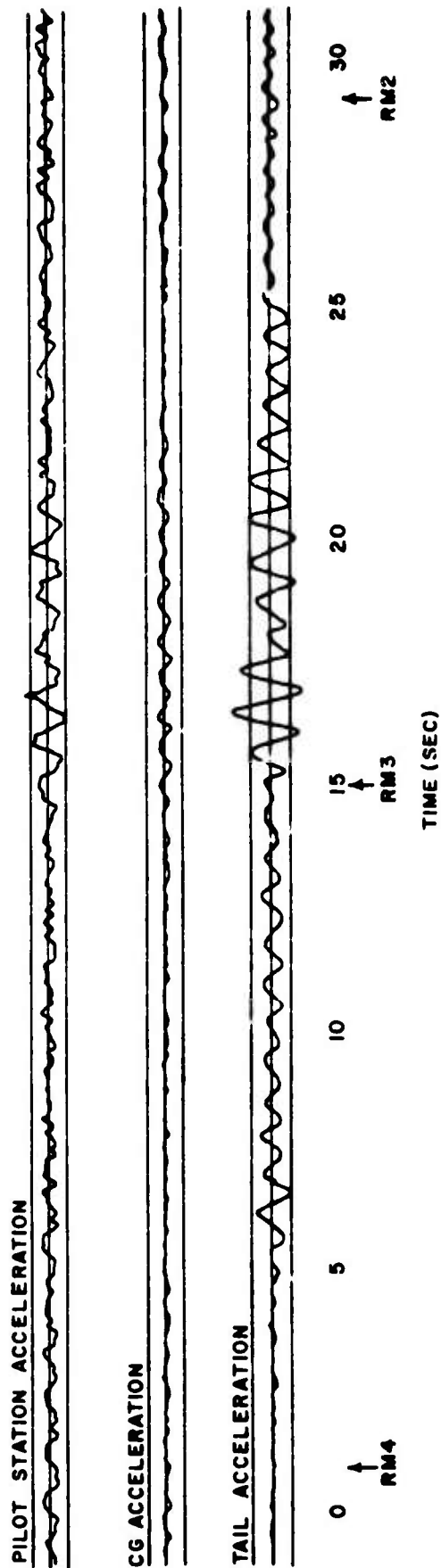
<sup>32</sup>P.N. Sonnenburg, *Determination of Runway Roughness Criteria*.

<sup>33</sup>C.M. Harris and C.F. Crede, *Shock and Vibration Handbook*, 3 Vols (McGraw-Hill Book Company, Inc., 1961).

<sup>34</sup>A.G. Gerardi and A.K. Lohwasser, "A Digital Computer Program for Aircraft Runway Roughness Studies."



## SIMULATED



24

## EXPERIMENTAL

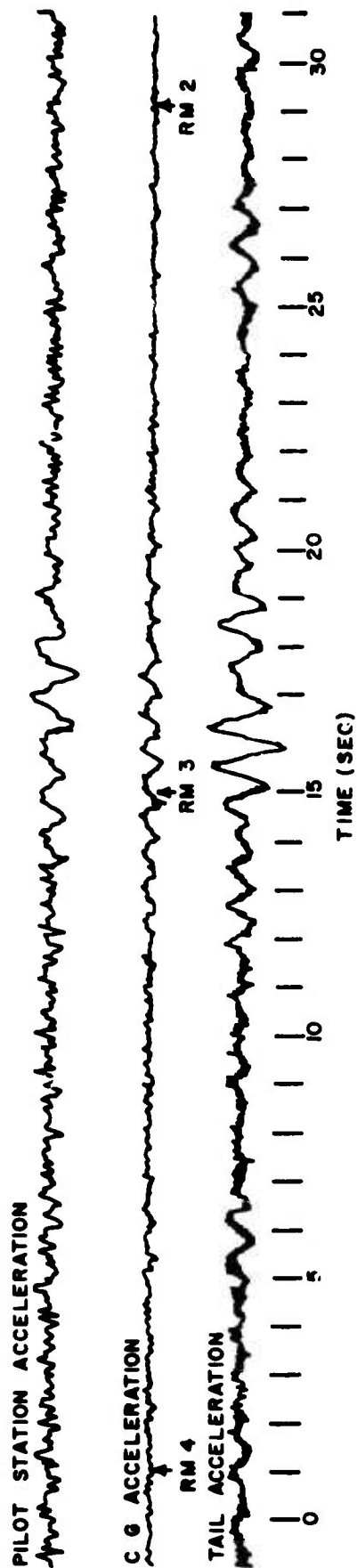


**Figure 12.** Simulated and measured acceleration time histories of a 400,000-lb B-52 during a 40-knot taxi over the U-TAPAO runway 18 profile.

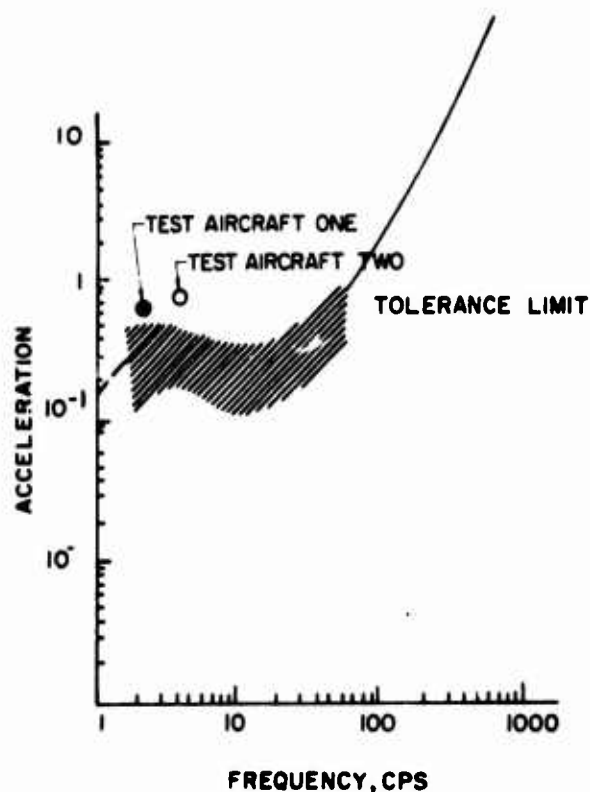


Figure 13. Human tolerance vibration criteria. (Adapted from A. G. Gerardi and A. K. Lohwasser, *Computer Program for the Prediction of Aircraft Response to Runway Roughness*, AFWL-TR-73-109, Vol 1 [AFWL, 1973].)

#### Absorbed Power

Extensive studies into human vibrational tolerance levels by the Mobility Systems Laboratory, U.S. Army Tank Automotive Command (ATC) led to development of the absorbed power concept. ATC concluded that time-averaged values of absorbed power correlated well with human subjective comfort and were the most descriptive parameter to predict the loss of mental and physical ability of an individual to control a vehicle.<sup>35</sup> Lins concludes the following:

Attempts to characterize vibration severity objectively usually involve measurements of the accelerations to which

<sup>35</sup>W. F. Lins, *Human Vibration Response Measurement*, Technical Report No. 11551 (U.S. Army Tank—Automotive Command, 1972).

a subject is exposed. Such measurements cannot be simply correlated with subjective response criteria, however, because perceived vibration severity is a complicated function of both frequency and amplitude of vibration.<sup>36</sup>

A review of literature shows that subjective human tolerance level is a function of several factors such as acceleration, time of exposure, frequency, and environment.<sup>37,38,39,40</sup> The effect of both frequency and acceleration on human vibrational tolerance is shown in Figure 13.

Absorbed power represents the rate of flow of energy into a vibrating body. It is defined as the time average of the product of force and velocity to which a body is subjected. It can be calculated in the time domain from the following expression:<sup>41</sup>

$$\bar{P} = \lim_{T \rightarrow \infty} \frac{1}{T} \int_0^T F(t)V(t)dt \quad [\text{Eq 3}]$$

where:  $\bar{P}$  = average absorbed power  
 $F(t)$  = force on subject  
 $V(t)$  = velocity of subject  
 $T$  = averaging time interval.

Since instrumentation limitations make it impractical to measure this force except in the laboratory, a transfer function which relates force to acceleration is used. The acceleration of a subject can easily be measured as a function of time, and absorbed power can then be calculated.<sup>42,43,44</sup>

An important characteristic of absorbed power is that it has physical significance and therefore can be measured as well as computed analytically. (Measurement equipment is described later in this report.) An example of absorbed power measurement is

<sup>36</sup>W. F. Lins, p 4

<sup>37</sup>C. M. Harris and C. E. Crede, *Shock and Vibration Handbook*, 3 Vols (McGraw-Hill Book Company, Inc., 1961).

<sup>38</sup>W. F. Lins

<sup>39</sup>C. K. Butterworth and D. E. Boozer, *C-141A Computer Code for Runway Roughness Studies*, AFWL-TR-70-71 (AFWL, 1970).

<sup>40</sup>R. A. Lee and F. Pradko, "Analytical Analysis of Human Vibration," *SAE Transactions*, Vol 77, Paper 680091 (1968).

<sup>41</sup>W. F. Lins

<sup>42</sup>W. F. Lins

<sup>43</sup>C. K. Butterworth and D. E. Boozer

<sup>44</sup>R. A. Lee and F. Pradko

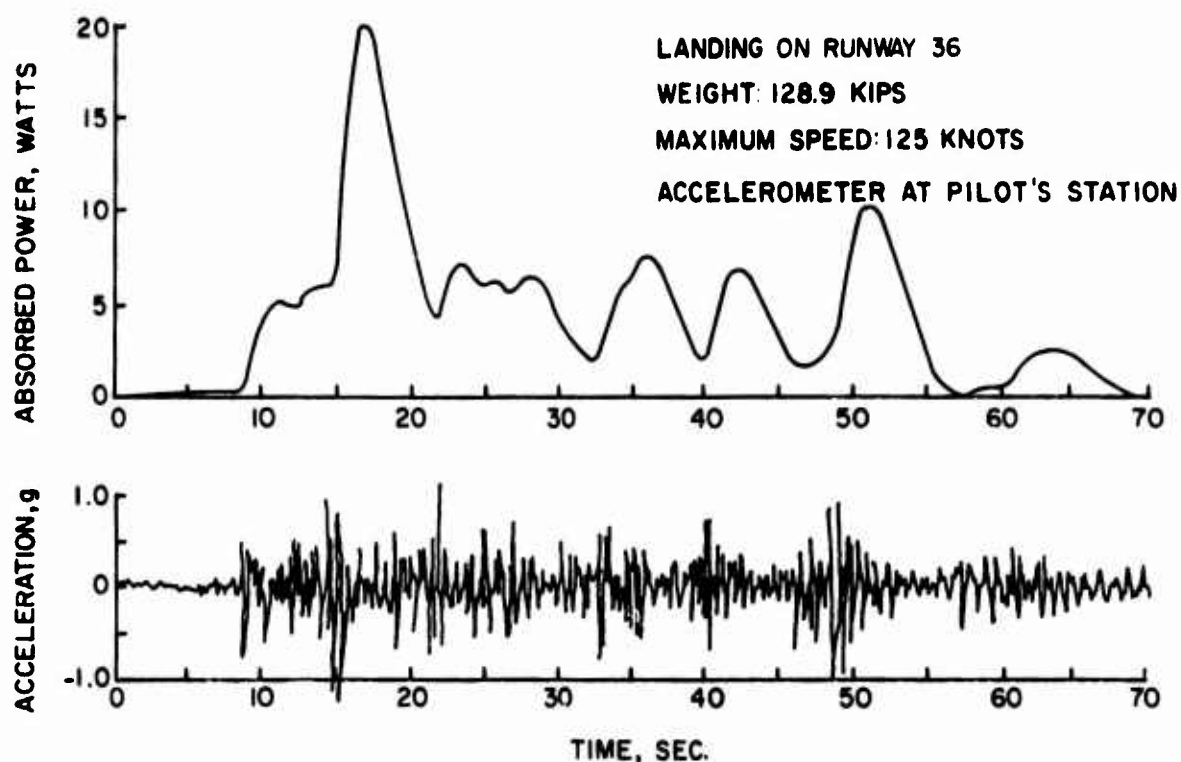


**Figure 14.** Absorbed power and vertical accelerations determined in the cockpit of B-727 on a runway at a major U.S. airport. (From W. Horn, *Private Communication* [Waterways Experiment Station, 1974].)

shown in Figure 14. Both absorbed power and vertical acceleration in the cockpit of a B-727 aircraft are shown as a function of time for a runway at a major civil airport in the United States. Vertical accelerations are shown to exceed the 0.4g level at several locations and even to exceed 1g at three locations. Absorbed power also shows very large magnitudes and at one location exceeds 20 watts. For off-road vehicles, the ATC determined a human failure level (when the driver lost control of the vehicle) of 6 watts of absorbed power regardless of the associated accelerations or frequencies;<sup>45</sup> it can be seen that this level is exceeded at several locations along this particular runway. Lee and Pradko suggest that the physical surroundings in which the vibration occurs have a strong influence on the acceptable absorbed power level:

For example, an upper acceptable absorbed power for automobile ride may be 0.2-0.3 watts. If one were to ride in

an automobile above this level, the opinion would very likely be that the ride is rough, and the vehicle uncomfortable. On the other hand, the upper acceptable limit for off-road vehicles may be 6-10 watts . . .<sup>46</sup>

Hence, the measurement of absorbed power for each application allows a comparison on an absolute scale.

Another important advantage of absorbed power is that it is a scalar quantity; therefore, the power determined in various directions such as fore-aft, vertical, and side-to-side, can be added together to give total absorbed power into a human.

The concept of absorbed power as an indicator of runway roughness is presently being investigated at the E. H. Wang Civil Engineering Research Facility at the University of New Mexico, under contract with the Air Force Weapons Laboratory (AFWL).<sup>47</sup> A

<sup>45</sup>W.F. Lins, *Human Vibration Response Measurement*. Technical Report No. 11551 (U.S. Army Tank—Automotive Command, 1972).

<sup>46</sup>R.A. Lee and F. Pradko, "Analytical Analysis of Human Vibration," *SAE Transactions*, Vol 77, Paper 680091 (1968).

<sup>47</sup>P.N. Sonneburg, *Determination of Runway Roughness Criteria*. Interim Report to AFWL (1974).

ACCEPTABLE ?

YES ☐

NO ☐

UNDECIDED ☐

5 - VERY GOOD

4 - GOOD

3 - FAIR

2 - POOR

1 - VERY POOR

0

SECTION IDENTIFICATION \_\_\_\_\_ RATING \_\_\_\_\_

RATER \_\_\_\_\_ DATE \_\_\_\_\_ TIME \_\_\_\_\_ VEHICLE \_\_\_\_\_

**Figure 15.** Serviceability rating form used at the AASHO Road Test.

computer program for calculating absorbed power as a function of time has also been written at the Waterways Experiment Station (WES). The plan is to use the TAXI code (previously described) along with a given pavement profile to estimate aircraft acceleration, and then calculate absorbed power experienced by aircraft passengers.

Although considerable work remains in development of the absorbed power method, it appears to be a very promising technique.

#### Human Evaluation

A pavement's "ride quality" can be evaluated subjectively by the users—the automobile and aircraft occupants. The human response approach basically involves pavement users riding over a pavement in a vehicle at a specified speed and rating the ride quality according to their opinion of the vibrating environment. This subjective response, or psychological impression, can be rated according to a scale such as "very poor," "poor," "fair," "good," or "very good." The mean subjective rating given to the pavement by all users is termed the present serviceability rating (PSR).

The pavement serviceability concept was developed for highway pavements at the AASHO Road Test and first reported by Carey and Irick.<sup>48</sup> A similar concept was developed concurrently by the

<sup>48</sup>W.N. Carey and P.E. Irick, *The Pavement Serviceability—Performance Concept*, Bulletin 250 (Highway Research Board, 1960).

10

9 - VERY GOOD

8

7 - GOOD

6

5 - FAIR

4

3 - POOR

2

1 - VERY POOR

0

RATER: \_\_\_\_\_

HWY. NO.: \_\_\_\_\_

SECTION NO.: \_\_\_\_\_

DATE: \_\_\_\_\_

#### IS PAVEMENT OF ACCEPTABLE QUALITY

YES \_\_\_\_\_ ☐

NO \_\_\_\_\_ ☐

UNDECIDED \_\_\_\_\_ ☐

#### REMARKS: \_\_\_\_\_

**Figure 16.** Performance rating form used by the Canadian Good Roads Association.

Canadian Good Roads Association (CGRA).<sup>49,50,51,52</sup> The rating form used by an individual rater at the AASHO Road Test is shown in Figure 15; the rating form developed by CGRA is shown in Figure 16. At the Road Test, the individual raters were allowed not only to ride over the pavement, but also to walk the

<sup>49</sup>Canadian Good Roads Association, "Manual on Pavement Investigations," Technical Publication No. 11 (CGRA, 1959).

<sup>50</sup>Canadian Good Roads Association, Pavement Design and Evaluation Committee, "Pavement Evaluation Studies in Canada," *Proceedings, International Conference on Structural Design of Asphalt Pavements* (University of Michigan, 1962).

<sup>51</sup>Canadian Good Roads Association, Pavement Design and Evaluation Committee, *A Guide to the Structural Design of Flexible and Rigid Pavements in Canada* (CGRA, 1965).

<sup>52</sup>Canadian Good Roads Association, Pavement Design and Evaluation Committee, "Field Performance Studies of Flexible Pavements in Canada," *Proceedings, Second International Conference on Structural Design of Asphalt Pavements* (University of Michigan, 1967).

length of the pavement and visually examine its surface. This procedure led Hutchinson to conclude:

... that rating efforts at the Road Test were directed toward obtaining subjective estimates of the pavement distortion and deterioration, and not to obtaining estimates of the subjective experiences of riding quality.<sup>53</sup>

However, the regression equations developed to predict the subjective user rating showed measured longitudinal roughness as by far the most significant parameter affecting subjective user evaluation.

Hutchinson describes some specific characteristics of subjective pavement roughness evaluation:

The riding quality afforded by a particular pavement section is a subjective experience and must be measured as such. The absolute riding quality is not a unique subjective characteristic but depends on the interrelationship of the pavement roughness, vehicle, and vehicle occupants. An absolute scale of riding quality would require the establishment of absolute levels of subjective experience that result from particular vibrational environments.<sup>54</sup>

Therefore, a user's subjective rating of pavement ride quality (or relative index of roughness) depends on many factors other than individual rater differences. While individual differences can be somewhat diminished by using the mean rating of a large group of raters, vehicle characteristics and speed are also very important factors. A pavement may have roughness characteristics such that its quality is rated relatively high at 20 mph but relatively low at 70 mph.

Three major systematic rating errors have been recognized in subjective rating:

1. The error of leniency which refers to the constant tendency of a rater to rate too high or too low for whatever reasons.
2. The halo effect which refers to the tendency of raters to force the rating of a particular attribute in the direction of the overall impression of the object rated.
3. The error of central tendency which refers to the fact that raters hesitate to give extreme judgments of stimuli and tend to displace individual ratings toward the mean of the group.<sup>55</sup>

<sup>53</sup>B.G. Hutchinson, *Principles of Subjective Rating Scale Construction*, HRR 46 (Highway Research Board, 1964), p 62.

<sup>54</sup>B.G. Hutchinson, *Principles of Subjective Rating Scale Construction*, p 69

<sup>55</sup>B.G. Hutchinson, *Principles of Subjective Rating Scale Construction*, pp 63-64

These problems tend to diminish the reliability of subjective evaluation if the rating system is not properly designed. Also, the subjective evaluation does not give information on structural damage or component failure of the vehicle. Its value is, of course, that it is a direct assessment of the users' evaluation of the level of service provided by the pavement. Also, it may be that the most critical limitation is human tolerance. Vehicle structural or component failures may be insignificant as long as pavement ride quality is acceptable to a majority of users.

The subjective evaluation of highway pavements has been correlated with quantitative roughness measurements. Predictive regression equations for flexible and rigid pavements were developed at the AASHO Road Test to estimate the users' subjective present serviceability rating from objective measured pavement surface data. The estimated rating is called a *present serviceability index (PSI)* to distinguish it from the actual, subjectively estimated PSR. However, it must be remembered that PSI is an estimate of the true PSR value. The AASHO model is as follows:

$$PSI = C + A_1 R_1 + B_1 D_1 + B_2 D_2 \quad [\text{Eq 4}]$$

where C = coefficient (3.03 for flexible pavements and 5.41 for rigid pavements)

A<sub>1</sub> = coefficient (-1.91 and -1.30 for flexible and rigid pavements, respectively)

R<sub>1</sub> = function of profile roughness ( $\log [1 + \overline{SV}]$ , where  $\overline{SV}$  = mean slope variance from CHLCE profilometer)

B<sub>1</sub> = coefficient (-1.38 for flexible and 0 for rigid, respectively)

D<sub>1</sub> = function of surface rutting ( $\sqrt{\overline{RD}}$ , where  $\overline{RD}$  = mean rut depth along pavement)

B<sub>2</sub> = coefficient (-0.01 for flexible and -0.09 for rigid)

D<sub>2</sub> = function of surface deterioration ( $\sqrt{C+P}$ , where C+P = amount of cracking (in linear feet for rigid and square feet for flexible) and patching in square feet per 1,000 ft<sup>2</sup> of pavement).

The accuracy of these models can be judged by the following statistics:

Flexible: R<sup>2</sup> = 84% (multiple correlation coefficient)

$S_e = 0.38$  (standard error of estimate of PSR)

Rigid:  $R^2 = 92\%$   
 $S_e = 0.32$

Further work by Yoder and Milhous<sup>56</sup> provided extensive correlations between various equipment measurements and subjective panel ratings. Their results showed that the standard error in predicting panel ratings from equipment measurement alone was only slightly larger than when pavement condition factors were included (such as cracking, patching, etc.).

Similar regression equations to predict the subjective present serviceability rating from measured pavement data were developed by the Texas Highway Department in 1968.<sup>57</sup> Similar  $R^2$  and standard error of estimates were obtained. It was also determined that a model containing only slope variance or roughness index explains about 67 percent of the mean rating panel's opinion ( $R^2 = 67$  percent).<sup>58</sup>

Walker and Hudson developed a regression model using profile wavelength/amplitude characteristics.<sup>59</sup> The basis for this model can be seen in Figure 9, which shows the relationships between power, wavelength, and PSR. The form of the equation is as follows:

$$\text{PSR} = B_0 + B_1X_1 + B_2X_2 + B_3X_3 + \dots B_NX_N \quad [\text{Eq 5}]$$

where  $B_i$  = the linear model coefficients determined from regression, and

$X_i$  = the average amplitude for  $i$ th wavelength.

For this regression model the  $R^2$  was 0.89 and the standard error of estimate was 0.33, which indicates

<sup>56</sup>E.J. Yoder and R.T. Milhous, *Comparison of Different Methods of Measuring Pavement Condition*, NCHRP Report No. 7 (Highway Research Board, 1964).

<sup>57</sup>Freddy L. Roberts and W. Ronald Hudson, *Pavement Serviceability Equations Using the Surface Dynamics Profilometer*, Research Report 73-3 (Center for Highway Research, The University of Texas at Austin, 1970).

<sup>58</sup>R.S. Walker and W.R. Hudson, *The Use of Spectral Estimates for Pavement Characterization*, Research Report 156-2 (Center for Highway Research, University of Texas at Austin, 1973).

<sup>59</sup>R.S. Walker and W.R. Hudson, *The Use of Spectral Estimates for Pavement Characterization*

that it can be used to estimate the users' subjective PSR with about the same accuracy as the models that include the pavement surface deterioration characteristics of rutting, cracking, and patching. This model has been used extensively—and successfully—by the Texas Highway Department to estimate PSR. This work shows that it is possible to accurately estimate the subjective user rating or serviceability of a highway pavement if the wavelength/amplitude characteristics of the longitudinal profile of the pavement are determined by the power spectral density technique. Prediction of PSR using only slope variance or roughness index is less accurate.

The development of subjective evaluation techniques for runway pavements has not paralleled that for highways. Subjective evaluation techniques are available only from a limited study conducted by Steitle,<sup>60</sup> which developed rating forms for obtaining pilots' evaluations of runway pavements (Figures 17 and 18). Actual ratings of two runways at Dallas Love Field were obtained from about 50 airline pilots. As can be seen in Figures 17 and 18, the basic AASHO rating scheme of five categories was used for each evaluation criterion. Typical rating results obtained for takeoffs on Runway 31R are shown in Figure 19. Profile measurements were made on both Love Field runways using the Surface Dynamics Profilometer.

Steitle suggests two methods for analyzing the pilots' subjective ratings and the measured runway profiles. One approach is to determine the effect of cockpit accelerations on the pilots' ratings. Cockpit accelerations along the runway can be determined for each aircraft using the TAXI Code computer program and the runway profile. A possible technique would be to determine a single summary roughness indicator, such as average absorbed power, to correlate with the pilot rating. A regression equation might thus be developed which would relate absorbed power to the pilots' subjective evaluation of a runway.

Another approach is to determine the profile amplitude/wavelength characteristics of the pavement through power spectral analysis and develop a

<sup>60</sup>David C. Steitle, *Development of Criteria for Airport Runway Roughness Evaluation*, MS Thesis (The University of Texas at Austin, 1972).

## TAKE - OFF

PILOT'S NAME \_\_\_\_\_ AIRPORT NAME \_\_\_\_\_

AIRLINE NAME \_\_\_\_\_ TYPE OF AIRCRAFT \_\_\_\_\_

SURVEY USED \_\_\_\_\_ TIME \_\_\_\_\_

### LOCAL CONDITIONS

DAY ☐ NIGHT ☐ WET ☐ DRY ☐ WIND \_\_\_\_\_  
DIR. / VEL.

### OVERALL RIDING QUALITY

ACCEPTABLE ☐ UNDECIDED ☐ UNACCEPTABLE ☐

### OVERALL RATING

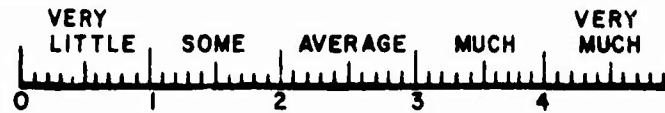


### PREMATURE LIFT-OFF

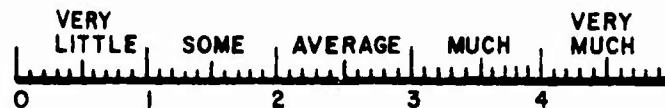
NO ☐ POSSIBLY ☐ YES ☐

LONGITUDINAL LOCATION OF PREMATURE LIFT-OFF OR T/O ROTATION  
(INDICATE ON A SKETCH IN SPACE BELOW)

### PORPOISING



### ROLL

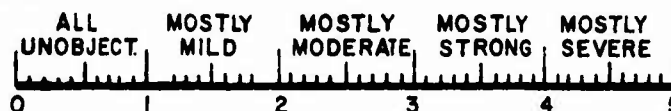


### OBJECTIONABLE COCKPIT ACCELERATIONS

NUMBER OF



### MAGNITUDE OF



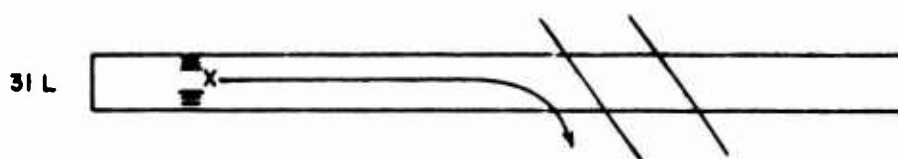
REMARKS ON RUNWAY CONDITION

Figure 17. Pilot's subjective roughness rating form. (From David C. Steile, *Development of Criteria for Airport Runway Roughness Evaluation*, MS Thesis [The University of Texas at Austin, 1972].)

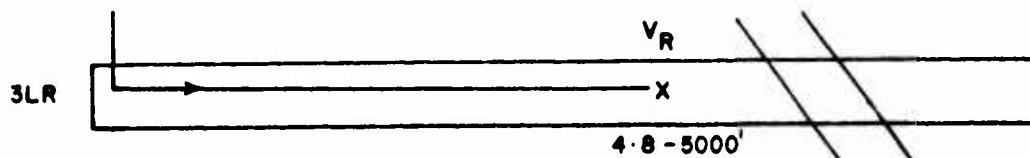
## INSTRUCTIONS

The rating form provides one side for take-off information and one side for landing information, as indicated on the form. The initial information to be filled in at the top of either side is self-explanatory. However, for "Type of Aircraft", the specific model is desired, such as B727-200 Stretch or DC-9-30. Check marks should be placed in appropriate boxes. And, where a longitudinal location is requested, a sketch such as the ones below is appropriate.

LONGITUDINAL LOCATION OF TOUCHDOWN (Indicate on a sketch in space below)

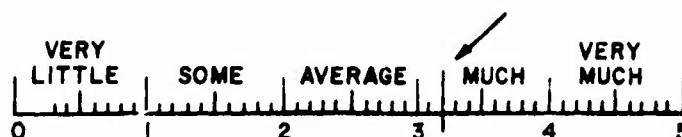


LONGITUDINAL LOCATION OF PREMATURE LIFE-OFF OR T/O ROTATION  
(Indicate on a sketch in space below)



The information desired from the sketch is the portion of the runway used in the maneuver. Also, feel free to indicate on the sketch areas of roughness, waviness, etc. For the items which have a scale from zero to five and the "LATERAL LOCATION OF TOUCHDOWN" scale, a vertical line through the appropriate value is desired such as is indicated by the arrows below.

PROPOISING



LATERAL LOCATION OF TOUCHDOWN



Finally, space is provided on the right of the sheet for any remarks which you think may be appropriate.

**Figure 18.** Pilot's subjective roughness rating instruction sheet. (From David C. Steitle, *Development of Criteria for Airport Runway Roughness Evaluation*, MS Thesis [The University of Texas at Austin, 1972].)



AIRPLANE	OVERALL RATING	OVERALL RIDING QUALITY
DC-9-10	0.6	Acceptable
DC-9-151	1.3	Acceptable
B-727-100	1.7	Acceptable
B-727-100	3.5	Unacceptable
B-727-100	4.5	Undecided
B-727	3.2	Unacceptable
B-727-200	2.5	Acceptable
B-727-200	3.0	Acceptable
B-727-200	3.5	Unacceptable
B-727-200	3.5	Unacceptable
B-727-200	4.5	Unacceptable
B-727-200	5.0	Unacceptable
B-707-388	2.9	Acceptable
B-707	0.5	Acceptable
B-707-320H	3.5	Unacceptable
B-707-320H	3.5	Unacceptable
B-747	4.0	Unacceptable

**Figure 19.** Pilot's rating data for take-off on Runway 31R, Love Field, Dallas. (From David C. Steitle, *Development of Criteria for Airport Runway Roughness Evaluation*, MS Thesis [The University of Texas at Austin, 1972].)

predictive model similarly to the way in which Equation 5 was developed, to relate pilot subjective response to pavement profile characteristics. Even from an examination of the limited data obtained by Steitle, it seems probable that to achieve an acceptable level of accuracy a different model would be needed for each aircraft type.

The subjective evaluation of a pavement's ride quality, and therefore its index of roughness, has definite advantages and disadvantages. Possibly its greatest advantage is that it gives a direct user-evaluation of the functional serviceability of a pavement. Its greatest disadvantage is that human response to vibrational environment is highly variable and, therefore, the rating panels must be large if reasonable serviceability ratings are to be obtained.

### Roughness Measurement Equipment

Several types of equipment systems presently available are capable of measuring roughness and/or processing the data to provide roughness indicators previously described. The equipment can be classified into systems that measure (1) pavement surface profile, (2) axle/vehicle body displacement, (3) acceleration and absorbed power, and (4) slope variance. Table I lists the equipment described in this section.

**Table I**

#### Summary of Major "Roughness" Measurement Equipment

1. PAVEMENT PROFILE MEASUREMENT (PROFILOMETERS)
  - a. Precise Leveling
  - b. Surface Dynamics Profilometer
  - c. AFWE Inertial Profilometer
  - d. AFWE Laser Profilometer
  - e. Rolling Straightedge
  - f. British Road Research Laboratory Profilograph
2. VEHICLE AXLE/BODY DISPLACEMENT MEASUREMENT (ROUGHOMETERS)
  - a. U.S. Bureau of Public Roads Roughometer
  - b. P.C.A. Roadometer
  - c. Mass' Ride Meter
3. ACCELERATION/ABSORBED POWER MEASUREMENT
  - a. Kentucky DOT Accelerometer
  - b. Absorbed Power Meter
4. SLOPE VARIANCE MEASUREMENT
  - a. CHLOI Profilometer

#### Profile Measuring Equipment

1. **Precise Leveling (LEVEL):** The actual pavement surface profile can be obtained by using precise leveling techniques, a method that has been used often in airport runway research. Before inertial-type profilometers were developed, this was the only method for obtaining accurate profile data. The accuracy of measurement depends upon the type of level and rod and the surveying techniques. Probably the most satisfactory procedure consists of setting bench marks along the edge of the runway with precise leveling instruments (to an accuracy of  $\pm 0.001$  ft), and then obtaining the actual profile elevations with normal leveling instruments. This provides profile accuracy of better than  $\pm 0.01$  ft.<sup>61</sup>

The profile data must usually be adjusted by removing the natural grade before the data can be used to determine such indicators as power spectral density. This technique obviously requires much time and manpower, but can result in accurate profiles.

2. **Surface Dynamics Profilometer (SDP):** This inertial-type profilometer, initially developed by

<sup>61</sup>W.H. Rayner and M.O. Schmidt, *Surveying Elementary and Advanced* (D. Van Nostrand Co., 1960).

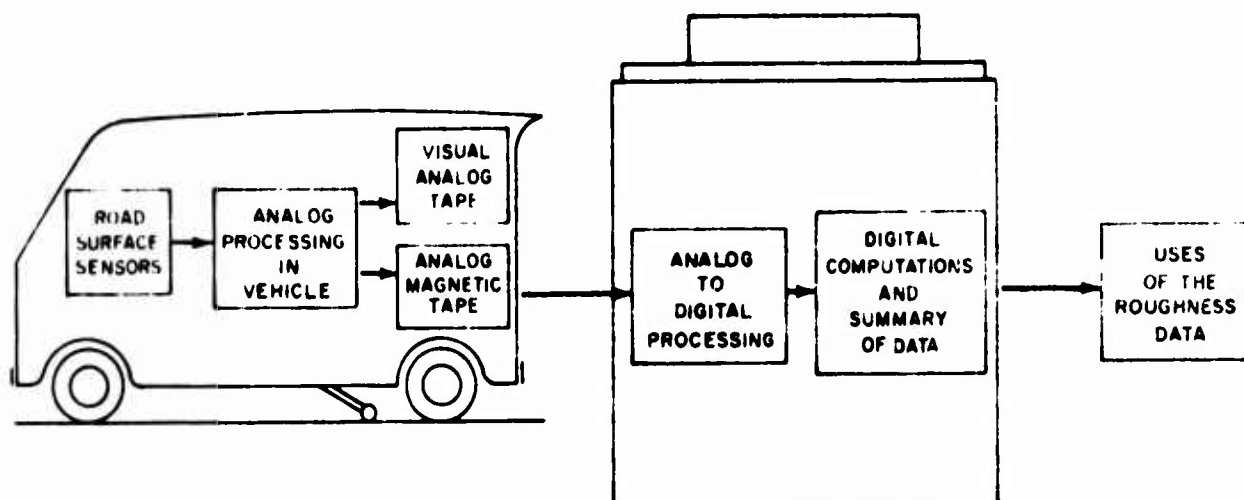


**Figure 20.** Surface Dynamics Profilometer measurement system used by Texas Highway Department. (From R.W. Walker and W.R. Hudson, *A Road Profile Data Gathering and Analysis System*, paper presented at the 49th Annual Meeting of the Highway Research Board, Washington, D.C. [1970].)

General Motors Corporation in the early 1960's, was originally named the GMR Road Profilometer.<sup>62,63,64</sup> The initial version was evaluated by the Michigan Department of Transportation;<sup>65</sup> another evaluation was by Spangler et al.<sup>66</sup> The first commercial SDP was manufactured in 1967 and has since undergone further development by the Texas Highway Department.<sup>67,68,69,70</sup>

<sup>62</sup>E. B. Spangler and W. J. Kelley, *Servo-Seismic Method of Measuring the Road Profile*, Bulletin 328 (Highway Research Board, 1962).

<sup>63</sup>E. B. Spangler and W. J. Kelley, *GMR Road Profilometer: A Method for Measuring Road Profile* (General Motors Corp., 1964).

<sup>64</sup>E. B. Spangler and W. J. Kelley, *GMR Road Profilometer—A Method for Measuring Road Profile*, HRR 121 (Highway Research Board, 1965), pp 27-54.

<sup>65</sup>J. R. Darlington, *Evaluation and Application Study of the General Motors Corporation Rapid Travel Profilometer*, Research Report Number R-73 (State of Michigan Department of State Highways, 1970).

<sup>66</sup>E. B. Spangler et al., *Evaluation of the Surface Dynamics Profilometer for Runway Profile Measurement*, Technical Report No. AFWL-TR-68-43 (AFWL, 1968).

<sup>67</sup>W. R. Hudson, *High-Speed Road Profile Equipment Evaluation*, Research Report No. 73-1 (Center for Highway Research, The University of Texas at Austin, 1968).

<sup>68</sup>Roger S. Walker, Freddy L. Roberts, and W. Ronald Hudson, *A Profile Measuring, Recording, and Processing System*, Research Report 73-2 (Center for Highway Research, The University of Texas at Austin, 1970).

<sup>69</sup>Roger S. Walker and W. Ronald Hudson, *Analog-to-Digital System*, Research Report 73-4 (Center for Highway Research, The University of Texas at Austin, 1970).

<sup>70</sup>Roger S. Walker, W. Ronald Hudson, and Freddy L.

The complete road profile data system developed in Texas consists of a Surface Dynamics Profilometer and an analog-to-digital (A-D) subsystem (see Figure 20). The actual road profile is measured by the SDP profile-sensing subsystem and recorded in *analog form* on magnetic tape. Then the analog record of the profile is converted to a *digital* record of road profile. This digital record can then be used to calculate several roughness statistics such as power spectral density, roughness index, and slope variance.

The measurement process is shown in Figure 21 and described by Walker and Hudson as follows:

The SD Profilometer contains all the necessary sensors and equipment to obtain an analog signal directly proportional to a roadway profile: two road-following wheels, each mounted to the vehicle and held firmly in contact with the road by a 300-pound spring force exerted by a torsion bar and a linear potentiometer, an accelerometer, and a small analog (profile) computer sense and record data. A linear potentiometer is mounted between a sensor wheel and vehicle body, and the difference in sensor wheel and vehicle body displacements ( $W-Z$ ) is obtained by the potentiometer. The accelerometer, mounted directly above the potentiometer, induces a voltage proportional to the vertical vehicle body acceleration  $Z$  and the analog computer double integrates the vertical body acceleration to

Roberts, *Development of a System for High-Speed Measurement of Pavement Roughness, Final Report*, Research Report 73-SF (Center for Highway Research, The University of Texas at Austin, 1971).

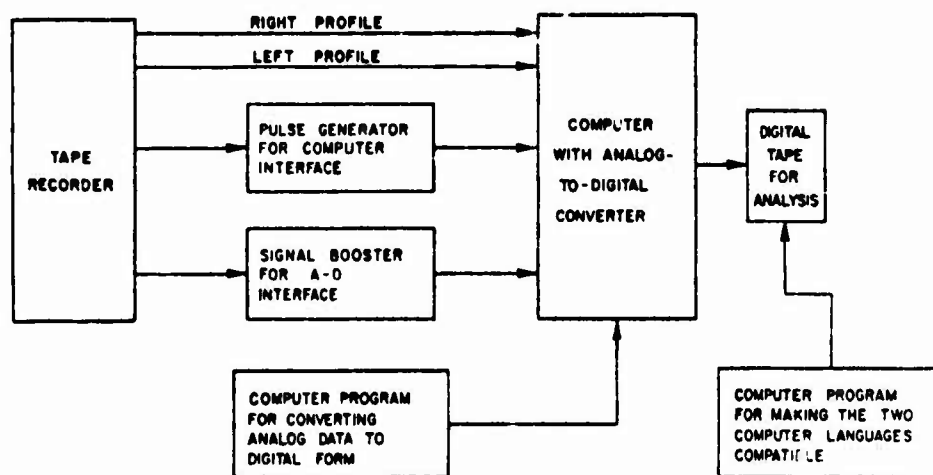
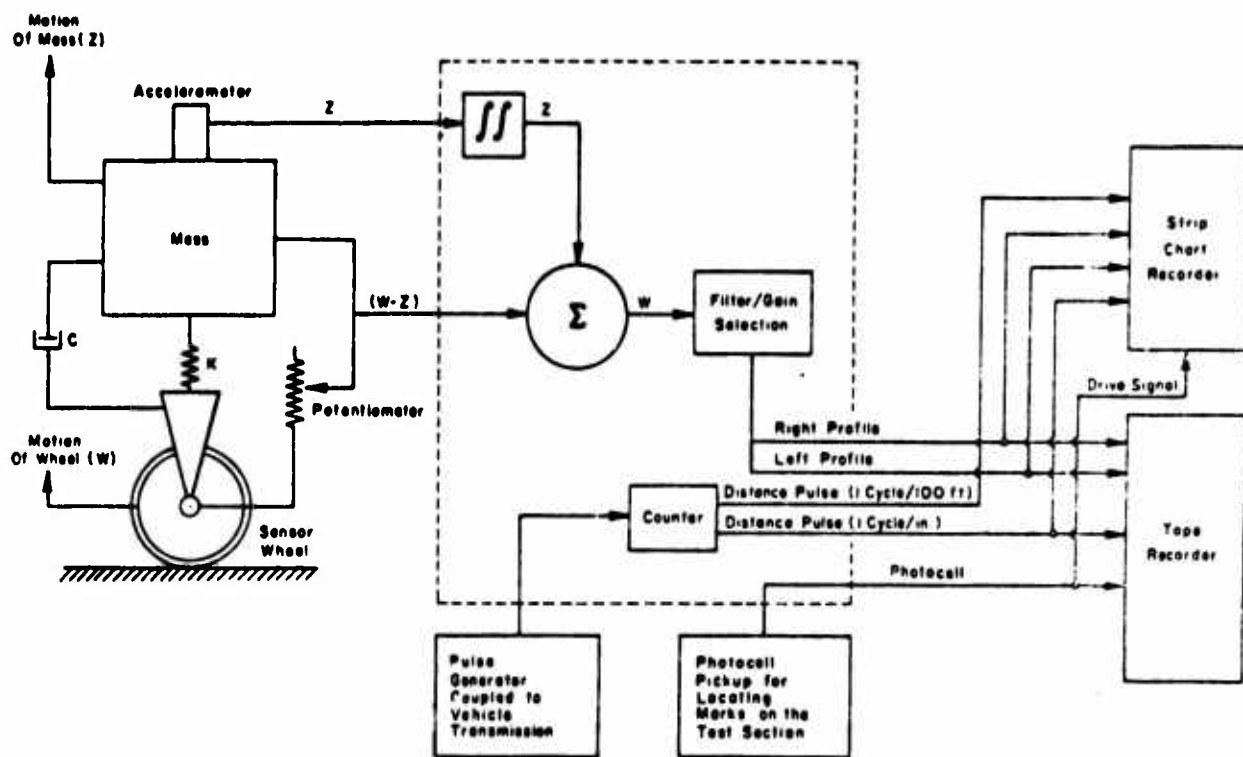


**Figure 21.** Detailed diagram of SDP measurement system of Texas Highway Department. (From R.S. Walker and W.R. Hudson, *A Road Profile Data Gathering and Analysis System*, Paper presented at the 49th Annual Meeting of the Highway Research Board, Washington, D.C. [1970].)

obtain the vertical body displacement  $Z$ . A voltage directly proportional to the vertical wheel movement (the road profile) is then obtained by the analog summing of the vertical body displacement  $Z$  and the sensor wheel and body displacement difference  $W/Z$ . An active high-pass filtering network is employed in the integrator and summing circuitry for filtering low frequency or long wavelength profiles, such as hills. Two independent measuring subsystems are used for measuring profiles, one right and one left (wheel paths).<sup>21</sup>

Some specific advantages of the SDP are:

(1) It provides a sufficiently accurate profile at a relatively high operating speed of about 20 mph, compared to other devices.

(2) It provides an accurate pavement surface profile in analog and digital form that may be used to determine various roughness statistics such as roughness index and slope variance, or used for power spectral analysis. The system can handle large amounts of data by automated means.

(3) It can measure fairly long pavement surface wavelengths (up to about 200 ft). Longer wavelengths may be required for high-speed runway pavement evaluation, however.

(4) It has excellent repeatability.

The SDP also has several disadvantages:

(1) Wheel bounce at operating speeds above 34 mph distorts the profile.

(2) Initial equipment cost is high; operating cost is also relatively high because skilled operators are required. In addition, there are significant data processing costs.

(3) The equipment and computer facilities necessary for obtaining digital data are complex.

(4) Operational traffic hazard problems occur because the SDP cannot obtain accurate profile data at normal traffic speed.

Despite these disadvantages, many pavement

engineers consider the SDP to be one of the best systems available for measuring pavement surface roughness.

**3. AFWL Inertial Profilometer:** This profilometer was recently developed by the Dynasciences Corporation under contract with the Air Force Weapons Laboratory (AFWL) and is being used extensively in AFWL's pavement roughness studies. The inertial profilometer shown in Figures 22 and 23 is similar in concept to the SDP. It has only one road-following wheel, which is located approximately at the center of the vehicle.

The measurement system consists of a vertical gyro erecting an accelerometer in a two-axis gimbal system with a LVDT attached to the spring-loaded road-following wheel. The gyro and accelerometer are served through the gimbals to keep the platform in a horizontal plane. The outputs from the accelerometer are doubly integrated to give the instantaneous position of the platform in the vehicle. This displacement, added to the displacement output from the LVDT, gives the actual instantaneous relative altitude of the pavement surface from an imaginary inertial datum line. A filter screens out long-term accelerations which represent wavelengths longer than 400 ft, enabling the system to establish a floating datum which is the average over about 400 ft of pavement. Hence, the system is capable of accurately measuring pavement surface wavelengths up to approximately 400 ft.

A laser beam system provided with the profilograph can be used to facilitate accurate horizontal alignment. This control allows the profile to be run along a specific alignment on a runway. The inertial profilometer is run at a speed of 20 mph.

The relative pavement profile is recorded and converted from analog form to digital form within the profilometer for further use in pavement roughness analyses. The advantages and disadvantages listed for the SDP apply to the inertial profilometer; however, the AFWL inertial profilometer is capable of measuring longer surface wavelengths, an advantage on runway pavements.

The AFWL inertial profilometer has been compared to rod and level surveys that have had comparable filtering techniques applied. A standard deviation of the difference between the inertial profilom-

<sup>21</sup>R.W. Walker and W.R. Hudson, *A Road Profile Data Gathering and Analysis System*, paper presented at the 49th Annual Meeting of the Highway Research Board, Washington, D.C. (1970).



**Figure 22.** View of profilometer vehicle and laser setup for horizontal control. (From M. Womack, Private Communication, AFWL [1974].)

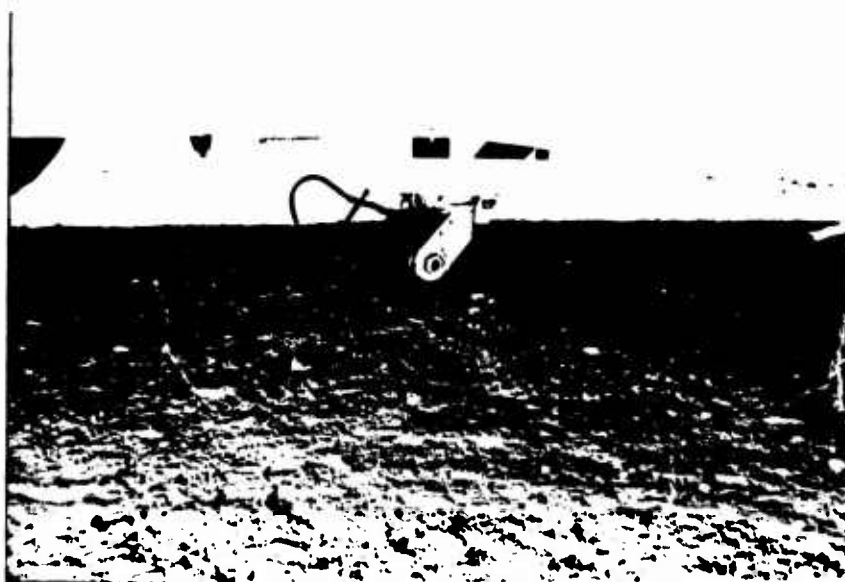


**Figure 23.** View of profilometer road-following wheel. (From M. Womack, Private Communication, AFWL [1974].)

eter and the rod and level survey profile was computed to be  $\pm 0.107$  in.<sup>72</sup>

4. AFWL Lasar Profilometer (LASAR): The Lasar Profilometer was developed by General Applied Science Laboratories under contract with AFWL. The system consists of two separate components: the lasar, which is mounted in a small vehicle as shown in Figure 24; and a light-sensing target connected directly to a road-following wheel, which is supported by another small vehicle as shown in Figure 25. Figure 26 shows the vehicles containing the lasar and the light-sensing target. The vehicle in which the lasar is located remains stationary, while the vehicle containing the light-sensing target moves along the pavement being measured at a rate of approximately 3 mph. As the road-following wheel moves along pavement surface, the light-sensing

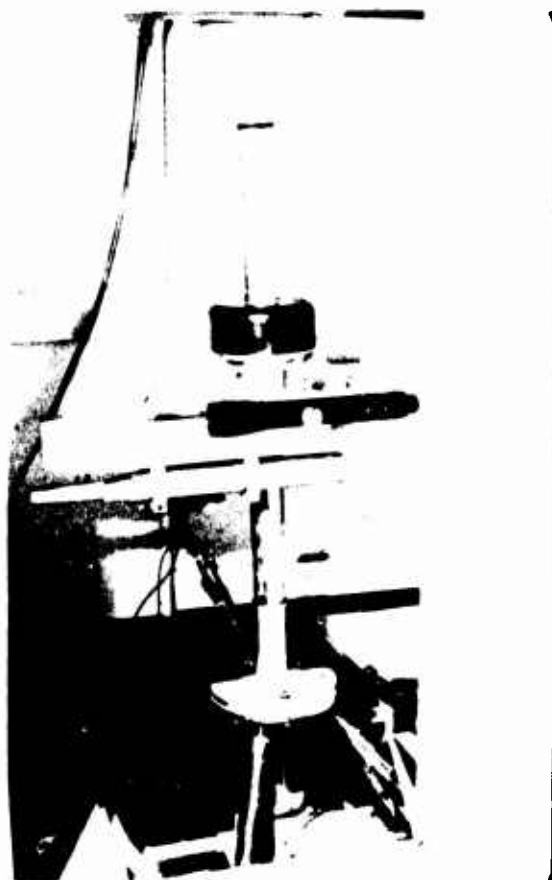


Figure 24. Lasar and lasar-leveling assembly in lasar vehicle. (From M. Womack, Private Communication, AFWL [1974].)

<sup>72</sup>M. Womack, Private Communication, AFWL (1974).

target remains locked onto the lasar beam by moving up and down automatically, to keep the lasar beam on the target. A recording device connected to the target provides a sampling interval of 6 in. This record is converted to digital form on magnetic tape and used for pavement roughness analysis. Although the equipment is currently capable of operating only at night, it could be modified for daylight operation. This profilometer is capable of giving accurate profile measurements. A standard deviation of the difference between the lasar profile and a rod and level profile was determined to be  $\pm 0.12$  in.<sup>73</sup> A single 9000-ft line of survey (18,000 data points) can be accomplished in approximately one hour. The equipment necessary for this system is also relatively expensive and generally requires a three-man crew.

5. Rolling Straightedge (RSE): Several varieties of this type of profilometer exist. Both the California Division of Highways and the University of Michigan have developed truck-mounted versions.<sup>74,75</sup> An excellent review of the development of various RSE profilometers is given by Hveem.<sup>76</sup>

The RSE profilometer used in Utah Highway Department research (Figure 27) is described here to illustrate the characteristics of this type of profilometer. The recording wheel in the center of the profilometer is connected to a recorder chart mounted on the profilometer frame, which plots the change in displacement between the recording wheel and the frame support wheels located about 25 ft apart. Several support wheels are used to minimize or average out the relative errors involved with this device. A vertical displacement integrator is used to sum one-direction deviation of the recording wheel. The relative profile is plotted continuously on the chart at a scale of 1 in. = 1 in. vertically and 1 in. = 25 ft horizontally. These profilometers operate at a relatively slow speed (usually less than 3 mph).

The RSE can provide a roughness index automatically. The relative profile can also be scaled from the chart, but with questionable accuracy. Because of the limited wheel base of the profilometer frame,

<sup>73</sup>M. Womack, Private Communication, AFWL (1974).

<sup>74</sup>F.N. Hveem, *Devices for Recording and Evaluating Pavement Roughness*, Bulletin 264 (Highway Research Board, 1960).

<sup>75</sup>W.R. Hudson, W.E. Teske, H. Karl Dunn, and E.B. Spangler, *State of the Art of Pavement Condition*, Special Report 95 (Highway Research Board, 1968).

<sup>76</sup>F.N. Hveem.

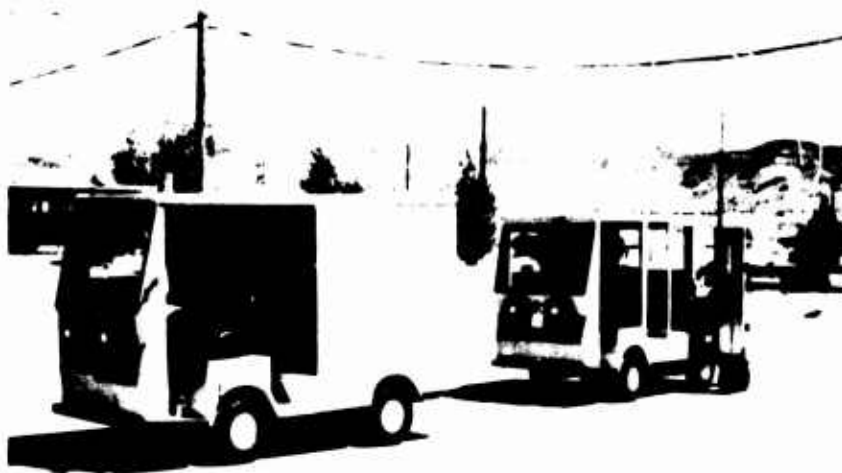
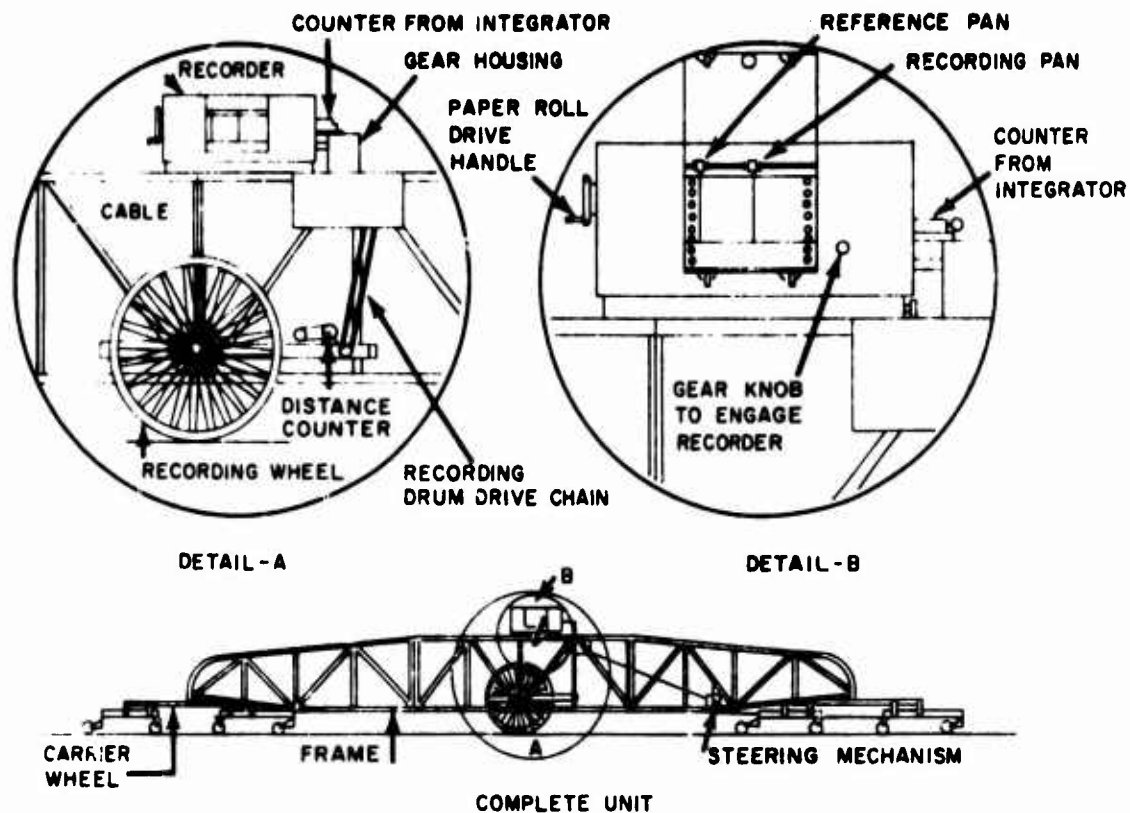


**Figure 25.** Lasar system tacking vehicle (note the light-sensing target at right end of vehicle mounted on road-following wheels . (From M. Womack, Private Communication, AFWL [1974].)



**Figure 26.** General view of AFWL lasar system profilometer. (From M. Womack, Private Communication, AFWL [1974].)



## PROFILOGRAPH

**Figure 27.** Rolling straightedge-type profilometer. (From W.J. Liddle et al., *Evaluation of Pavement Serviceability on Utah Highways*, Interim Report 1969 [Utah Highway Department, 1969].)

wavelengths longer than 25 ft (needed for runways or high-speed highways) cannot be obtained from the relative profile.

The RSF profilometers are used primarily for research studies and for checking the roughness of newly constructed pavement surfaces.

6. **British Road Research Laboratory Profilometer (RRL):** The RRL profilometer was originally developed at the Road Research Laboratory in Great Britain and has been used extensively by several Canadian agencies (Figure 28). This profilometer provides: (1) a continuous profile of the pavement surface (profile drum), (2) a roughness index in inches per distance (integrator), and (3) the number and size of surface irregularities, an increment of 0.1 in. from 0.1 to 1.5 in. (classifier).<sup>77</sup>

<sup>77</sup>R.W. Culley, *Roughness Index Standards for Saskatchewan Pavements*, Technical Report 1 (Saskatchewan Department of

The RRL profilometer is further described by Chong and Phang as follows:

The profilometer is basically a 16-wheeled articulated carriage that supports a detecting and recording device at a constant height above the main level of the road surface. The 16 wheels and their axles support four 4-wheeled bogies that cover a total width of 4 ft and provide a 21-foot long wheel base. The design of the unit is such that only  $\frac{1}{16}$  of the vertical movement of any single wheel is transmitted to the mounting of the detector wheels. The tires of the wheels are made of soft rubber and are inflated to a low pressure to ensure that very small irregularities in the road surface are not introduced into the measurement.

The detector assembly is located at the center of the chassis and consists of a detector wheel mounted centrally on a vertical detector shaft positioned in vertical guides. Two trailing (flanking) wheels, mounted on elbows and pivoted on the detector shaft, ensure that the detector wheel

Highways, 1966).



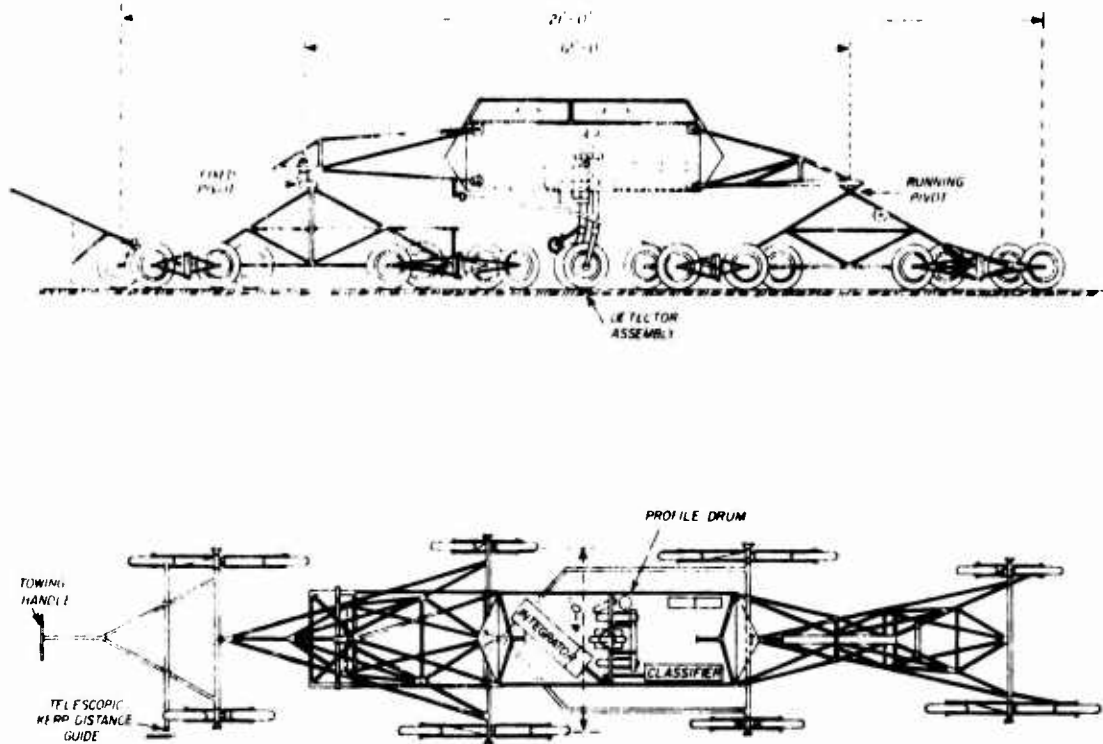


**Figure 28.** Ontario's RRL-type profilometer. (From G.J. Chong, *Measurement of Road Rideability in Ontario*, Report IR 29 [Department of Transportation and Communications of Ontario, 1969].)

"tracks" the line of travel properly. This results in a compensating forward movement of the profile pen, which keeps the plot of each vertical drop vertical.<sup>78</sup>

The device is towed by a small tractor at approximately 1 mph. The RRL profilograph gives good repeatability and could be used for long-term roughness measurements on special test sections, or for construction control.<sup>79</sup> However, it is not capable of measuring wavelengths longer than about 25 ft, which greatly limits its usefulness.

#### *Vehicle Axle/Body Displacement Measuring Equipment*

1. U.S. Bureau of Public Roads Roughometer (BPR): Several highway agencies have used the BPR roughometer over the past years. The basic device

commonly used today is shown in Figure 29 and described as follows:

The roughometer is a single-wheeled trailer having a recording wheel located centrally in a frame that represents the top of a suspension system; it is comprised of 2 standard leaf-springs and 2 standard hydraulic dashpot dampers. An integrator capable of moving in both directions (but which is arranged to integrate only in one direction) is coupled to an electric counter that is calibrated to record inches of vertical movement. The integrator that is fixed to the framework attached to the suspension system is connected to the axle of the recording wheel by a steel cable.

The recording system thus measures the inches of vertical movement of the axle relative to the top of the suspension system. A second counter records the revolutions of the recording wheel so that between the 2 counters the roughness of any length of road may be recorded.<sup>80</sup>

The BPR roughometer outputs a roughness index in inches/longitudinal distance and operates at a

<sup>78</sup>G.J. Chong and W.A. Phang, *PCA Road Meter Measuring Road Roughness at 50 mph*, Special Report No. 133 (Highway Research Board 1973), p 53.

<sup>79</sup>G.J. Chong, *Measurement of Road Rideability in Ontario*, Report IR 29 (Department of Transportation and Communications of Ontario, 1969).

<sup>80</sup>G.J. Chong and W.A. Phang, *PCA Road Meter Measuring Road Roughness at 50 mph*

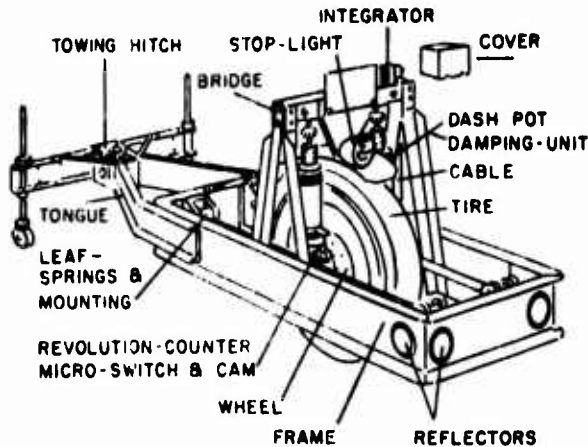


Figure 29. Bureau of Public Roads roughometer.

speed of 20 mph. Its most significant limitation is that the roughness index measured at 20 mph by a trailer device may not adequately represent the roughness experienced by an automobile traveling at much higher rates of speed. According to Hudson et al.,<sup>81</sup> the roughometer amplifies shorter wavelengths that cause automobile shake but attenuates the longer wavelengths, distorting the roughness characteristics. The 20 mph operating speed is also significantly below that of other roughometers mounted in actual automobiles.

**2. Portland Cement Association Roadometer (PCA):** The Portland Cement Roadometer was developed by M. P. Brokaw in 1965 and many agencies have since constructed versions of it.<sup>82,83</sup> A simple electromechanical device installed in a passenger automobile, it measures the number and magnitude of vertical displacements between the automobile body and the rear axle. Figure 30 is a schematic illustration of the device. Its measuring system is described by Phillips and Swift:

Its cable from the rear axle is attached to a switch or commutator so arranged that each successive  $\frac{1}{8}$ -in. departure from a preselected "zero" or midposition results in energizing a different contact of the switch. A series of electromagnetic counters registers the number of times

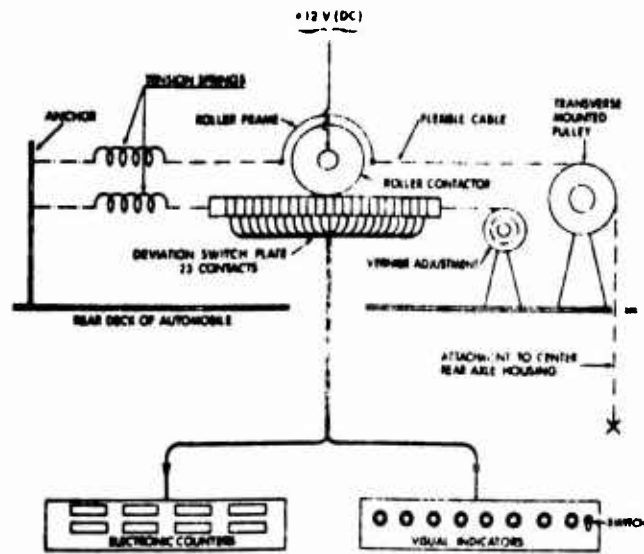


Figure 30. Schematic illustration of PCA roadometer.

that the moving arm encounters each particular contact. Thus, in the course of driving over a given section, contacts near the midposition will generally be reached frequently and those farther away will be seldom encountered, because there are ordinarily many small surface irregularities and only a few large ones. Accordingly, at the end of any traverse, the several counters indicate the number of times their respective contacts have been energized. The indication of surface roughness is obtained by multiplying the readings of the individual counters each by an appropriate constant, then summing the resulting numbers.<sup>84</sup>

Brokaw showed that this procedure in effect gives greater weight to the larger deviations in proportion to their magnitudes, and has a square law effect which renders the summed roughness count similar to a slope variance measurement, although the instrument does not actually measure slope variance. The summed PCA roadometer count (divided by 64 times the section length) provides a roughness index in square inches per mile of pavement traversed.<sup>85</sup>

Researchers have discovered several factors which significantly affect the PCA roughometer output:<sup>86,87</sup>

(1) Different automobiles usually do not provide the same numerical roughness count.

<sup>81</sup>W.R. Hudson, W.E. Teske, Karl H. Dunn, and E.B. Spangler, *State of the Art of Pavement Condition Evaluation*, Special Report 95 (Highway Research Board, 1968).

<sup>82</sup>M.P. Brokaw, *Development of an Automatic Electromechanical Null-Seeking Device for the PCA Road Meter*, Special Report 133 (Highway Research Board, 1973).

<sup>83</sup>H.L. Wagner and B.P. Shields, *Development of a Modified PCA Road Meter for Pavement Roughness Testing* (Research Council of Alberta, Highway Research Division, 1969).

<sup>84</sup>M.B. Phillips and G. Swift, *A Comparison of Four Roughness Measuring Systems*, HRR 291 (Highway Research Board, 1969).

<sup>85</sup>M.B. Phillips and G. Swift

<sup>86</sup>Patrick C. Hughes, *Evaluation of the PCA Road Meter*, Special Report 133 (Highway Research Board, 1973).

<sup>87</sup>G.H. Argue, *A Canadian Evaluation Study of Road Meters*, HRR Special Report 133 (Highway Research Board, 1973).

(2) The roughometer will correlate reasonably well with subjective panel evaluation if the panel is large.

(3) Roughness counts vary significantly with speed of the vehicle, load in automobile, low air temperatures ( $<15^{\circ}\text{F}$ ), wind velocity ( $>15$  mph), and mechanical condition of the test vehicle.

Perhaps the major limitation of the roadometer is that its roughness measurement will change with time because of test vehicle wear-out, thus it cannot be used as a standard to determine change in roughness with time, unless extensive calibration procedures are followed. These procedures include direct correlation with a rating panel or a non-changing profilograph device as described later. The major advantages of the PCA roadometer are its low cost, efficiency, and ease in obtaining data at high speed.

**3. Mays' Ride Meter (MRM):** The Mays' Ride Meter was initially developed by Ivan Mays to provide a simple method of obtaining roughness data. Various agencies have determined this device to be very useful and somewhat preferable to other roughometers.<sup>88,89,90</sup> Manufactured by the Rainhart Company of Austin, Texas,<sup>91</sup> the MRM is a simple electromechanical device mounted in a standard automobile.

The basic measuring technique is similar to the PCA and BRP equipment as described by Walker and Hudson:

Roughness measurements are proportional to the vertical changes between the vehicle body and its rear axle as the vehicle travels over a paved surface. These vertical motions are accumulated and are recorded on an advancing paper type or strip chart by a recording pen simultaneously moving at a rate proportional to the movements of the vehicle body and its differential. Vehicle distance traveled is also indicated on the roughness chart by an automatic event

marker connected to the speedometer drive system. By measuring the amount of chart moving per unit of road length traveled, a roughness measurement directly proportional to the total body-differential movement, in inches per mile can be obtained.<sup>92</sup>

A typical MRM measurement record is shown in Figure 31.

The MRM system has limitations similar to those described for the PCA device. Although it has been found to correlate well with panel ratings,<sup>93,94</sup> the roughness index values change with vehicle wear-out. The Texas Highway Department uses several MRM's in extensive data-gathering activities, but calibrates the devices with the SDP at regular intervals to avoid the problem associated with test vehicle wear-out.<sup>95,96</sup>

An excellent comparison between the BRP, PCA, MRM, and CHLOE roughness measurement devices was made by Phillips and Swift,<sup>97</sup> who developed information which is helpful in determining the various operational characteristics of these devices (see Table 2).

#### *Acceleration/Absorbed Power Measurement*

**1. Kentucky DOT Accelerometer:** The Kentucky Department of Transportation has used various instrumentation systems in the past, such as a tri-axial arrangement of accelerometers mounted on the chest of a passenger riding in a standard-size automobile.<sup>98</sup> Instrumentation has now been developed to automatically sum the vertical accelerations measured in the same position over a length of pavement. The automatic system is diagrammed in Figure 32.

<sup>88</sup>M.B. Phillips and G. Swift, *Comparison of Four Roughness Measuring Systems*, HRR 294 (Highway Research Board, 1969).

<sup>89</sup>Roger S. Walker and W. Ronald Hudson, *A Correlation Study of the Mays' Road Meter with the Surface Dynamics Profilometer*, Research Report 156-1 (Center for Highway Research, The University of Texas at Austin, 1973).

<sup>90</sup>S.M. Law and W.T. Burr III, *Road Roughness Correlation Study*, Research Report No. 48 (Louisiana Department of Highways, 1970).

<sup>91</sup>*Mays' Ride Meter Booklet* (Rainhart Co., 1972).

<sup>92</sup>Roger S. Walker and W. Ronald Hudson, *A Correlation Study of the Mays' Road Meter with the Surface Dynamics Profilometer*, Research Report 156-1 (Center for Highway Research, The University of Texas at Austin, 1973), p. 5.

<sup>93</sup>M.B. Phillips and G. Swift.

<sup>94</sup>R.S. Walker and W.R. Hudson, *Method for Measuring Serviceability Index with the Mays' Road Meter*, Special Report 133 (Highway Research Board, 1973).

<sup>95</sup>Roger S. Walker and W. Ronald Hudson, *A Correlation Study of the Mays' Road Meter*.

<sup>96</sup>R.S. Walker and W.R. Hudson, *Method for Measuring Serviceability Index*.

<sup>97</sup>M.B. Phillips and G. Swift.

<sup>98</sup>W.F. Lums, *Human Vibration Response Measurement*, Technical Report No. 11551 (U.S. Army Tank-Automotive Command, 1972).

**Table 2**  
**Comparison of Road Roughness Devices\***

Description	CHLOE Profilometer	BPR Roughometer	PCA Roadmeter	Mays Road Meter
1. Apparatus	Trailer and car	Trailer and car	Car only	Car only
2. Basic response	Slope	Height	Height	Height
3. Proportionality	Square-law	Linear	Square-law	Linear
4. Accepted designation of measurement	Slope-variance	Roughness	$2(D^2)$ , sum of road car deviations squared	Roughness index
5. Speed while measuring	3 to 5 mph	20 mph	40 or 50 mph	40 or 50 mph
6. Speed while traveling to and from sections	Legal limit	Legal limit	Legal limit	Legal limit
7. In-field set-up time	15 minutes	5 minutes	1 minute	None
8. In-field set-up requirements	Unload CHLOE from transport trailer, hook up cables, calibrate	Lower wheel, hook up roughness integrator and counters	Stop vehicle to set to zero	None
9. Maximum section length	Less than 0.5 mile	Limited only by roughness exceeding counter capacity	Limited only by roughness exceeding counter capacity	Unlimited
10. Minimum section length	Not recommended for less than 0.1 mile	Not recommended for less than 0.1 mile	Not recommended for less than 0.1 mile	Not recommended for less than 0.1 mile
11. Data presentation form	Number of 6-in. units traversed, counts and counts squared	Single numerical counter	Plurality of numerical counters	Length of chart record
12. Location of presentation	Adjacent to driver	Adjacent to driver	Adjacent to driver	Adjacent to driver or in trunk
13. Determination of section length	Counter	Counter	Car odometer or roadside marker	Car odometer or roadside marker
14. In-field data requirements (when measuring sections of known lengths)	Record three readings	One reading at end of each section	Eight counter readings at end of each section and reset counters	Merely keep track of the sequence in which the sections are traversed
15. In-field adjustments	None required	Frequent check of dash pot fluid level	Frequent zero adjustment recommended—requires vehicle halt	None required
16. At-home data processing to determine roughness	Calculating $\sqrt{SV}$ from three readings	Tabulating (may be done in-field)	Summing and tabulating	Measuring chart lengths and tabulating
17. Additional data obtainable from record	None	None	Frequency distribution of roughness heights	Approximate location and heights of roughness within sections
18. Maintenance requirements	Frequent malfunction requiring repairs	Frequent servicing of grease fittings and dash pots	Frequent polishing of commutator to ensure contact	Minimal

\*M.B. Phillips and G. Swift, *A Comparison of Four Roughness Measuring Systems*, HRR 291 (Highway Research Board, 1969).

and the complete system is described by Rizenbergs et al.<sup>99</sup>

Many parameters—such as the test vehicle dynamic characteristics, test passenger weight, vehicle load, and vehicle speed—affect the accelera-

tion readings. Although some of these parameters have been standardized, the accelerometer procedure has some of the limitations of the PCA and MRM roadmeters. To accurately measure pavement roughness changes over several years, Kentucky has attempted to correlate each new vehicle with the existing vehicle and also to use reference surfaces for day-to-day calibration.

2. Absorbed Power Meter: The power that a person absorbs (or the rate of flow of energy into a

<sup>99</sup>R.L. Rizenbergs et al., *Pavement Roughness: Measurement and Evaluation*, HRR 471 (Highway Research Board, 1973), pp 46-61.

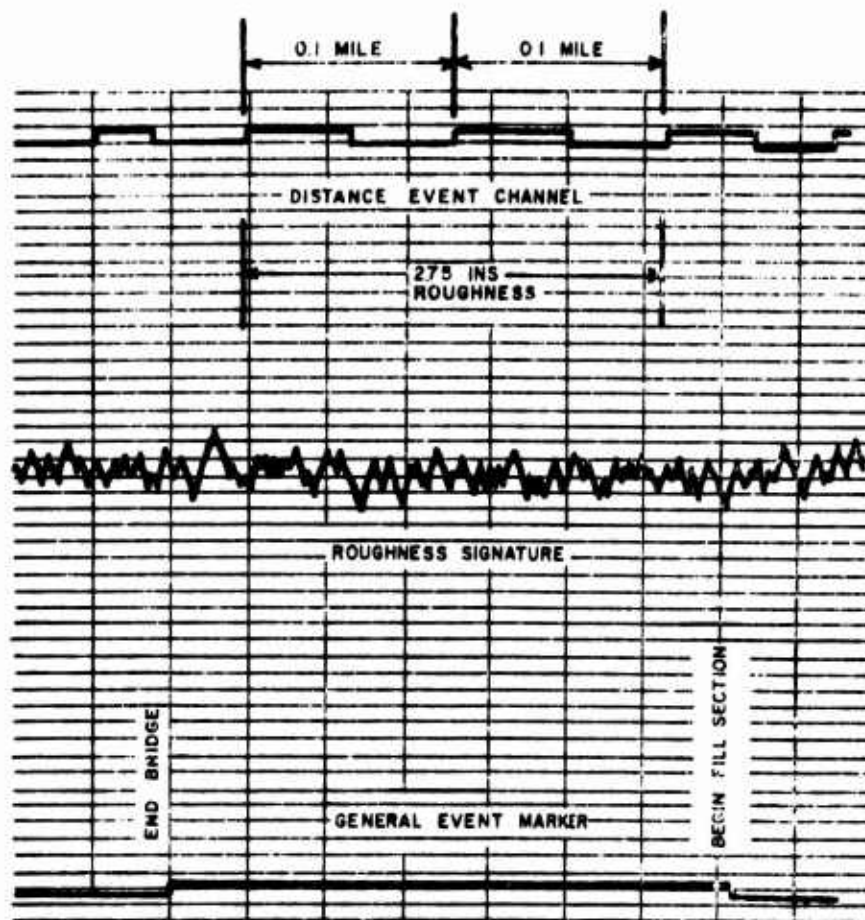


Figure 31. Typical Rainhart MRM measurement record.

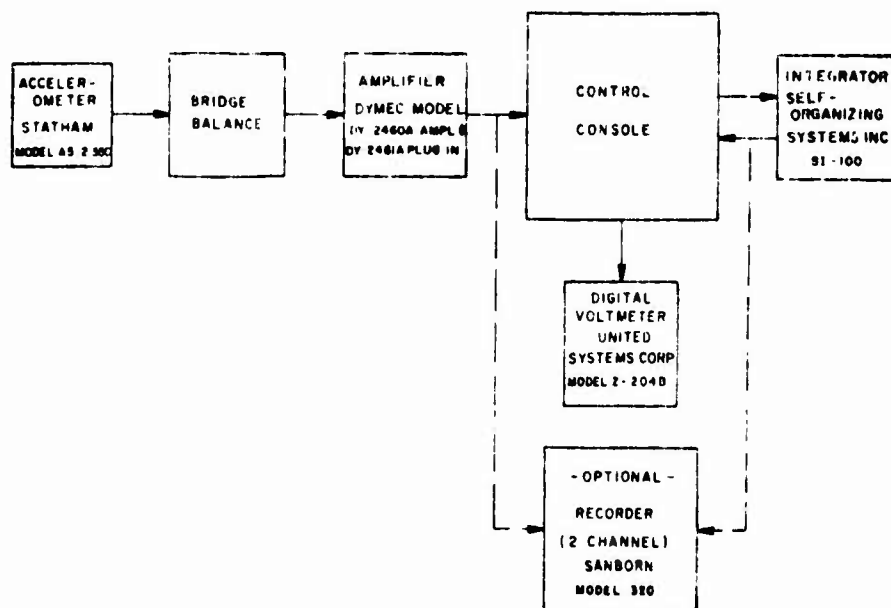


Figure 32. Kentucky DOT automatic acceleration measuring system. (From R.L. Rizenbergs et al., *Pavement Roughness: Measurement and Evaluation*, HRR 471 [Highway Research Board, 1973], pp 46-61.)

person) when subjected to vibrations in an automobile or aircraft can be determined by one of two methods: (1) direct measurement of the absorbed power with an absorbed power meter, or (2) calculation of absorbed power from acceleration/frequency information.

The FACOM Absorbed Power Meter is a portable electronic instrument consisting of the meter, which contains the electronics and input/output connections, a power supply, and an accelerometer which can be placed beneath the test passenger or in any position desired. Lins describes this instrument in detail.<sup>100</sup> Other absorbed power meters, developed by Switzer of WES,<sup>101</sup> include the ability to measure absorbed power from three axes. WES is currently studying the usage and measurement of absorbed power.

The method of computing absorbed power from acceleration/frequency records for a pavement profile is also described by Lins. Agreement between the two methods is excellent according to Switzer.

#### *Slope Variance Measurement*

Slope variance can be determined from actual profile elevation data, or measured directly with the CHLOE profilometer. This profilometer was developed by the AASHO Road Test staff to enable slope variance to be obtained more easily than was possible with the AASHO longitudinal profilometer.<sup>102</sup> Profile slope is measured by the change in angle between two reference lines. Two road-following wheels about 9 in. apart form one reference line. The other line is determined by a 20-ft long member supported by a trailer hitch on the back of a towing vehicle and a wheel which supports the rear end of the member.<sup>103</sup> Slope variance is determined from the measured slopes along a specific pavement section.

<sup>100</sup>W. F. Lins, *Human Vibration Response Measurement*, Technical Report No. 11751 (U. S. Army Tank—Automotive Command, 1972).

<sup>101</sup>G. Switzer, Private Communication, WES (1974).

<sup>102</sup>*The AASHO Road Test Report 5—Pavement Research*, Special Report 111 (Highway Research Board, 1962).

<sup>103</sup>W. R. Hudson, W. E. Teske, Karl H. Dunn, and E. B. Spangler, *State of the Art of Pavement Condition Evaluation*, Special Report 95 (Highway Research Board, 1968).

The CHLOE profilometer has good repeatability and correlates fairly well with subjective panel ratings.<sup>104</sup> However, the device has serious limitations: it will not measure wavelengths longer than the space between the two road-following wheels; its test speed is only 3-5 mph; it requires frequent repairs; and it is sensitive to surface texture, requiring adjustments of serviceability equations when pavements with large surface textures are encountered.<sup>105</sup> Table 2 compares the operational characteristics of the CHLOE profilograph and three other devices.

#### **Roughness Summary**

Several indicators are available to characterize pavement roughness: roughness index, slope variance, profile wavelength amplitude characteristics, acceleration, absorbed power, and human subjective evaluation have been defined here.

Several types of equipment and methods are available to measure these indicators. The question which must be answered is which roughness indicators and equipment systems provide the most useful information for a specific purpose.

There are several important reasons for characterizing roughness of a pavement:

1. To control initial pavement smoothness during construction.
2. To gather historical pavement roughness data for use in verifying or developing design procedures or developing pavement deterioration models.
3. To determine priority rehabilitation and maintenance needs relative to pavement roughness, for inventory purposes.
4. To determine if the limiting functional roughness condition of a pavement has been reached and locate areas of excessive roughness for possible repair.

<sup>104</sup>M. B. Phillips and G. Swift, *A Comparison of Four Roughness Measuring Systems*, HRR 291 (Highway Research Board, 1969).

<sup>105</sup>F. H. Scrivner, *A Modification of the AASHO Road Test Serviceability Index Formula*, Technical Report No. 1 (Texas Transportation Institute, 1963).

The type of pavement being considered is also important in determining the appropriate roughness indicator and measurement equipment. A highway pavement might be a local road or street with relatively low speeds, or a primary highway with relatively high speeds. An airfield pavement might be a runway where very high speeds must be considered, or a taxiway with lower speeds. The selection of specific roughness indicators should therefore consider (1) the purpose of the measurement, (2) the function and type of pavement, and (3) availability of funds and the cost of the equipment system. Although it is beyond the scope of this report to make detailed recommendations for each of these conditions, Tables 3 and 4 summarize tentative recommendations for various pavement types and measurement objectives.

Table 3

Tentative Recommendations for Use of Roughness Indicators

Roughness Indicator	Objective of Measurement		
	Construction Control	Long-Term Monitoring of Pavement	Inventory and Maintenance Needs
1. Roughness Index	*Q NA	Q/NA	A/NA
2. Slope Variance	NA NA	Q NA	Q/NA
3. Wavelength Amplitude	A A	A A	A/A
4. Acceleration	Q Q	A A	A A
5. Absorbed Power	Q Q	A/A**	A/A**
6. Subjective Evaluation	NA NA	Q Q	A/Q

#### Rating Symbols

A—Acceptable

Q—Questionable

NA—Not Acceptable

\*Highways Airfields

\*\*Has not yet been completely developed, but appears promising.

## 4 SKID RESISTANCE EVALUATION AND MEASUREMENT STATE OF THE ART

### Introduction

Skid resistance is the force that resists the sliding of tires on a pavement when they are prevented from rotating. This force depends on many variables such as:

1. Pavement surface texture condition

2. Tire tread (pattern and amount of wear)
3. Speed at which sliding occurs
4. Water depth on surface
5. Tire inflation pressure
6. Load
7. Temperature

Dynamic hydroplaning is a phenomenon that occurs with high water depth and/or speed on the pavement. Although water depth is the most significant variable, the speed at which hydroplaning occurs for a given water depth is dependent on the rest of the variables mentioned above.

Viscous hydroplaning occurs when the surface is contaminated with a thin film of water, oil, or other slippery material. This phenomenon does not depend on the water depth and can be minimized by keeping the surface clean.

The problem of skidding is becoming increasingly important on runways, because of the improved performance and higher landing speeds of aircraft. Figure 33 shows the annual increase in accidents due to hydroplaning experienced by the U.S. Air Force.

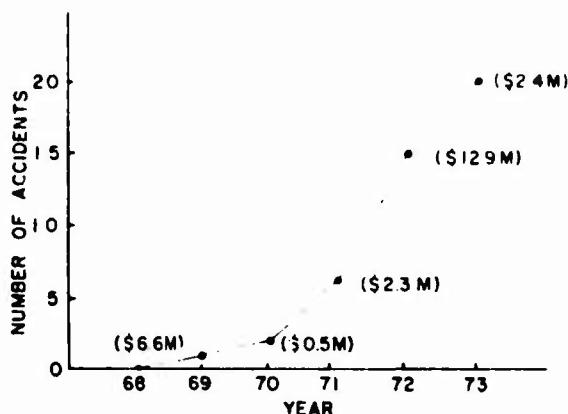


Figure 33. Reported U.S.A.F. hydroplaning accidents (by permission of U.S.A.F.).

Although pavement surface condition is only one of the variables that contribute to skidding, it is significant and should be maintained at acceptable levels. In a study of skidding resistance of wet runway surfaces, Lander et al. conclude the following:

A study of the effects of surface texture, load, inflation pressure and tire wear of aircraft tires under wet conditions has shown that it is the surface texture of the runway which

**Table 4**  
**Tentative Recommendations of Roughness Indicators and Equipment for Determining Maintenance Needs**

Roughness Indicator	Equipment	Highways		Airfields	
		Local Roads & Streets	Primary Highway	Runways	Taxiways
1. Roughness Index	BPR	P	P	NA	NA
	PCA	HA	HA	NA	NA
	MRM	HA	HA	NA	NA
	SDP	P	P	P	P
	LEVEL	NA	NA	P	P
	RSE	P	P	NA	NA
	RRL	P	P	P	P
2. Slope Variance	CHLOF	P	P	NA	NA
	PROFILE	P	P	NA	NA
3. Wavelength Amplitude	SDP	P	HA	A	A
	AIP	P	A	HA	HA
	LASAR	P	P	A	A
	LEVEL	P	P	A	P
4. Acceleration	KAC	A	A	NA	NA
	ACC	A	A	A	A
5. Absorbed Power	APM	Q*	Q*	Q*	Q*
6. Subjective	PANEL	A	A	Q	Q

*Rating Symbols*

HA = Highly acceptable usage

A = Acceptable usage

P = Possible but not desirable usage (high cost is generally the reason)

Q = Questionable usage

NA = Not acceptable usage

*Equipment Code*

BPR = Bureau of Public Roads Roughometer

PCA = Portland Cement Association Roughometer

MRM = Mays' Ride Meter

SDP = Surface Dynamics Profilometer (Texas)

LEVEL = Precise Level

RSE = Rolling Straightedge Profilograph

RRL = Road Research Laboratory Profilograph

CHLOF = Slope Variance Profilograph

PROFILE = Slope Variance Calculated From Profile

AIP = AFWL Inertial Profilometer

LASAR = AFWL Lasar Profilometer

KAC = Kentucky Accelerometer Equipment

APM = Absorbed Power Meter

ACC = Accelerometers

PANEL = Rating Panel

\*Has not yet been completely developed, but appears promising.



is one of the main factors that influences braking performance. It also determines the degree of influence of other factors such as water depth and tread pattern on braking performance.<sup>106</sup>

A crucial question for the pavement engineer is the skid level at which the surface should be maintained to provide a safe skid resistance. In order to develop a relationship between surface condition and skid resistance, it is necessary to standardize the other variables. The next sections deal with methods for measuring skid resistance of pavements, the effect of some of the variables on skid resistance, and the correlations between various skid-resistance measuring methods.

### Methods for Measuring Skid Resistance

Friction is a force which always opposes motion. The coefficient of friction is defined as the ratio between the frictional force in the plane of interface and the force normal to the plane. In the field of pavements, the coefficient of friction is referred to as the "friction factor,"  $f = F/L$ , where  $F$  is the frictional force and  $L$  is the normal load. The friction factor depends on many variables other than the pavement itself—such as tire pressure, thickness of water film, speed, etc. To determine a friction value associated with the pavement surface, it is necessary to standardize these variables.

Before any of the methods of measuring skid resistance are described, it is important to understand the two basic characteristics of the pavement surface which influence its frictional capabilities: texture and drainage. *Surface texture* can be defined in terms of microtexture and macrotexture. A microtexture is what makes an aggregate smooth or rough to the touch. Its contribution to friction is through adhesion with the tire. The macrotexture is the result of the shape, size, and arrangement of the aggregates (for flexible pavements), or the surface finish (for concrete surfaces). Macrotexture's contribution to skid resistance is through developed hysteresis due to the tire deformation; the hysteresis reflects a loss in the moving vehicle kinetic energy and thus helps the vehicle to stop. Figure 34 is a schematic diagram

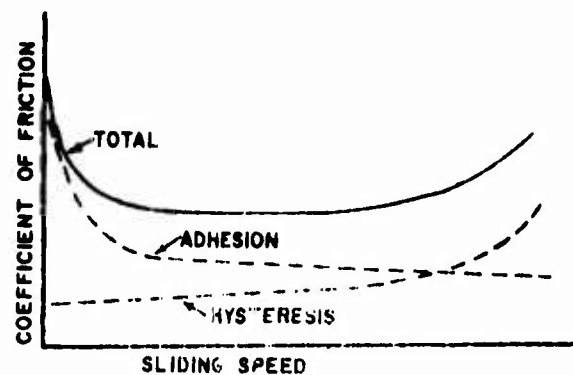


**Figure 34.** Generalized representation of coefficient of friction between a steel sphere and rubber as a function of sliding speed. (From *Skid Resistance*, NCHRP Synthesis of Highway Practice No. 14 [1972].)

of the contribution of microtexture and macrotexture to the friction factor. At low speed friction is due mainly to adhesion (microtexture). At high speed, the contribution of hysteresis becomes more significant. A pavement that is covered with a thin film of lubricant would provide only hysteresis.

Drainage is another significant characteristic of the pavement surface. On dry pavements the available skid resistance is usually sufficient to meet any requirement. On wet pavements, a good drainage system provides channels for the water to escape, allowing contact between the tire and the pavement. The effectiveness of a drainage system can be evaluated by applying water to the pavement and measuring the friction factor immediately after the application and at intervals afterward to study the increase in friction.

There are several methods for measuring the friction factor of a pavement.

#### *Trailer Methods*

1. **Locked-Wheel Mode:** Trailers with one or two wheels are towed at a given speed. The test wheel is then locked and water is applied in front of it. After the test wheel has been sliding on the pavement for a certain distance to stabilize the temperature, the friction force in the tire contact patch is recorded for a specified period of time. The results are reported as Skid Number (SN) where:

$$SN = 100 \times \text{friction factor.}$$

<sup>106</sup>F. I. W. Lander and I. Williams, *The Skidding Resistance of Wet Runway Surfaces with Reference to Surface Texture and Tread Conditions*, Road Research Laboratory, RRL Report LR 184 (Ministry of Transport, England, 1968).



**Figure 35.** Typical road friction testers. (From *Skid Resistance*, NCHRP Synthesis of Highway Practice No. 14 [1972].)

In order to minimize the variability of the results, a standard tire specified in ASTM Method E274 is used. Figure 35 is a photograph of typical locked-wheel skid trailers.

2. Slip Mode: Slip is defined as

$$S = 100 \frac{W_0 - W}{W_0}$$

where  $W_0$  = angular wheel speed at free rolling  
 $W$  = angular wheel speed at the time of measurement.

If the brake is applied on a straight-moving wheel, the slip increases until it reaches 100 percent when the wheel is locked. The friction factor increases with increasing slip until it reaches a maximum value,  $f_{\max}$ , at the "critical slip," and starts to decrease until the wheels are locked (Figure 36). The critical slip and the ratio  $f_{\max}/f_{\text{lock}}$  are functions of the surface texture and temperature;<sup>107</sup> therefore they can be obtained only by appropriate measurement. Figure 37 shows the effect of surface texture on the ratio  $f_{\max}/f_{\text{lock}}$ .

The critical slip phenomenon is very important since it indicates that the maximum friction does not occur when the wheels are locked, but rather in the range of 10 to 15 percent slip. This has brought about the automatic brake control systems which are used on most aircraft.

<sup>107</sup>*Skid Resistance*, NCHRP Synthesis of Highway Practice No. 14 (1972).

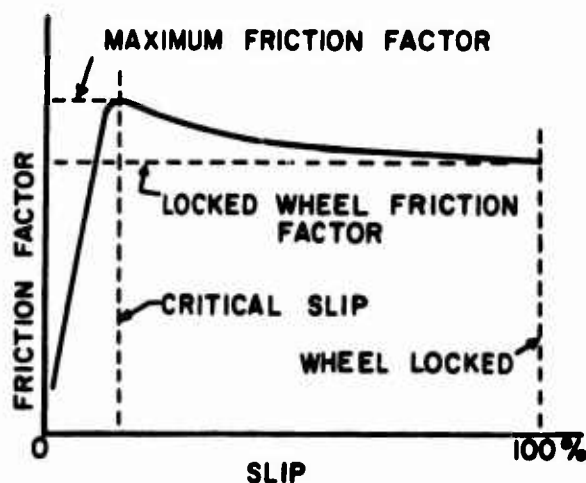


**Figure 36.** Friction factor as function of slip (wheel moving in direction of wheel plane while being braked). (From *Skid Resistance*, NCHRP Synthesis of Highway Practice No. 14 [1972].)

More than one type of equipment is available for measuring skid resistance in the slip mode. Figure 38 is a photograph of the equipment used by the Federal Aviation Administration, which features an adjustable slip so that the friction test can be performed at the critical slip for a given surface.

3. Yaw Mode: The yaw mode is a method of measuring the sideways friction factor by turning the test wheel (unbraked) to an angle with the direction of motion (yaw angle). Since the sideways friction factor varies with the magnitude of the yaw angle as shown in Figure 39, it is desirable to perform the testing at a yaw angle at which the friction factor

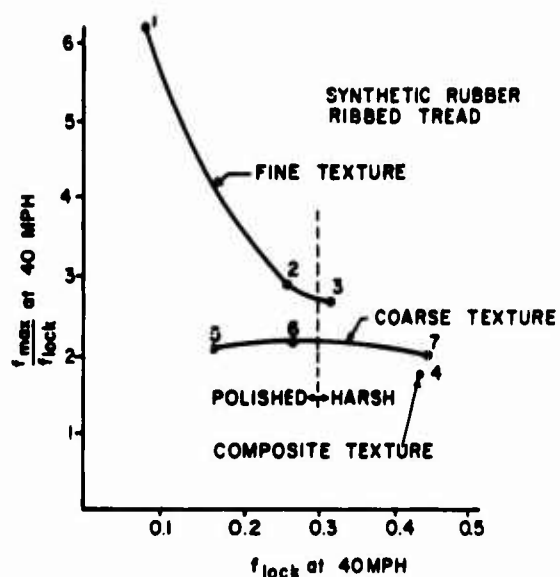


**Figure 37.** Ratio of maximum and locked-wheel friction factors at 40 mph on various wet surfaces. (From *Skid Resistance*, NCHRP Synthesis of Highway Practice No. 14 [1972].)

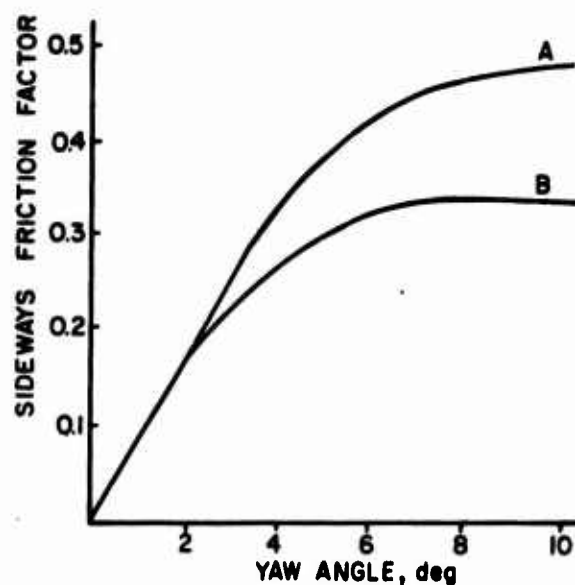


**Figure 39.** Typical sideways friction factor vs yaw angle relationships for two wet pavements (A and B). (From *Skid Resistance*, NCHRP Synthesis of Highway Practice No. 14 [1972].)



**Figure 38.** Runway friction tester with adjustable slip. (From *Skid Resistance*, NCHRP Synthesis of Highway Practice No. 14 [1972].)

becomes insensitive to small changes. A commercially available trailer for that purpose is the Mu-Meter, which was developed in England and uses two smooth tires yawed at equal and opposite angles ( $7\frac{1}{2}$  degrees) (Figure 40a). The U.S. Air Force is currently using it to make measurements at 40 mph (Figure 40b).

A more sophisticated machine for measuring side-way friction is the SCRIM (Sideways-Force Coefficient Routine Investigation Machine), which was developed by Britain's Transport and Road Research Laboratory and manufactured under license by W.D.M., Ltd<sup>108</sup> (Figure 41). The vehicle carries the necessary water supply, which is spread in advance of the test wheel. The test wheel is mounted 20 degrees to the direction of motion of the vehicle (Figure 41b), and can be lifted clear of the road when not in use. The machine measures the sideways-force coefficient (SFC), which is expressed as follows:

$$\text{SFC} = \frac{\text{sideway force}}{\text{vertical reaction between tire and road surface}}$$

SCRIM has the capability of continuous recording and allows for high operating speeds (more than 40 mph).

<sup>108</sup>W.D.M. Limited, *SCRIM, Information Brochure* (Western Works, Staple Hill, Bristol BS16, 4NX, Great Britain, 1972).

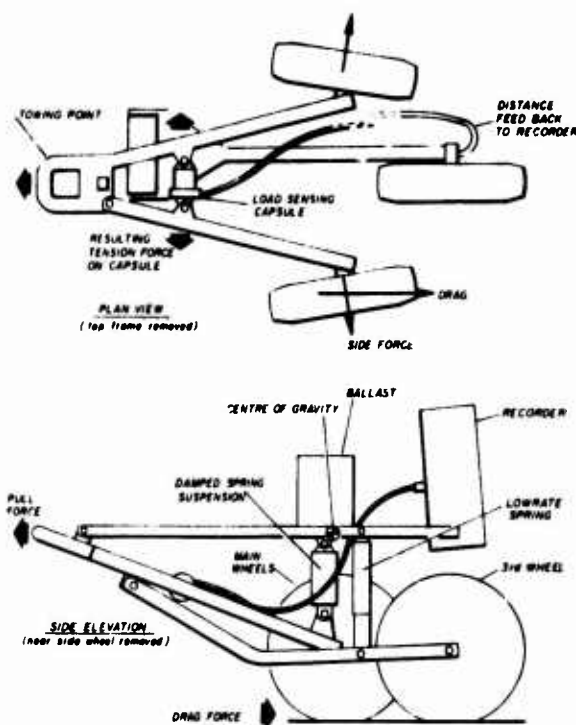
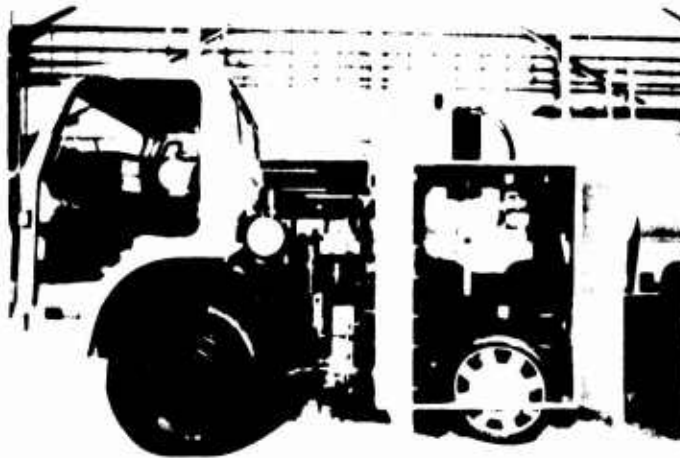


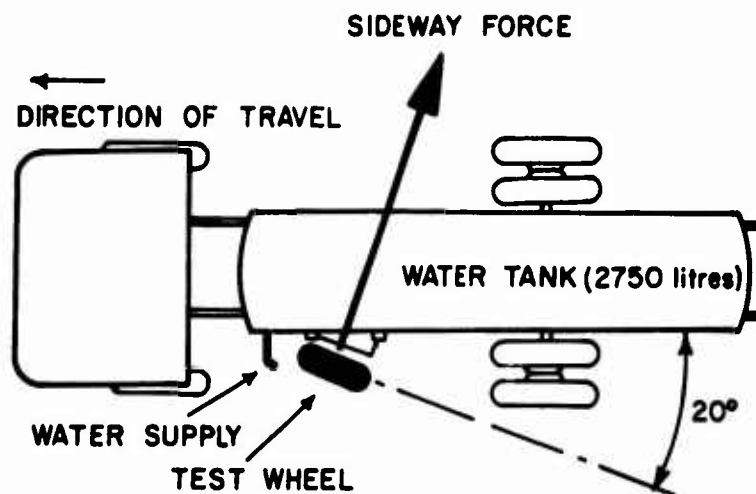
**Figure 40a.** Diagrammatic layout of Mu-Meter. (From *Measurement of Runway Friction Characteristics on Wet, Icy, or Snow-Covered Runways*, Report No. FS-160-65-68-1 Federal Aviation Administration [Department of Transportation, 1971].)



**Figure 40b.** Mu-Meter used by U.S.A.F.



(a)



(b)

**Figure 41.** Sideways-Force Coefficient Routine Investigation Machine. (From W.D.M. Limited, *SCRIM, Information Brochure* [Western Works, Staple Hill, Bristol BS16, 4NX, Great Britain, 1972].)

### Automobile Methods

One of the problems with using automobiles for skid measurements is the possibility of accidents during testing. Since the braking of all four wheels increases likelihood of a spin-out, it is best to brake only the front wheels or a diagonal pair of wheels. Figure 42 shows the braking system for the Diagonal-Braked Test Vehicle (DBV) developed by NASA. Figure 43 is a photograph of the DBV used by the U.S. Air Force. Its diagonally braked wheels are equipped with ASTM bald-tread tires (ASTM-E249) and the unbraked wheels are equipped with conventional tires. The skid resistance indicator used with this vehicle is the ratio between wet and dry stopping distance when the diagonal wheels are braked at 60 mph.

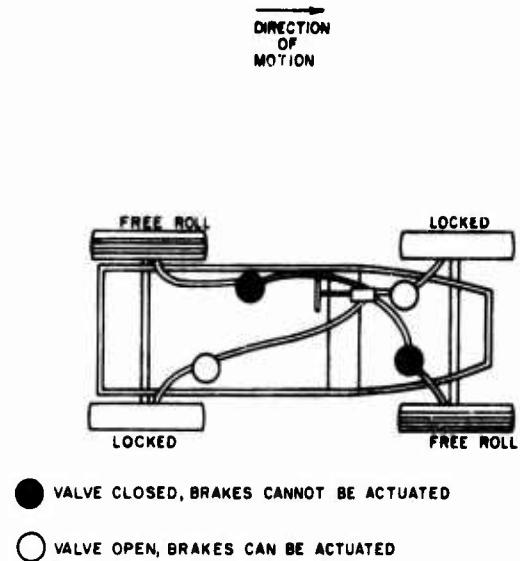


**Figure 42.** Braking system for NASA diagonal-braked test vehicle.



**Figure 43.** Diagonally braked vehicle (DBV) used by U.S.A.F.

Another automobile method, which was used by the Air Force on snow- or ice-covered pavements, is the Runway Condition Reading (RCR). RCR numbers are obtained by making maximum braking measurements on the runway at 20 to 30 mph, with an airport ground vehicle employing a James brake decelerometer.<sup>109</sup>

There are several other testing methods which use vehicles, one of which is ASTM Method E445-71T.

#### *Portable Field and Laboratory Methods*

Portable field machines can be moved easily to different locations. One of the available devices is the Keystone Tester developed by Pennsylvania State University, which employs a rubber shoe that slides along the pavement as the operator "walks" the tester (Figure 44).

Another example of a portable field tester is the California Skid Tester (Figure 45), which operates on the principle of "spinning up a rubber-tired wheel while it is off the ground, lowering it to the pavement, and noting the distance it travels against the resistance of a spring before it stops."<sup>110</sup> The towing vehicle is stationary during the test and glycerine, rather than water, is the pavement lubricant.

Although there are numerous devices for measuring friction in the laboratory, their applicability for measuring runway skid resistance is rather limited. One of the most common laboratory devices is the British Portable Tester developed by the British Road Research Laboratory (Figure 46). It consists of a rubber shoe attached to a pendulum, which slides over a sample of the surface under study. The method of testing is described under ASTM Method E303. The results are reported as British Pendulum Numbers (BPN).

#### *Texture Identification Methods*

There are several methods available for measuring the texture of a pavement surface,<sup>111</sup> but no success-

ful correlation has been developed between any of these individual measurements and skid resistance. However, Schonfeld, using stereophotographic techniques, developed a texture code which he showed to be correlated with skid resistance measured by the ASTM skid trailer.<sup>112</sup> To do this, he obtained color stereophotographs of approximately 6×6 in. sections of the pavement surface and identified seven texture features: the height, width, angularity, density and fine texture of the projections; and the fine texture and percent of cavities of the background (Figure 47). He then assigned a scale and weighting function to each feature in order to correlate the results with measured skid resistance.

#### **Effect of Individual Variables on Skid Resistance**

As mentioned earlier, skid resistance evaluation is complicated by the many variables that contribute to the friction value. The proper way to determine the relative significance and possible interactions of each variable is through a factorial experiment. However there is at present no one experiment that includes all the variables. The following sections summarize studies on the effects on skid resistance of traffic and seasonal variations, vehicle factors (speed, tire pressure, wheel load, and tire tread), and pavement factors (surface characteristics and drainage).

#### *Traffic and Seasonal Variations*

Two pavement sections built at the same time may have different friction coefficients because they have been subjected to different traffic. As the traffic rolls over the pavement, polishing of the surface microtexture takes place. Wear, dislocation, and/or reorientation of aggregates may also occur—especially under heavy traffic. In general, skid resistance deteriorates with increasing traffic until it reaches a level of equilibrium. There is no one specific value at which it levels off. Due to seasonal variations of skid resistance (see Figure 48) there can be only a mean equilibrium value, which is a function of traffic and surface characteristics. Figure 49 illustrates the effect of traffic on skid resistance, showing the side-way friction factor for six different locations. Although all six pavement sections had the same type of surface course and were installed at the same

<sup>109</sup>A Comparison of Aircraft and Ground Vehicle Stopping Performance on Dry, Wet, Flooded, Slush, Snow, and Ice Covered Runways, NASA Technical Note D-6098 (1970).

<sup>110</sup>Skid Resistance, NCHRP Synthesis of Highway Practice No. 14 (1972)

<sup>111</sup>Skid Resistance

<sup>112</sup>R. Schonfeld, *Photo Interpretation of Skid Resistance*, HRR 311 (Highway Research Board, 1970).

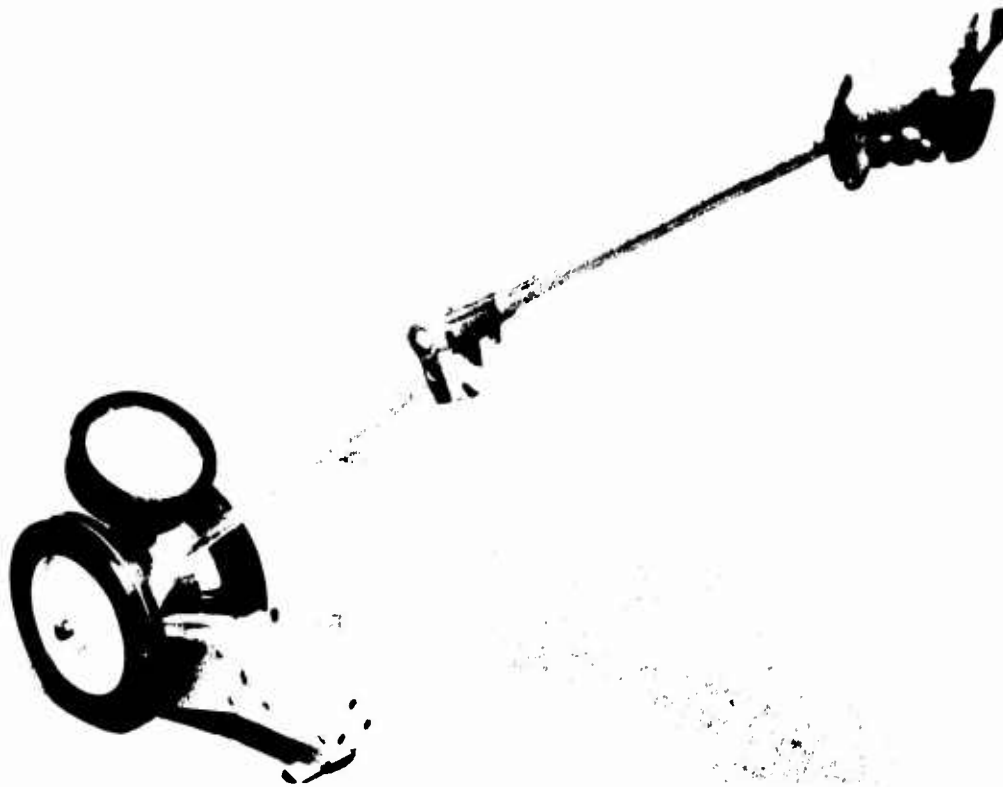


**Figure 44.** Keystone MARK IV skid resistance tester. (From *Skid Resistance*, NCHRP Synthesis of Highway Practice No. 14 [1972].)

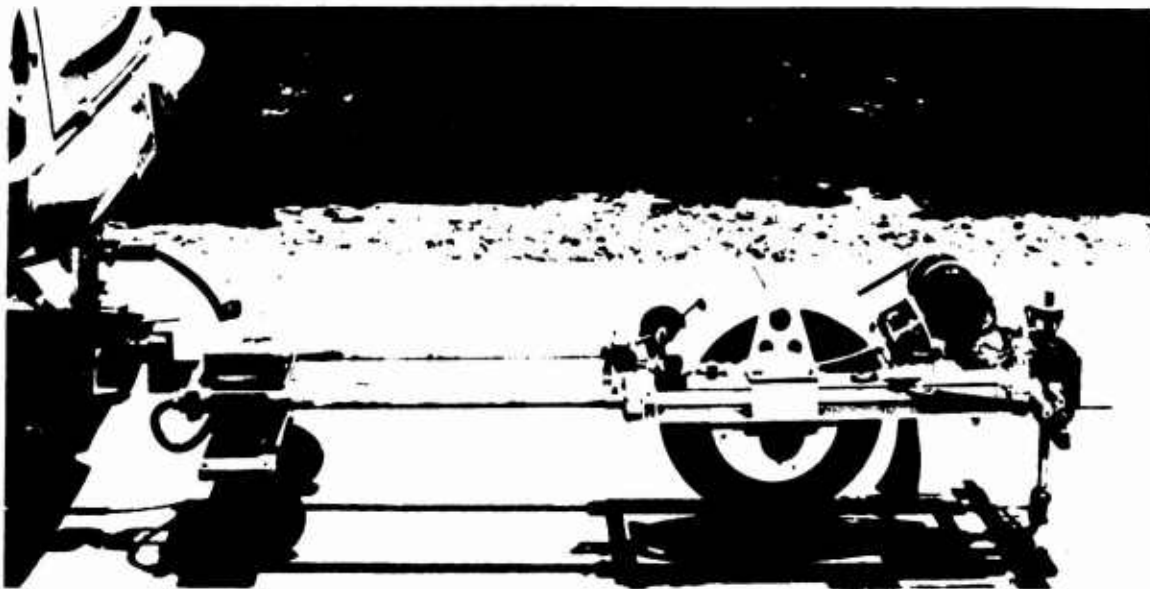


**Figure 45.** California Portable Skid Tester. (From *Skid Resistance*, NCHRP Synthesis of Highway Practice No. 14 [1972].)



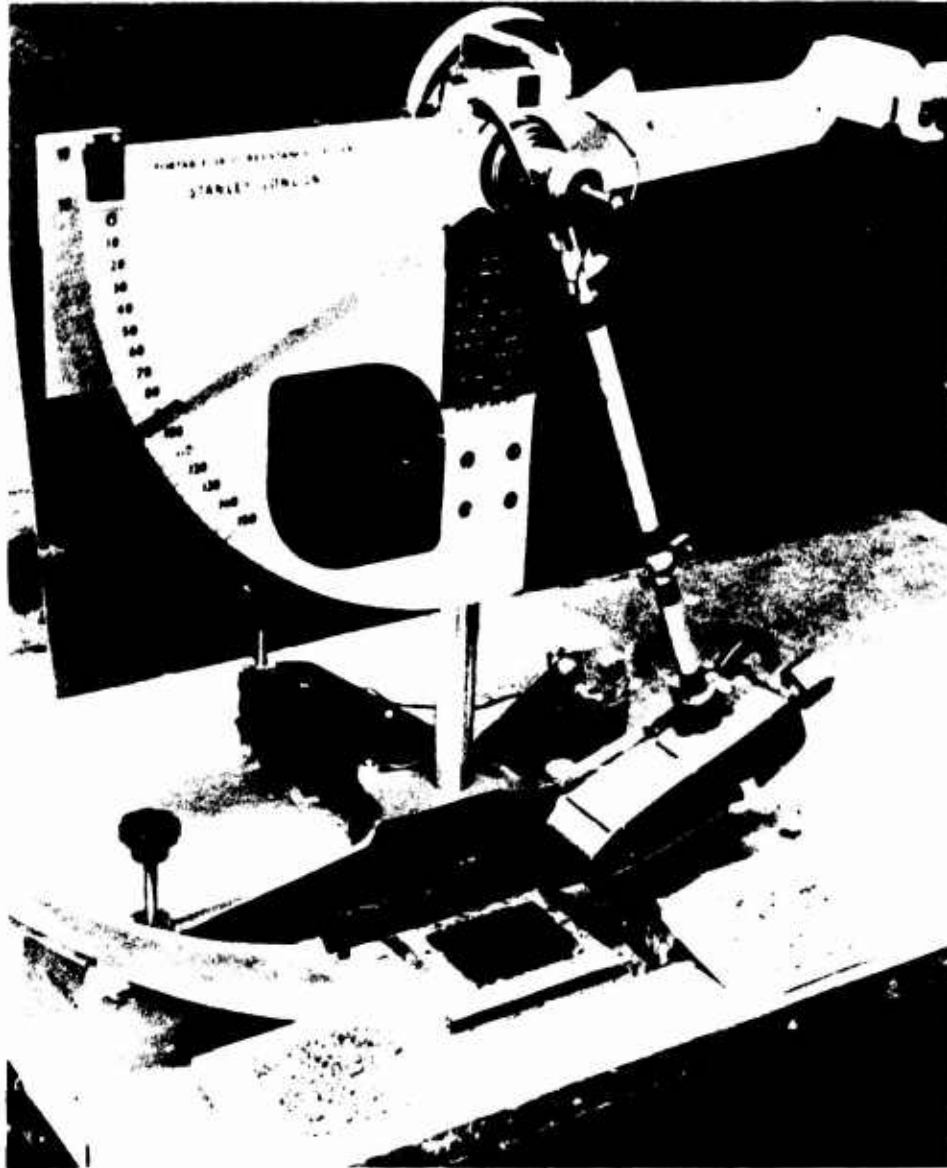


**Figure 46.** British Road Research Laboratory's pendulum friction tester (British Portable Tester). (From *Skid Resistance*, NCHRP Synthesis of Highway Practice No. 14 [1972].)



**Figure 47.** Components of surface texture as identified by Schonfeld. (From R. Schonfeld, *Photo Interpretation of Skid Resistance*, HRR 311 [Highway Research Board, 1970].)

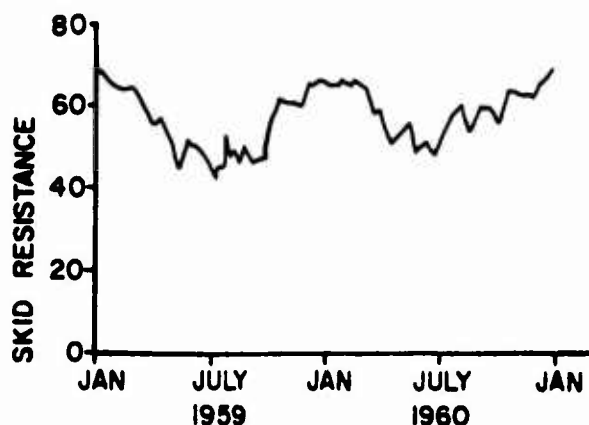


**Figure 48.** Seasonal change of skid resistance. (After *Skid Resistance*, NCHRP Synthesis of Highway Practice No. 14 [1972].)

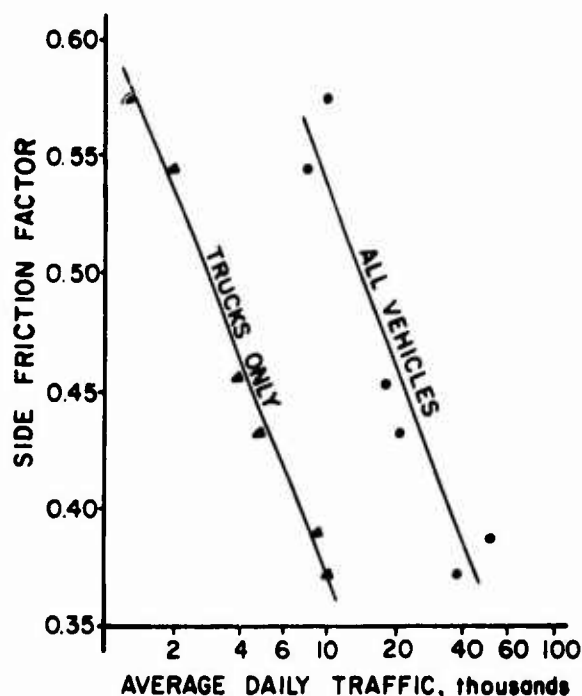


**Figure 49.** Deterioration of skid resistance with exposure to traffic. (After *Skid Resistance*, NCHRP Synthesis of Highway Practice No. 14 [1972].)

time, they were subjected to different traffic volumes. The daily traffic shown for each location is the average over a 3-year period. It is reported from the study<sup>113</sup> that the skid resistance had stabilized at all locations after 2 years. The figure indicates there is a better correlation with the number of trucks (heavy traffic) than with the total number of vehicles. Figure 50, from a different study reported in the same reference, illustrates the fact that skid resist-

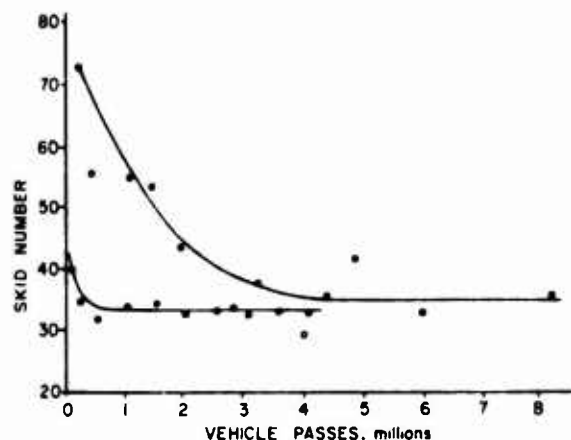


**Figure 50.** Loss of skid resistance of two pavements as a function of traffic exposure. (From *Skid Resistance*, NCHRP Synthesis of Highway Practice No. 14 [1972].)

ance reaches a mean equilibrium value after many applications of traffic.

#### Vehicle Factors

1. Speed: In general, the friction coefficient decreases with increase in speed. It has been found that on dry pavement surfaces, the friction factor changes very little with change in speed; however, on wet surfaces the decrease is significant.<sup>114</sup> In the

<sup>113</sup>*Skid Resistance*, NCHRP Synthesis of Highway Practice No. 14 (1972).

<sup>114</sup>M. Tomita, *Friction Coefficients Between Tires and Pavement Surfaces*, Technical Report R303 (U.S. Naval Civil Engineering Laboratory, 1964).

same reference, it was reported that studies in 1960 by the Ministry of Aviation, using an instrumented aircraft, "showed that the friction coefficients on wet concrete pavement decreased rapidly with increasing speed from zero to about 50 or 60 knots (57.5 to 69 mph). However, at speeds above 80 to 100 knots (92 to 115 mph), the friction coefficients tended to increase slightly with increase in speed."<sup>115</sup> The slight increase in the friction coefficients at high speed was attributed to the creation of wing lift, which caused differences in the vertical loads and tire pressures in the measuring technique employed. Figures 51 and 52 show the change in friction with speed for concrete and asphalt pavements under dry and wet conditions. As mentioned earlier, on dry surfaces the friction factor changes only slightly with speed. However, this may not be the case for asphalt surfaces if bleeding occurs (Figure 53).<sup>116</sup>

2. Tire Pressure: Experiments have shown that for a given wheel load, an increase in tire pressure will cause a decrease in friction coefficient (Figure 54).<sup>117</sup> This can be attributed to the increased area of contact at low inflation pressure--the heat created by skidding or deceleration is distributed over a large area, which results in a cooler tire and a high friction coefficient.

3. Wheel Load: Studies using varying wheel loads have shown that the friction coefficient decreases as the wheel load increases (Figure 55).<sup>118</sup> One of the explanations for such a phenomenon is that the increase in wheel load causes a decrease in the tire contact area per unit load and therefore a decrease in the friction coefficient. In contrast, it was also reported that on ice, a slight increase in friction coefficient occurred as the rear axle static load was increased.<sup>119</sup>

4. Tire Tread: Tread design has a significant influence on braking effectiveness. Tire grooves provide channels through which water at the tire-pavement interface can be displaced. At high speeds or in the presence of thick water films, there is not enough time for the water to be displaced and hydro-

planing may occur. Figure 56 shows a comparison between braking effectiveness of smooth and five-groove tires for the 990A aircraft. NASA has reported that calculations using the results of this experiment showed that the stopping distance of the 990A aircraft with the smooth tires on the wet, un-grooved concrete runway was approximately 1,500 ft more than that required for the aircraft with unworn five-groove tires.<sup>120</sup>

#### *Pavement Factors*

Essentially two pavement factors affect skid resistance: surface characteristics and drainage.

1. Surface Characteristics: This factor includes the type of surface binder (asphalt or concrete), surface finish (texture), and aggregate (more significant if asphalt binder is used). Yager et al.<sup>121</sup> experimented with three groups of aircraft (C-141A, 990A, and F-4D) on the landing research runway at NASA. The runway is composed of level test sections with differing surface and composition characteristics (Figure 57). Results for the 990A aircraft, shown in Figure 58, indicate that grooved pavement surfaces are superior to the ungrooved surfaces.

Figure 59 shows a comparison of the effect of two different surface-grooving configurations on the braking efficiency of the C-141A aircraft on a concrete surface. One of the configurations is a continuous  $\frac{1}{4}$  in.  $\times$   $\frac{1}{4}$  in.  $\times$  1 in. pitch. The other consists of  $\frac{1}{4}$  in.  $\times$   $\frac{1}{4}$  in.  $\times$  2 in. pitch grooves for 2 ft, followed by 2 ft of ungrooved surface.

It would be misleading to conclude from Figure 58 that asphalt binders offer better skid resistance than concrete. Studies by other investigators did not show the same trend. Tomita reported a study performed in Michigan to determine the effect of the pavement type on friction coefficient.<sup>122</sup> The study covered Portland cement concrete, bituminous concrete/crushed gravel, and bituminous concrete/crushed

<sup>115</sup>M. Tomita, *Friction Coefficients Between Tires and Pavement Surfaces*, Technical Report R303 (U.S. Naval Civil Engineering Laboratory, 1964), p. 25.

<sup>116</sup>M. Tomita

<sup>117</sup>M. Tomita

<sup>118</sup>M. Tomita

<sup>119</sup>M. Tomita

<sup>120</sup>A Comparison of Aircraft and Ground Vehicle Stopping Performance on Dry, Wet, Flooded, Slush, Snow, and Ice Covered Runways, NASA Technical Note D-6098 (1970).

<sup>121</sup>A Comparison of Aircraft and Ground Vehicle Stopping Performance on Dry, Wet, Flooded, Slush, Snow, and Ice Covered Runways

<sup>122</sup>M. Tomita

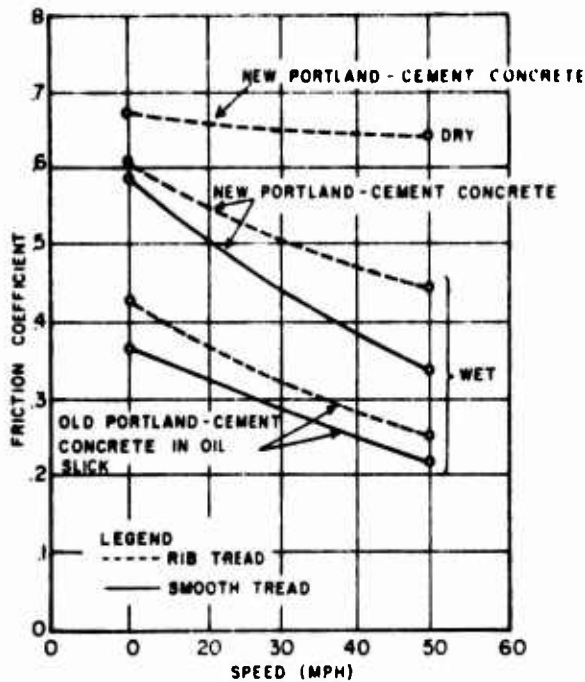


**Figure 51.** Friction values on new Portland cement concrete and in heavy oil slick on old Portland cement. Average daily traffic—9,000 vehicles [Moyer, 1959A]. (After M. Tomita, *Friction Coefficients Between Tires and Pavement Surfaces* [1964].)

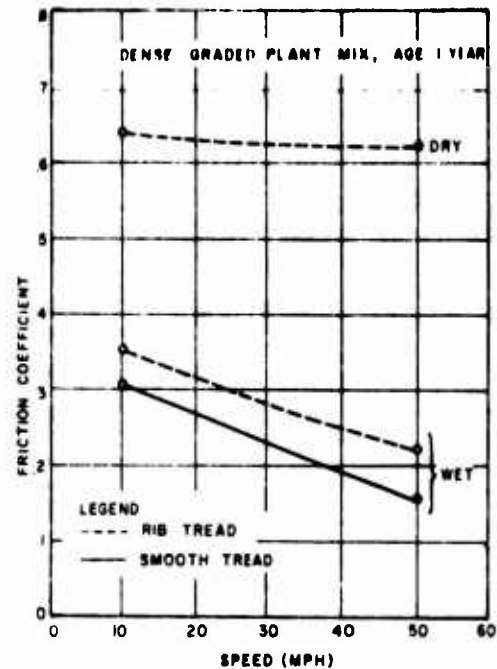


**Figure 52.** Friction values on a dense-graded plant-mix asphaltic surface constructed with partly crushed gravel aggregate. Average daily traffic—15,000 vehicles [Moyer, 1959]. (After M. Tomita, *Friction Coefficients Between Tires and Pavement Surfaces* [1964].)

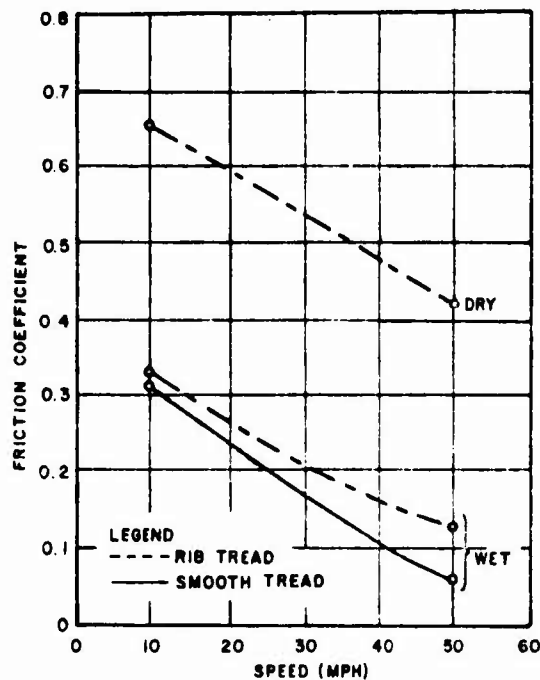


**Figure 53.** Friction values on asphalt seal-coat surface with excess asphalt contributing to bleeding in hot weather (Moyer, 1959). (From M. Tomita, *Friction Coefficients Between Tires and Pavement Surfaces*, Technical Report R 303 [U.S. Naval Civil Engineering Laboratory, 1964].)

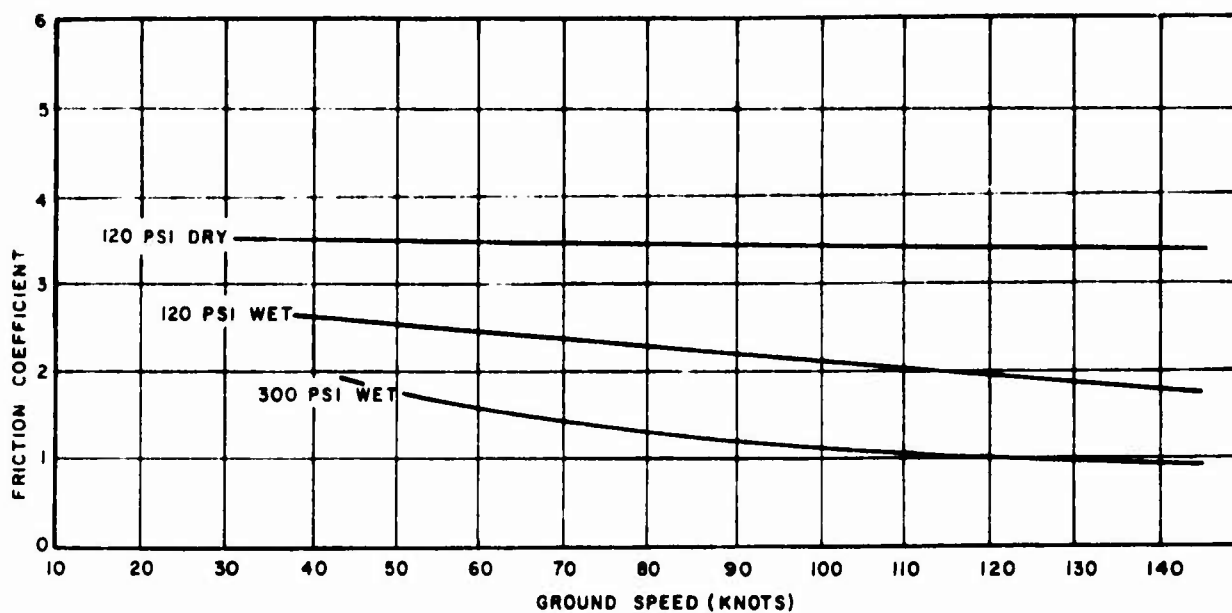


**Figure 54.** Comparison of friction coefficient for two types of pressure on wet surface and one type of pressure on dry surface, Portland cement concrete runway. Anti-skid braking throughout. Gross weight 18,350 lbs. (From M. Tomita, *Friction Coefficients Between Tires and Pavement Surfaces*, Technical Report R 303 [U.S. Naval Civil Engineering Laboratory, 1964].)

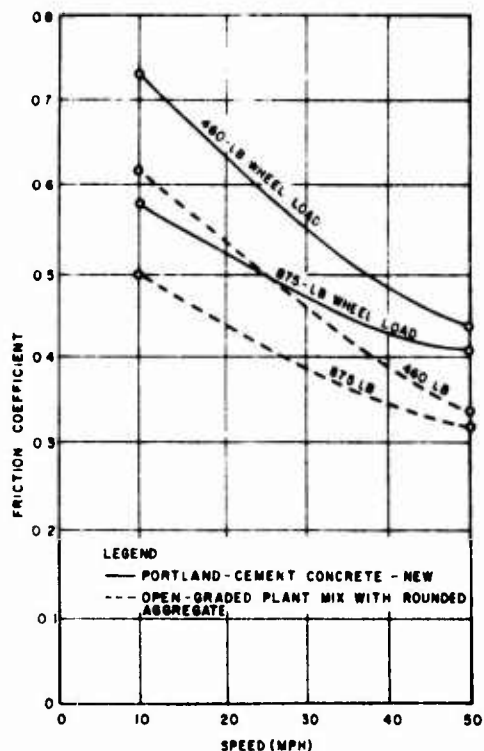


**Figure 55.** Effect of wheel load on skid resistance of wet Portland cement concrete and plant mix asphalt surfaces. (From M. Tomita, *Friction Coefficients Between Tires and Pavement Surfaces*.)

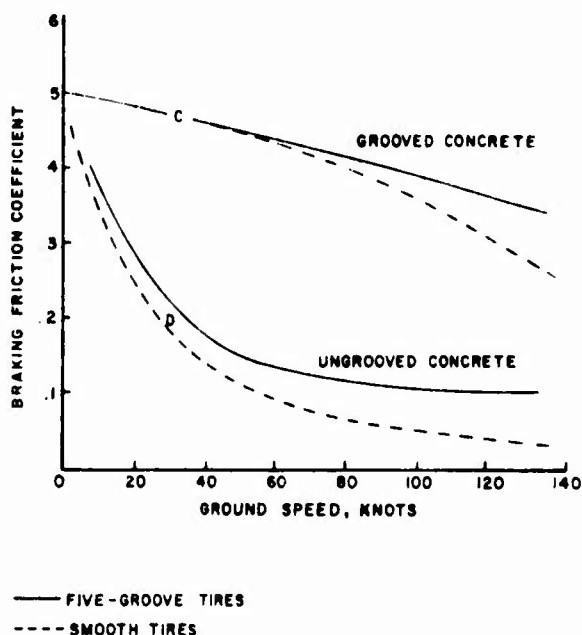


**Figure 56.** Tire-tread effects on wet and puddled runways for twin-tandem bogie arrangements. (From *A Comparison of Aircraft and Ground Vehicle Stopping Performance on Dry, Wet, Flooded, Slush, Snow and Ice Covered Runways*, NASA Technical Note D-6098 [1970].)

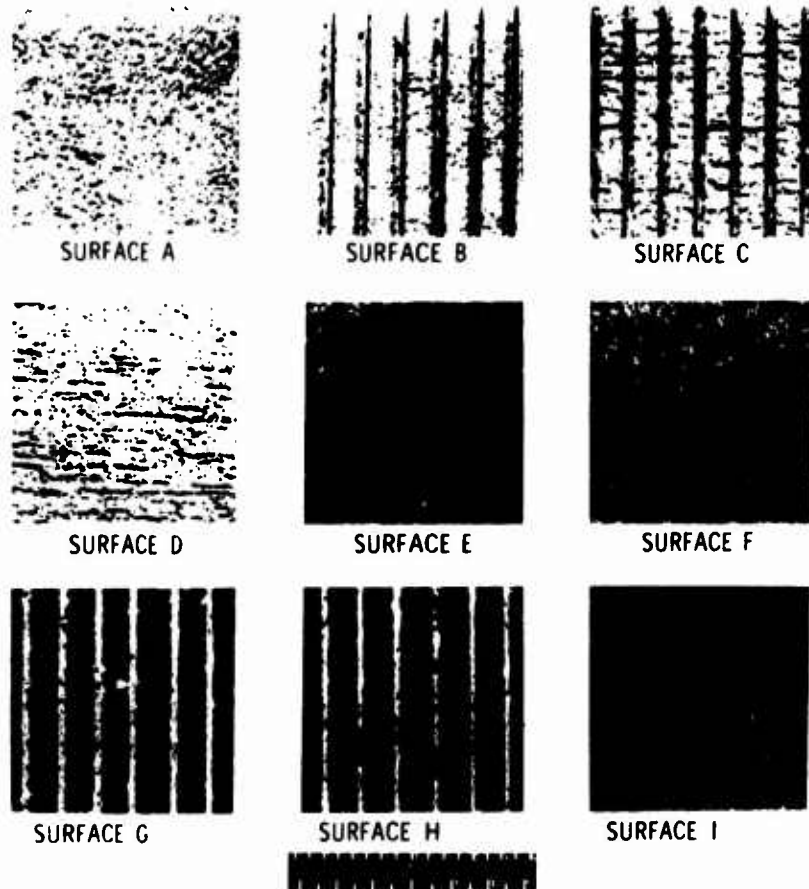
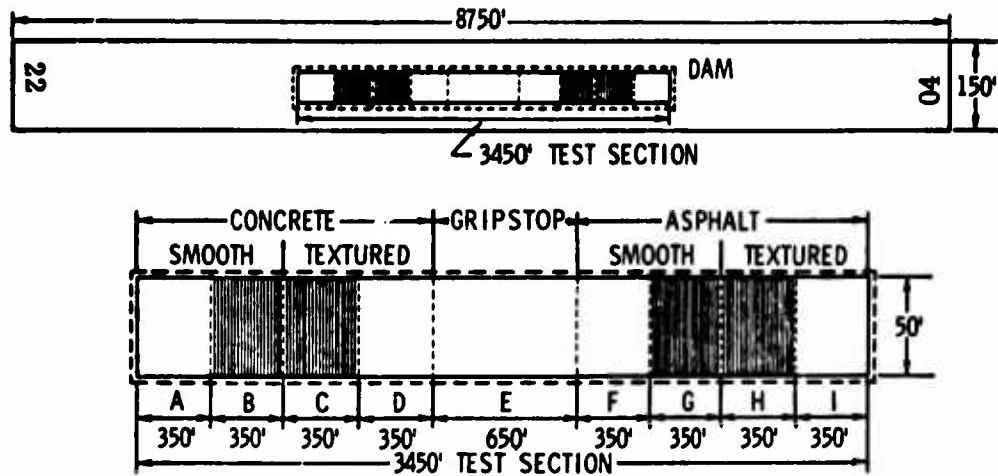
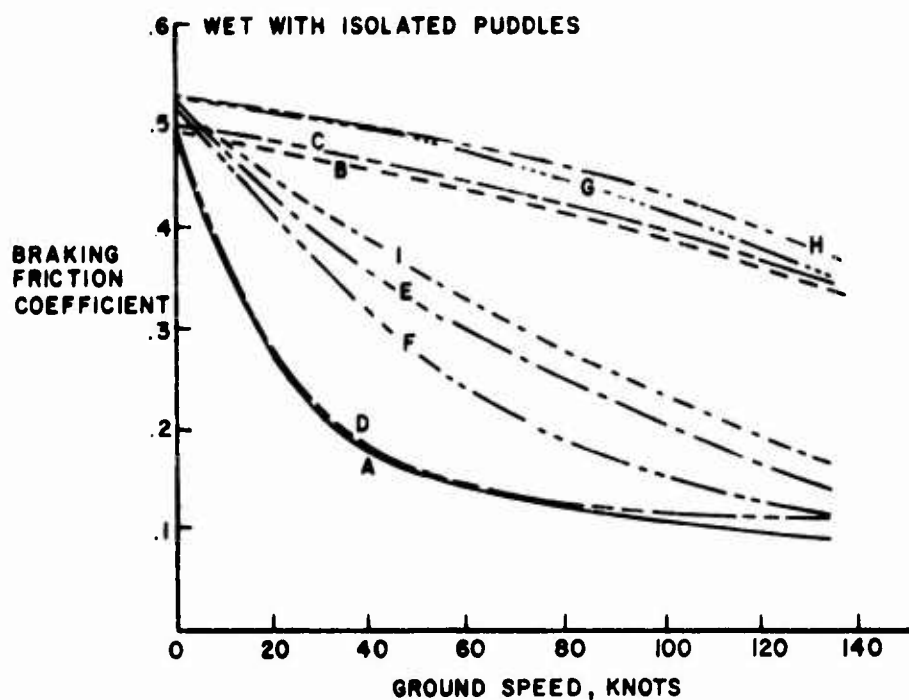


**Figure 57.** Landing research runway at Wallops Station, VA. (From *A Comparison of Aircraft and Ground Vehicle Stopping Performance on Dry, Wet, Flooded, Slush, Snow, and Ice Covered Runways*, NASA Technical Note D-6098 [1970].)



	SURFACE	MATERIAL	TREATMENT	GROOVES
————	A	CONCRETE	CANVAS BELT	UNGROOVED
-----	B	CONCRETE	CANVAS BELT	1 IN. BY 1/4 IN. BY 1/4 IN.
-----	C	CONCRETE	BURLAP DRAG	1 IN. BY 1/4 IN. BY 1/4 IN.
-----	D	CONCRETE	BURLAP DRAG	UNGROOVED
-----	E	ASPHALT	GRIPSTOP	UNGROOVED
-----	F	ASPHALT	SMALL AGGREGATE	UNGROOVED
-----	G	ASPHALT	SMALL AGGREGATE	1 IN. BY 1/4 IN. BY 1/4 IN.
-----	H	ASPHALT	LARGE AGGREGATE	1 IN. BY 1/4 IN. BY 1/4 IN.
-----	I	ASPHALT	LARGE AGGREGATE	UNGROOVED

**Figure 58.** Comparison of braking friction coefficients on wet and puddled runways obtained from 990A aircraft. (From *A Comparison of Aircraft and Ground Vehicles Stopping Performance on Dry, Wet, Flooded, Slush, Snow, and Ice Covered Runways*, NASA Technical Note D-6098 [1970].)

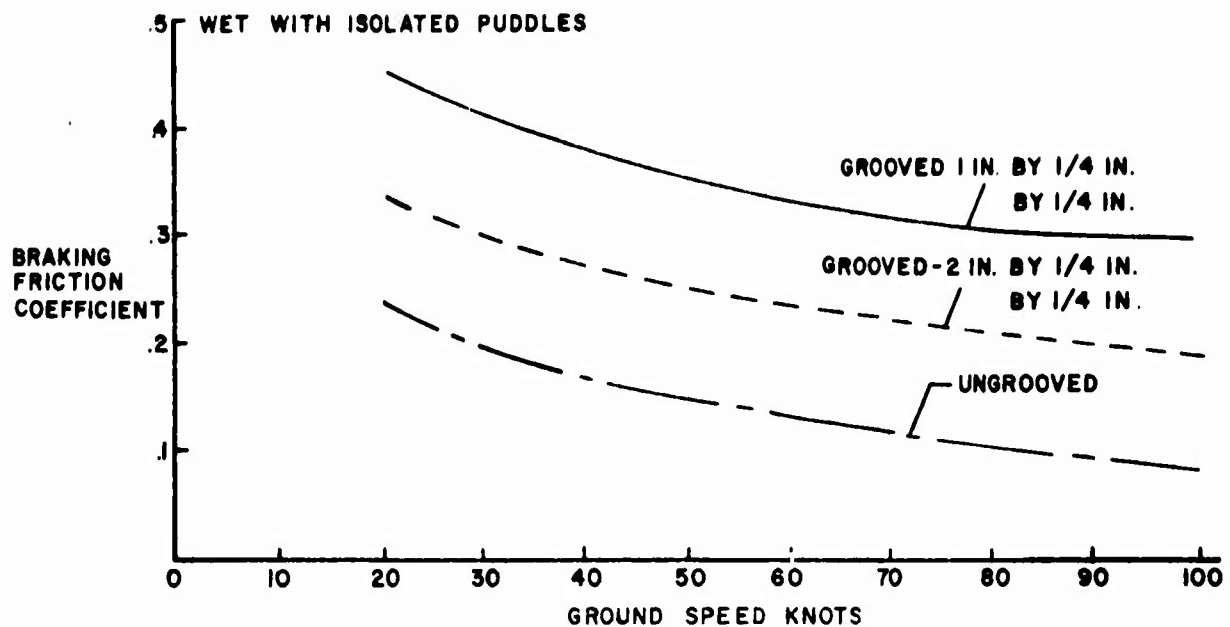


**Figure 59.** Effect of runway groove configuration on C-141A aircraft braking on landing research runway at NASA Wallops Station. (From *A Comparison of Aircraft and Ground Vehicle Stopping Performance on Dry, Wet, Flooded, Slush, Snow, and Ice Covered Runways*, NASA Technical Note D-6098 [1970].)

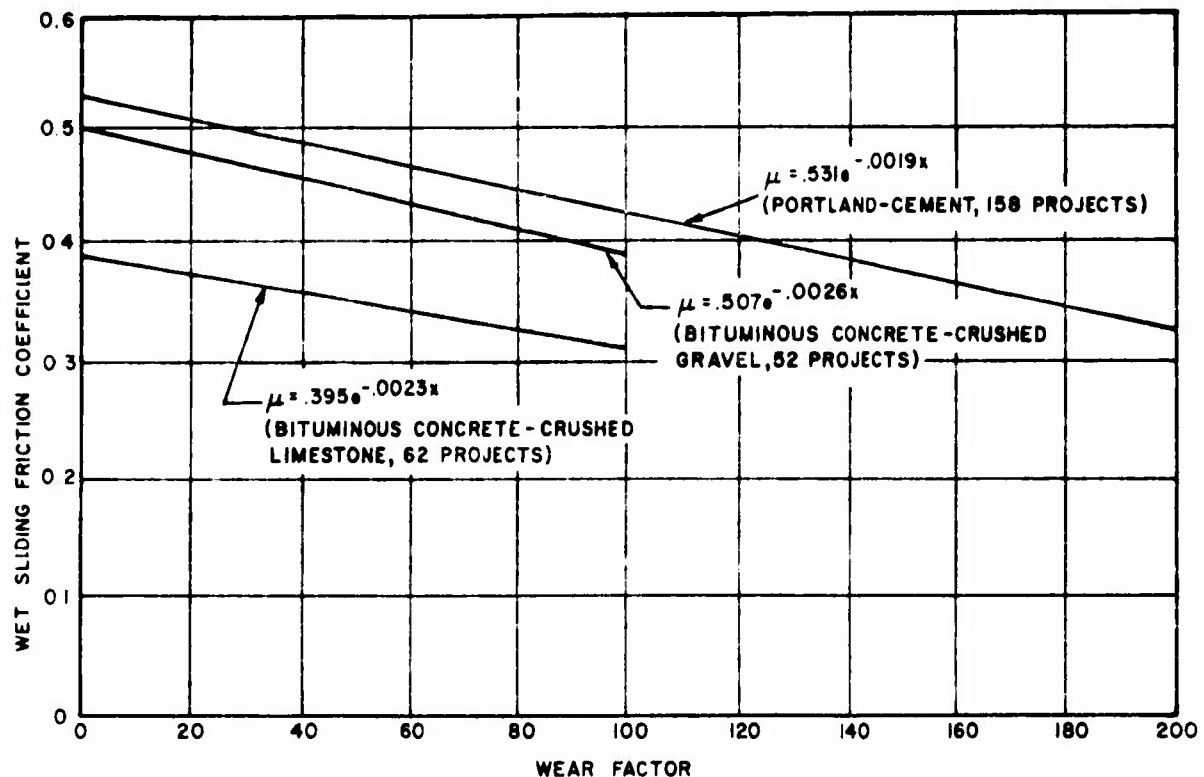


**Figure 60.** Comparison of friction-wear relationship: Portland cement concrete, and asphaltic concrete with gravel and limestone aggregates [Finney and Brown, 1959]. (From M. Tomita, *Friction Coefficients Between Tires and Pavement Surfaces*.)



limestone (Figure 60). The wear factor shown in the figure was computed as the product of average daily traffic volume per traffic lane since construction, weighted for percent of commercial traffic, divided by 1,000, and multiplied by the age of the project in years. Based on the results shown in Figures 58-60, no definite conclusion can be drawn about the effect of the type of binder on skid resistance.

2. Drainage: Good drainage conditions allow the pavement surface to recover its dry skid resistance characteristics shortly after wetting. In its runway skid resistance survey, the U.S. Air Force examined drainage conditions using the above concept.<sup>123</sup> A water truck applied water to the surface in two passes, with the truck calibrated so that each pass placed 0.1 in. of water on each 2,000 ft of the test strip. The "zero" water time was the time the water truck passed the midpoint of the test section during the second water pass. Figure 61 shows the effect of time-after-wetting on changes in sideways friction as measured by the Mu-Meter, and on the stopping distance ratio as measured by the DBV. These graphs demonstrate the natural drainage characteristics of the runway surface and the time required for the skid resistance to return to a dry pavement condition.

### Correlation Between Friction Measurements

From the previous discussion, it is clear that a one-to-one correlation should not be expected between two different skid testers. Each tester measures a different aspect of the developed friction based on mode of operation, speed, water application, and so forth. For example, performing the measurement at a low speed will give a friction factor which is caused mainly by the microtexture component of the surface (Figure 34). In order to compare testers, measurements must be made under comparable conditions.

#### *Mu-Meter vs Skid Trailer*

Field tests using the Soiltest ML-400 Mu-Meter friction recorder and the Texas Highway Department research skid trailer showed that the instruments compared favorably when test conditions were

the same (Figure 62).<sup>124</sup> The data were obtained by operating both instruments with smooth tires at 24 psi tire pressure, and having the pavement wetted by a water truck. The graph shows a good correlation between the instruments, although it is not 1:1. The Mu-Meter shows higher values than the skid trailer, which is to be expected since the Mu-Meter operates in the cornering-slip mode and the skid trailer operates in the skid mode. Another factor that might have caused the higher results from the Mu-Meter is that, because of its relatively narrow track width, only one of its test wheels can be made to run in the most-traveled wheel path.

#### *Automobile Method vs Skid Trailers*

While trailers are used to measure the friction coefficient at a given speed, friction coefficients determined by automobile methods correspond to a range of speeds—from the speed at which the brakes are applied down to zero as the car stops. Figure 63 shows the results of a study by Mahone et al.<sup>125</sup> to correlate Virginia's skid trailer and stopping distance car. The results cannot be generalized since different correlation may be obtained under different testing conditions.

#### *Automobile Method vs Mu-Meter*

It is to be emphasized that each of these methods measures a different indicator of friction. In addition, different testing conditions (e.g., tire-tread design, wheel load, etc.) make comparison of the methods rather difficult. Figure 64 shows a comparison between the friction factor measured by the Mu-Meter at 40 mph and the wet/dry stopping distance ratio measured by the NASA Diagonal-Braked Vehicle (DBV) by locking a diagonal pair of wheels at 60 mph. The data are from the results of the U.S. Air Force runway skid resistance survey at different bases.<sup>126</sup> For the survey, the surface was wet by a water truck each time measurements were taken. The results indicate poor correlation up to a Mu value of 0.65.

Burns et al. reported a good correlation between

<sup>123</sup>G.D. Ballentine and P.A. Compton, *Procedures for Conducting the Air Force Weapons Laboratory Standard Skid Resistance Test* (AFWL, 1973).

<sup>124</sup>B.M. Gallaway and J.G. Rose, *Comparison of Highway Pavement Friction Measurements Taken in the Cornering-Slip and Skid Modes*, HRR 376 (Highway Research Board, 1971).

<sup>125</sup>D.C. Mahone and S.N. Runkle, *Pavement Friction Needs*, HRR 396 (Highway Research Board, 1972).

<sup>126</sup>*Runway Skid Resistance Survey Reports* (Air Force Civil Engineering Center, Tyndall AFB, 1974).

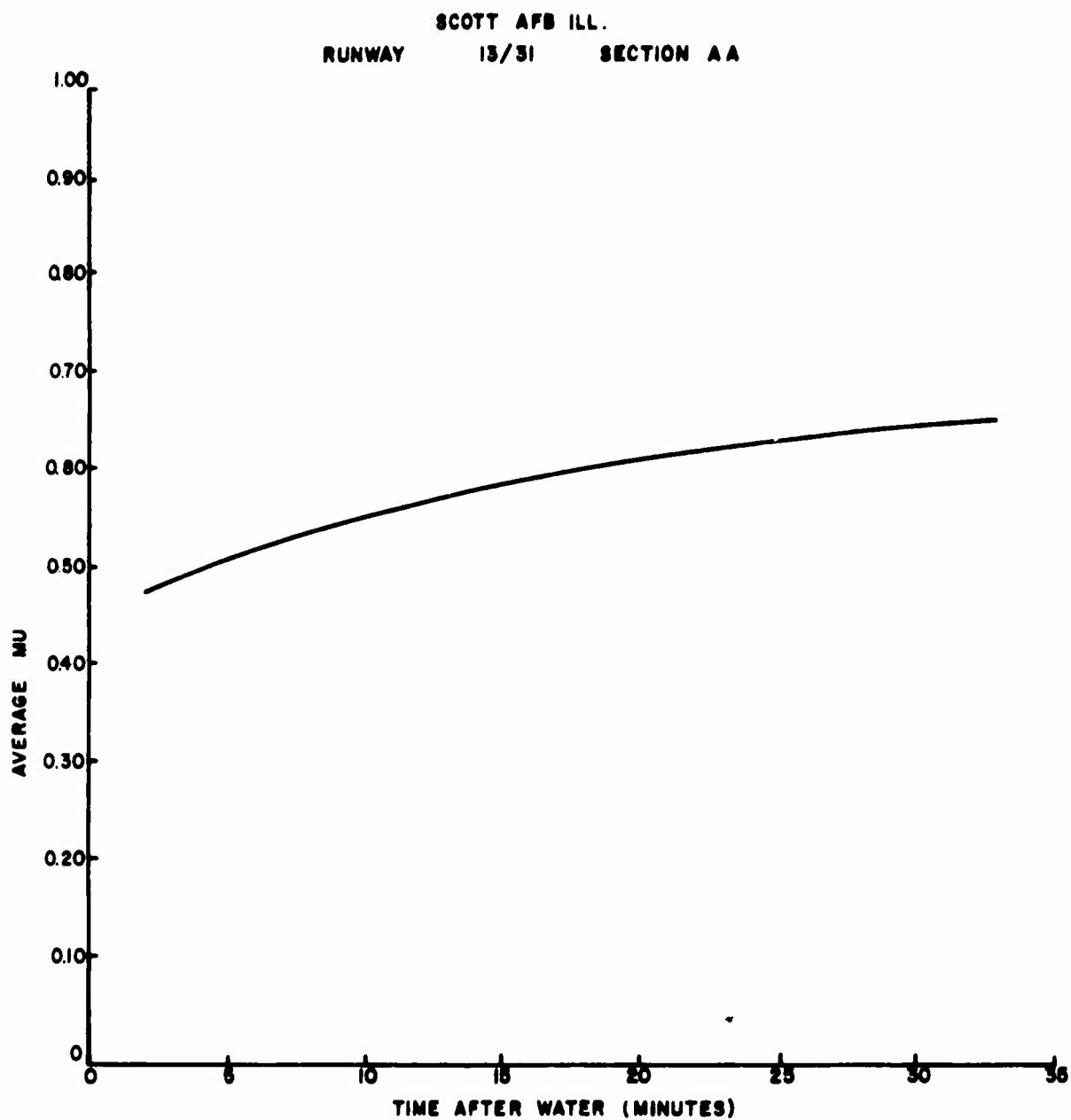


**Figure 61a.** Effect of time after surface-wetting on side friction coefficient as measured by Mu-Meter. (From *Runway Skid Resistance Survey Report, for Scott AFB, Illinois* [Air Force Civil Engineering Center, Tyndall AFB, 1974].)

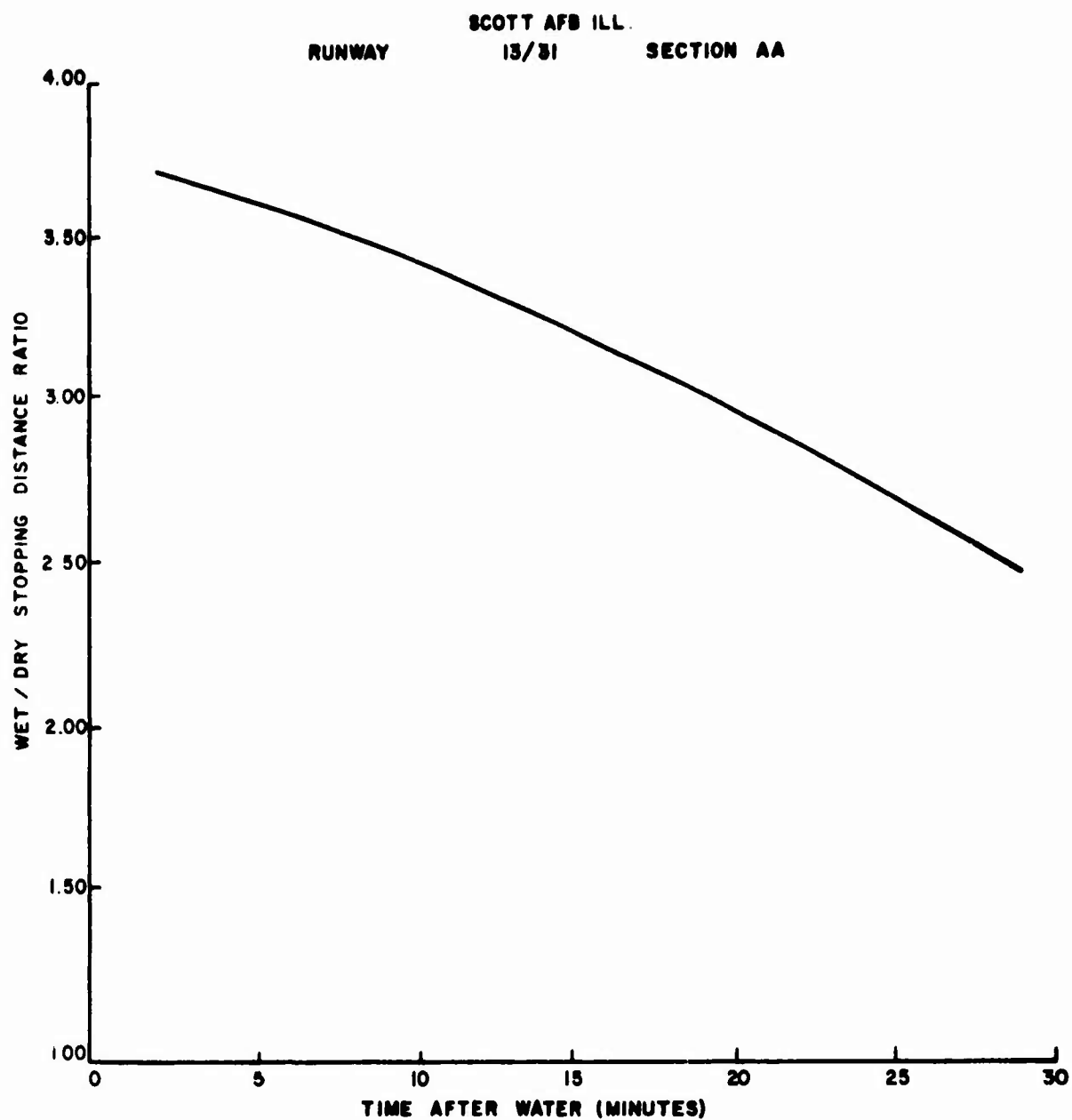


**Figure 61b.** Effect of time-after-surface-wetting on wet/dry stopping distance ratio as measured by Diagonal-Braked Vehicle [DBV]. (From *Runway Skid Resistance Survey Report for Scott AFB, Illinois* [Air Force Civil Engineering Center, Tyndall AFB, 1974].)

MU-METER VS. SKID TRAILER  
95% CONFIDENCE LIMITS

	Y	X
MEANS	50.	38.
S <sub>y</sub>	20.	18.

N = 21

R = .957

R<sup>2</sup> = .915

Y = 9.629 + 1.05 X

$\hat{\sigma}_y = 5.844$

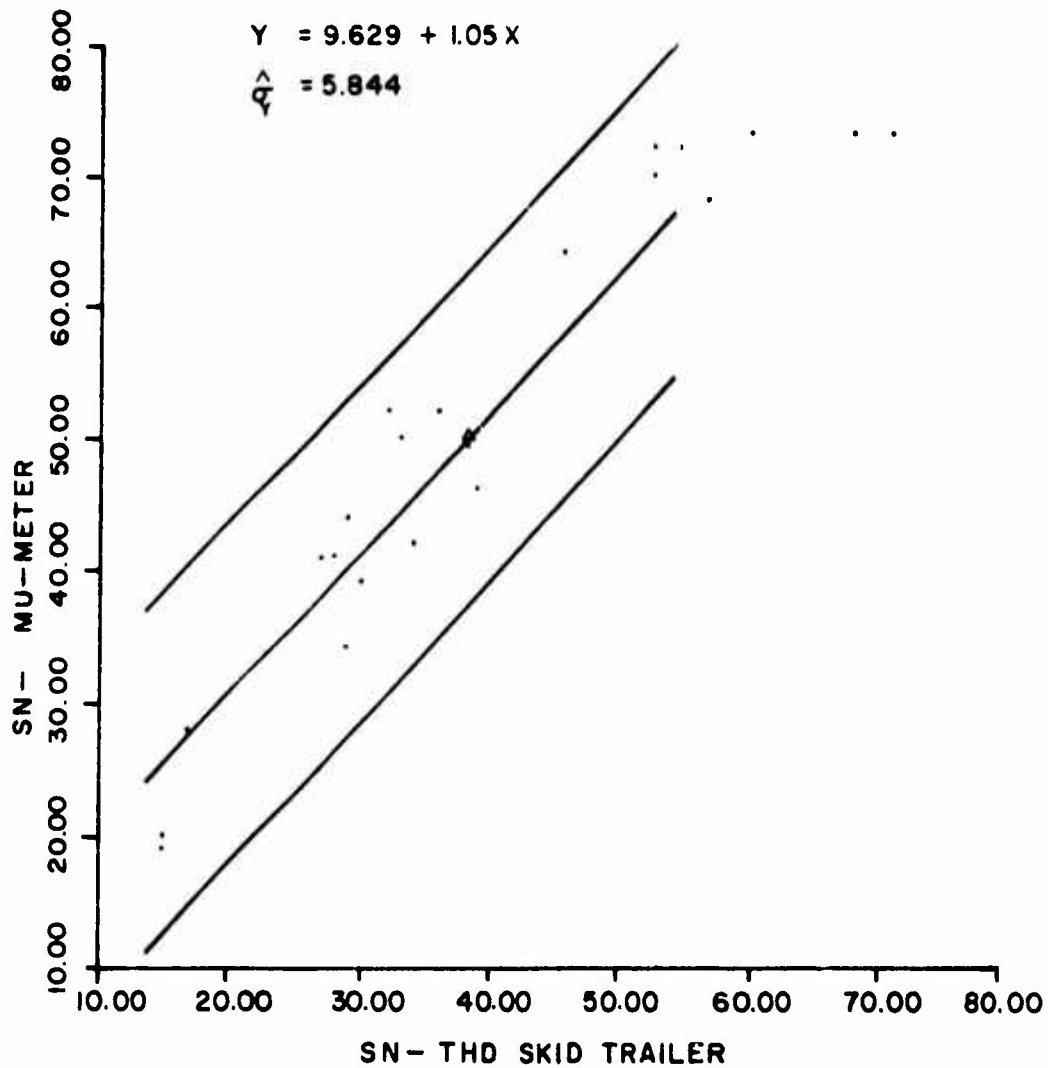


**Figure 62.** Correlation between Mu-Meter and Texas Highway Department locked-wheel trailer. (Data obtained from B.M. Gallaway and J.G. Rose, *Comparison of Highway Pavement Friction Measurements Taken in the Cornering-Slip and Skid Modes*, HRR 376 [Highway Research Board, 1971], p 113.)

**AUTOMOBILE VS. SKID TRAILER**  
**95% CONFIDENCE LIMITS**

MEANS	Y	X
	52.	65.
$S_v$	7.8	1.1

$N = 61$

$R = .910$

$R^2 = .828$

$Y = 11.92 + 0.6247 X$

$\hat{\sigma}_Y = 3.281$

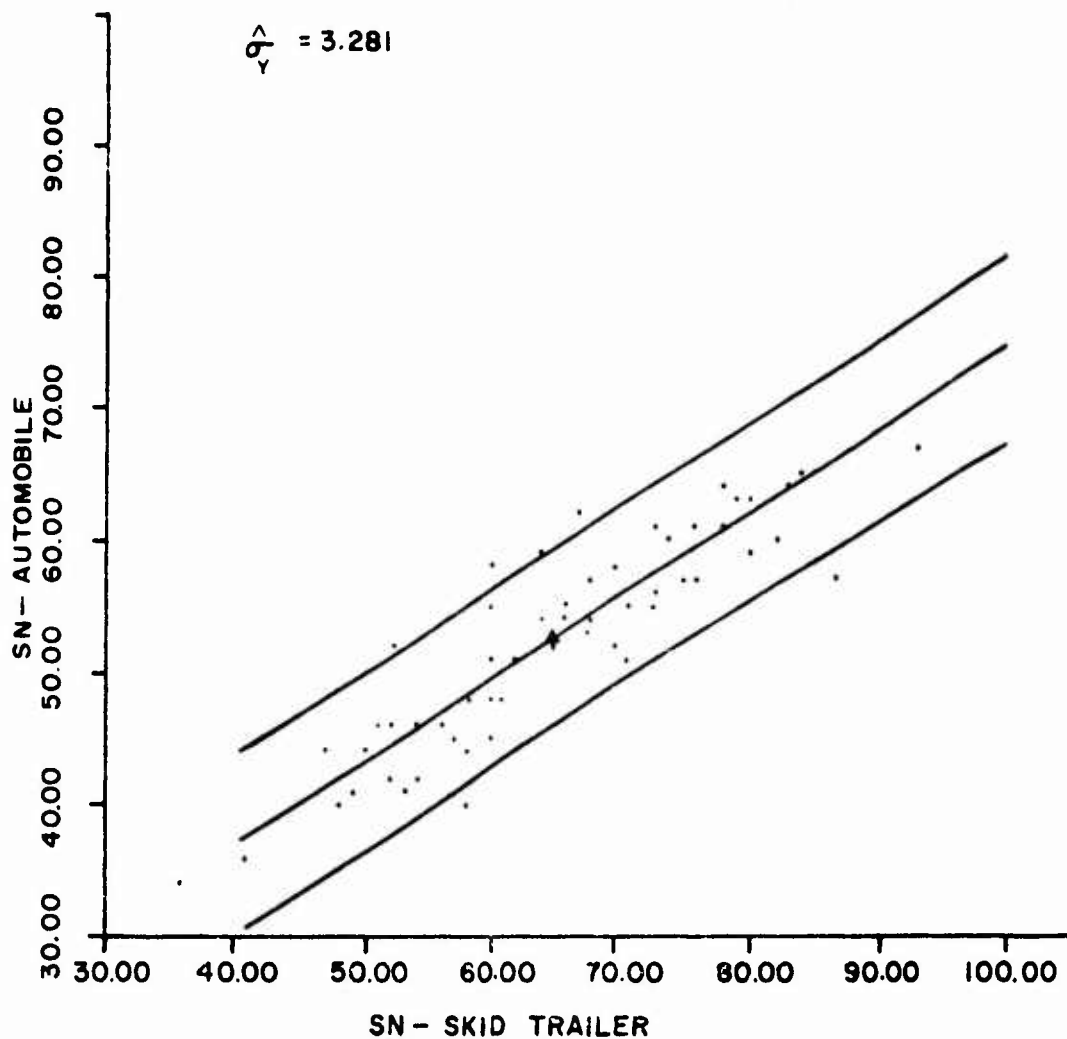


**Figure 63.** Correlation between skid number obtained from car stopping distance from 40 mph and Virginia skid trailer at 40 mph. (Data obtained from D.C. Mahone and S.N. Runkle, *Pavement Friction Needs*, HRR 396 [Highway Research Board, 1972], p 3.)

**AUTOMOBILE VS. MU-METER  
95% CONFIDENCE LIMITS**

	Y	X
MEANS	2.0	.68
S <sub>y</sub>	.76	.14

N = 51

R = -.836

R<sup>2</sup> = .698

Y = 5.005 - 4.409X

$\hat{\sigma}_Y = 0.419$

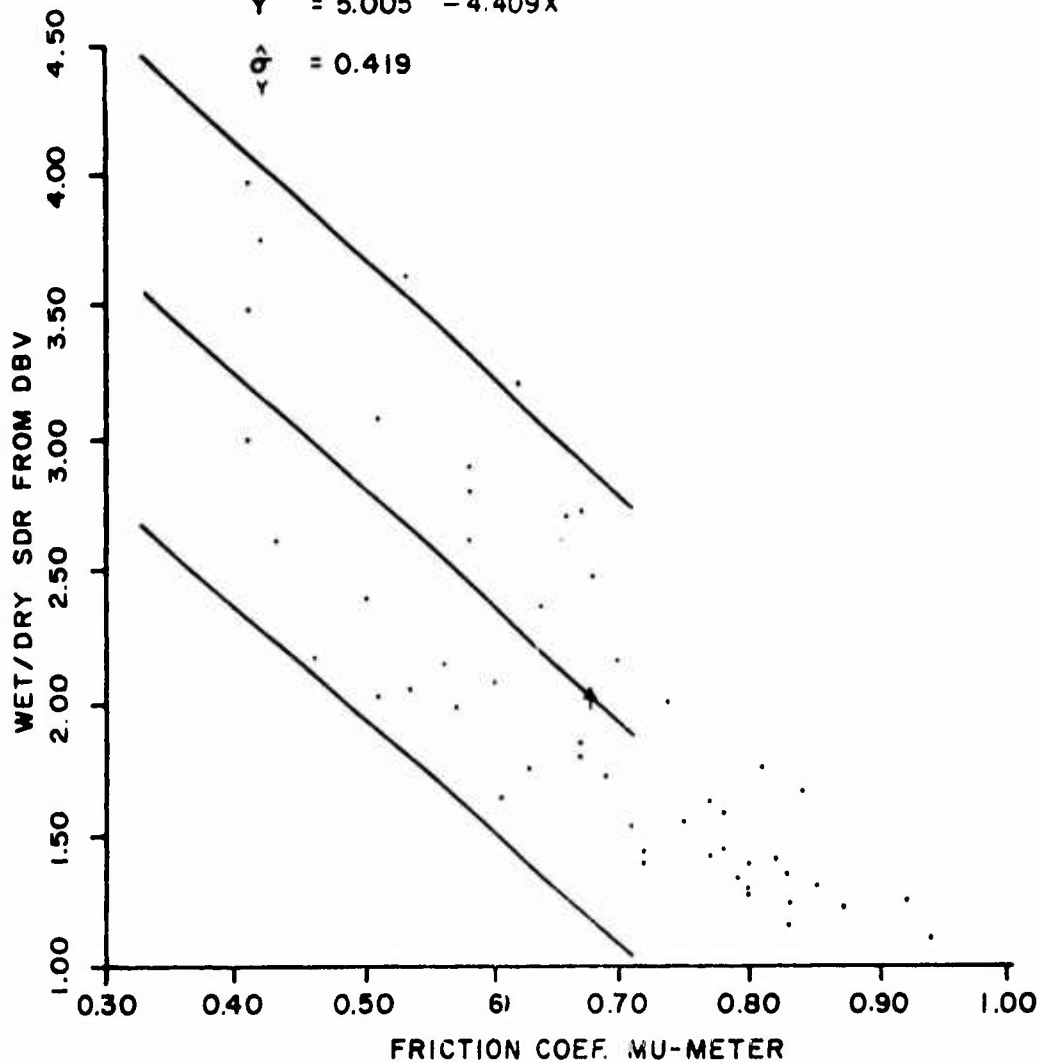


**Figure 64.** Sideway friction measured by Mu-Meter vs wet/dry stopping distance ratio measured by the Diagonal-Braked Vehicle.\* (From *Runway Skid Resistance Survey Reports* [Air Force Civil Engineering Center, Tyndall AFB, 1974].)

\*Measurements were taken at the following bases:

(1) Scott AFB, Illinois

(2) Royal AF Woodbridge, England

(3) Kincheloe AFB, Michigan

(4) Zqeibrucken AB, Germany

(5) Minot AFB, North Dakota

Arizona's Mu-Meter and a stopping distance car.<sup>127</sup> Their results do not contradict the results obtained from the Air Force data, but rather emphasize the importance of testing conditions.

#### *Trailers and Automobiles vs Portable Field and Laboratory Methods*

Little correlation has been found between these methods because of the different modes of operation and, particularly, because of the low speeds of most of the portable field and laboratory methods. Even correlation between portable field equipment operating at different speeds is unlikely. Zube et al., in comparing the Penn State Drag Tester and California Skid Tester, conclude the following:

A suitable correlation was not obtained between the Penn State Drag Tester and the California Skid Tester when different types of surfaces were compared. A significant correlation was obtained when only PCC surfaces were used in the analysis. It is apparent that the speed effect mentioned in the papers by Kummer is of considerable importance in attempting to correlate low speed skid testers with those based on much higher speeds. This is especially true when there are definite differences in surface texture.<sup>128</sup>

Figure 65 shows the results of the correlation study performed by Zube et al.

#### *Automobile vs Actual Aircraft*

A joint USAF-NASA research program studied the stopping performance of an instrumented C-141A four-engine jet transport and several instrumented ground vehicles under dry, wet, flooded, slush, snow, and ice conditions.<sup>129</sup> Tests were performed on concrete and asphalt runway surfaces. The concrete finishes included conventional, wire combed, and a variety of grooving patterns. The asphalt surfaces included slurry seal, plant mix, porous friction course, grooved, and others.

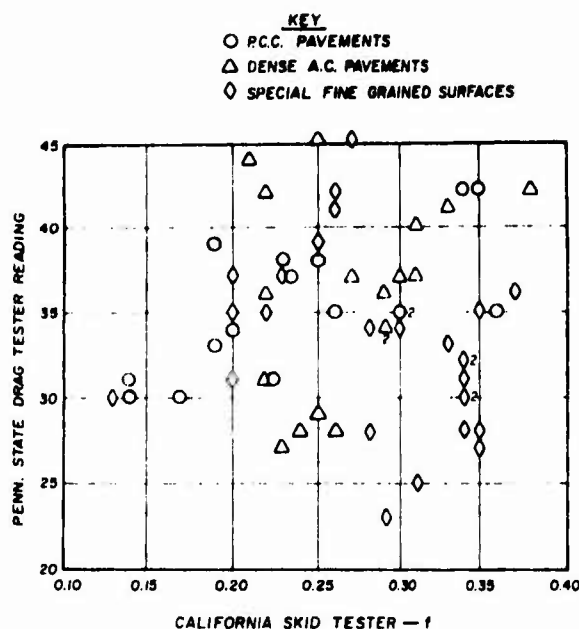


**Figure 65.** Correlation of California skid tester and Pennsylvania State drag skid tester. (From E. Zube and J. Skog, *A Study of the Pennsylvania State Drag Tester for Measuring the Skid Resistance of Pavement Surfaces*, Report M&R 633251 [Material and Research Department, California Division of Highways, 1967].)

Results showed that the NASA diagonal-braked ground vehicle (DBV) permits accurate prediction of the stopping distance of an aircraft under varied runway slipperiness conditions. Figure 66 shows the good correlation between the NASA DBV and the C-141A aircraft. Similar good correlations were obtained with the 990A and F-4D aircraft.<sup>130</sup> Figure 67 shows the correlation between the RCR vehicle and the C-141A aircraft. The correlation is particularly poor on wet surfaces because of the low speed (20-30 mph) at which brakes are applied on the RCR vehicle as compared to the high speed of the aircraft when it starts to brake.

<sup>127</sup> E. C. Burns and R. J. Peters, *Surface Friction Study of Arizona Highways*, HRR 471 (Highway Research Board, 1973).

<sup>128</sup> E. Zube and J. Skog, *A Study of the Pennsylvania State Drag Tester for Measuring the Skid Resistance of Pavement Surfaces*, Report M&R 633251 (Material and Research Department, California Division of Highways, 1967).

<sup>129</sup> *A Comparison of Aircraft and Ground Vehicle Stopping Performance on Dry, Wet, Flooded, Slush, Snow, and Ice Covered Runways*, NASA Technical Note D-6098 (1970).

<sup>130</sup> *A Comparison of Aircraft and Ground Vehicle Stopping Performance on Dry, Wet, Flooded, Slush, Snow, and Ice Covered Runways*.

WET RUNWAYS  
95% CONFIDENCE LIMITS

	Y	X
MEANS	1.7	1.7
$S_y$	.43	.38

N = 35  
R = .888  
R<sup>2</sup> = .789

$$Y = -1.086E-02 + 1.021E+00 X$$

$$\sigma_y = 0.202$$

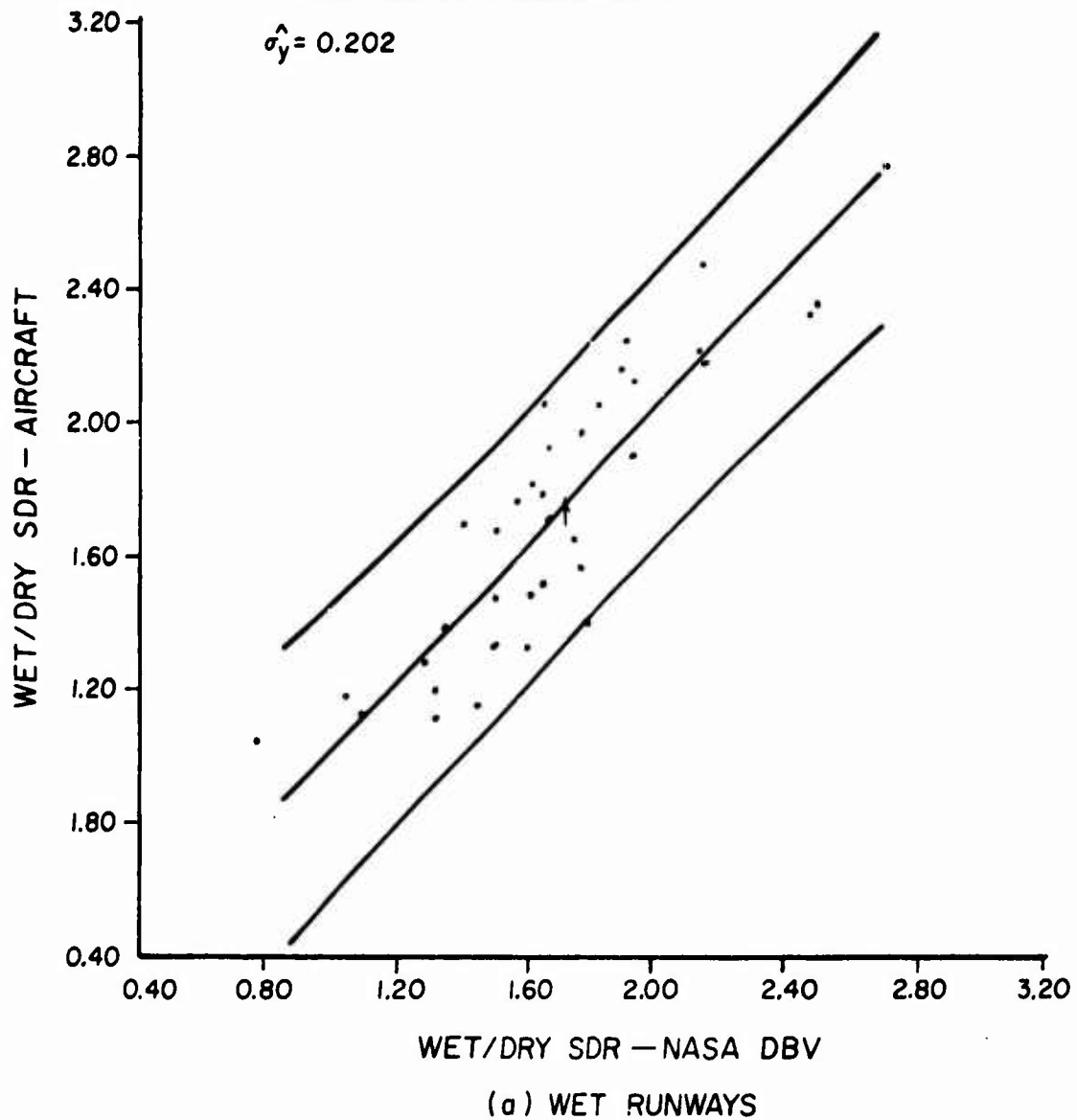


**Figure 66.** Correlation between the wet/dry stopping distance ratio obtained by the C-141A aircraft and NASA Diagonal-Braked Vehicle (DBV) with vehicle brakes applied at 60 mph.



SNOW-SLUSH-AND ICE-COVERED R/W  
95% CONFIDENCE LIMITS

	Y	X
MEANS	2.7	2.8
$S_y$	.70	.93

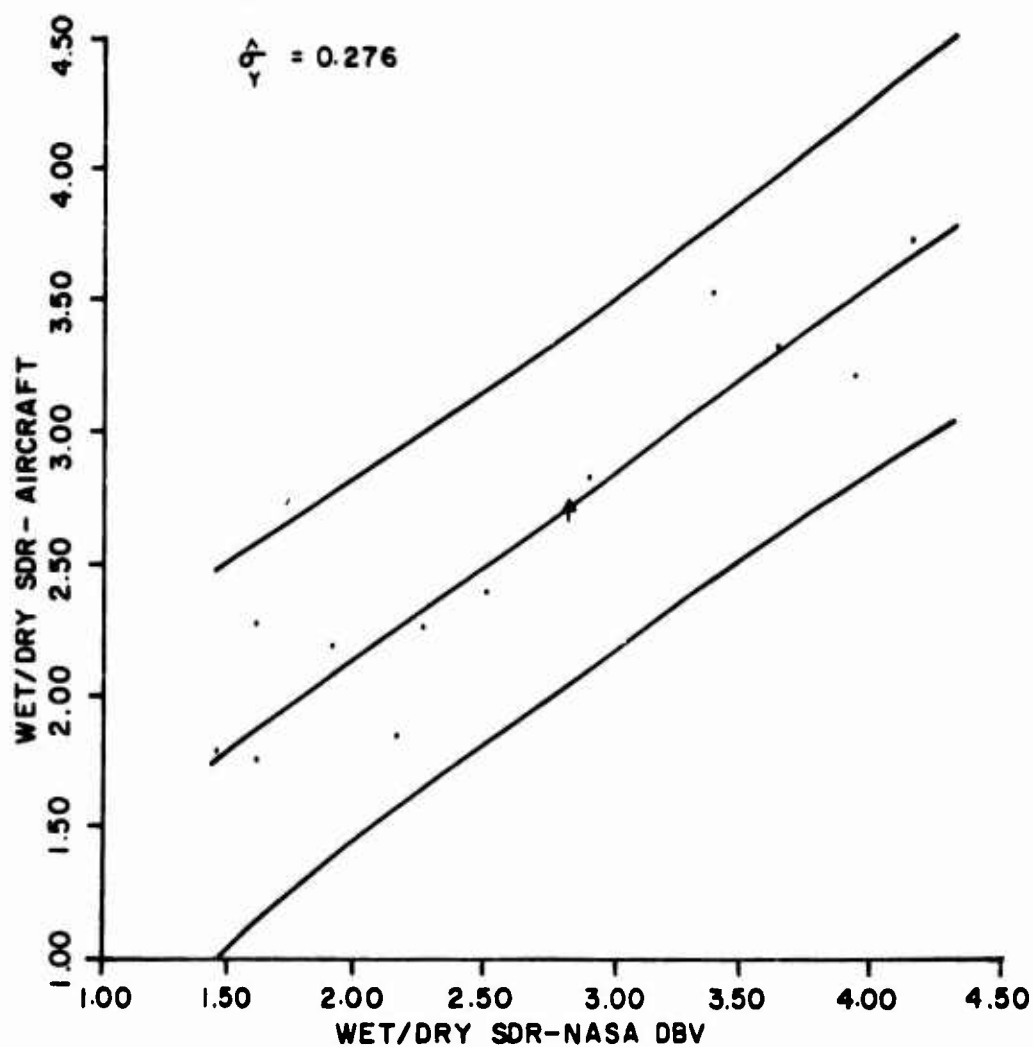
N = 10

R = .929

R<sup>2</sup> = .863

Y = 0.7227 + 0.7015 X

$\frac{\Delta}{Y} = 0.276$



(b) SNOW, SLUSH AND ICE-COVERED RUNWAYS

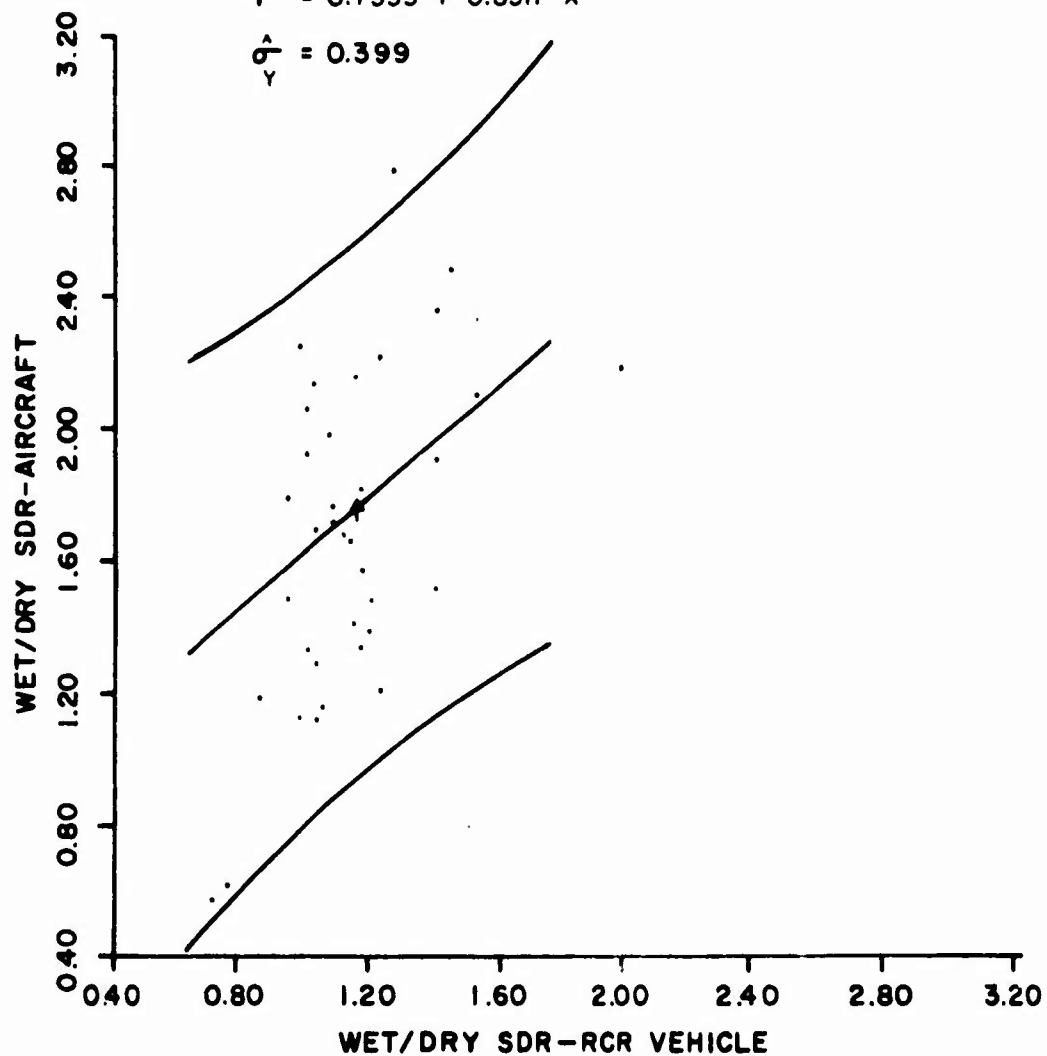
Figure 66. (cont'd).

**WET RUNWAYS**  
**95% CONFIDENCE LIMITS**

	Y	X
MEANS	1.7	1.2
S <sub>y</sub>	.43	.21
N	= 35	
R	= .415	
R <sup>2</sup>	= .172	

$$Y = 0.7533 + 0.8517 X$$

$$\sigma_Y^A = 0.399$$



**(a) WET RUNWAYS**

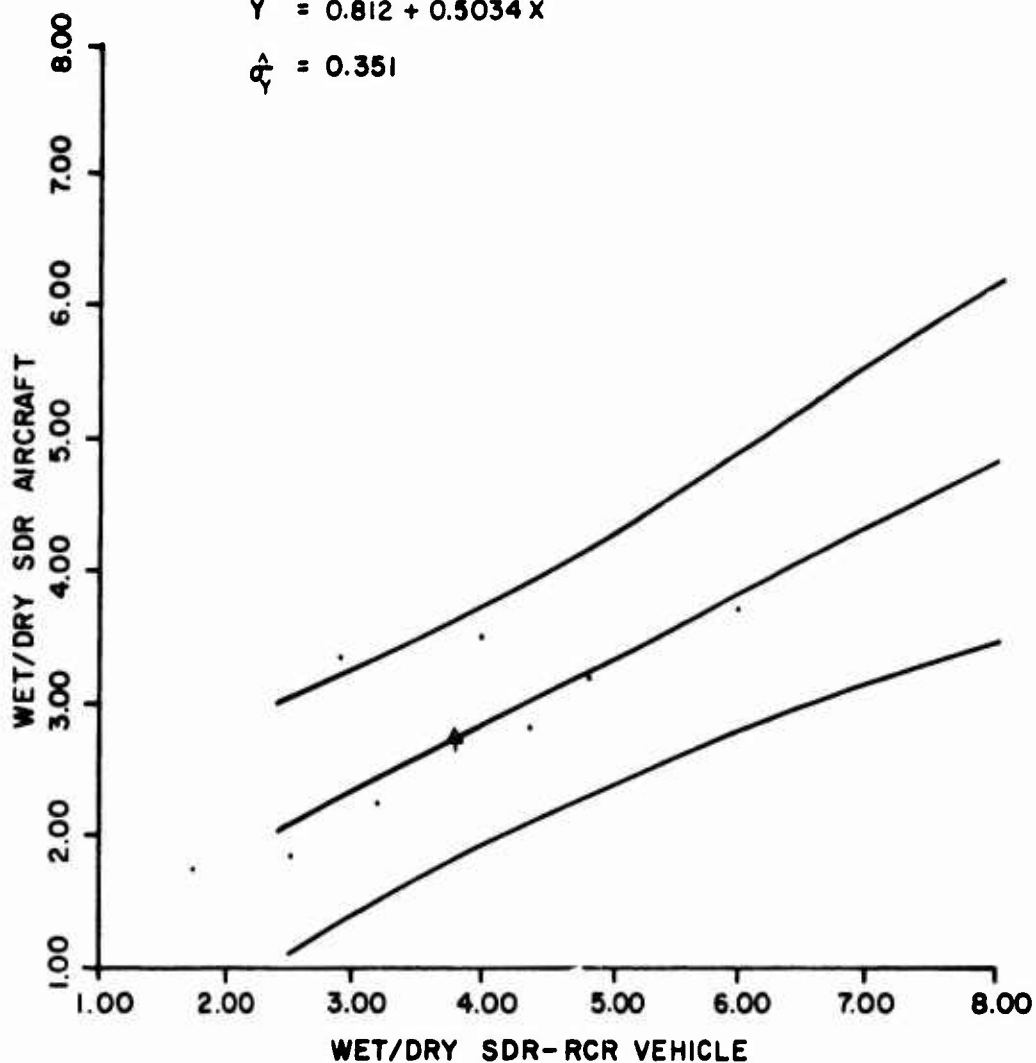
**Figure 67.** Correlation between the wet/dry stopping distance ratio obtained by C-141A aircraft and runway condition reading (RCR) vehicle with vehicle brakes applied at 20 mph.

**SNOW-SLUSH-AND ICE-COVERED R/W  
95 % CONFIDENCE LIMITS**

	Y	X
MEANS	2.7	3.8
$S_y$	.79	1.4
N	= 7	
R	= .915	
$R^2$	= .837	

$$Y = 0.812 + 0.5034 X$$

$$\sigma_Y = 0.351$$



**(b) SNOW, SLUSH AND ICE-COVERED RUNWAYS**

**Figure 67. (cont'd).**

## Skid Resistance Summary

The previous sections have discussed friction measuring methods, variables affecting the measured values, and correlation between different methods. A review of the state of the art revealed the following skid resistance and hydroplaning indicators:

1. Friction coefficient measured with trailers with locked wheels
2. Friction coefficient measured with trailers with unlocked wheels making a yaw angle with the direction of travel
3. Friction coefficient measured with trailers with rolling wheels in the slip mode
4. Reading obtained from a decelerometer installed in a vehicle
5. The ratio between wet and dry stopping distance for an automobile applying brakes at a given speed
6. Friction coefficient measured by portable field instruments

7. Friction coefficient measured by laboratory equipment

8. A code for the surface texture.

As mentioned, each of these indicators measures a different aspect of the friction factor. The degree of correlation between two indicators depends on testing conditions such as speed, tire-tread design, wheel load, and so forth. Therefore, when using one or more of the indicators to evaluate the skid resistance and hydroplaning potential of a pavement surface, test conditions should be selected specifically to satisfy the purpose of the evaluation. For example, in selecting indicators to evaluate runways, one should first eliminate those that are unlikely to correlate with actual aircraft stopping distance—such as stopping distance measured by automobiles braking at low speeds (20 mph), and friction coefficients measured by laboratory methods, some portable field equipment, or trailers with locked wheels. This will narrow the choice to trailers operating in the slip or yaw modes, stopping distance measured by automobiles braking at high speeds (60 mph), and perhaps some type of a texture code and water depth measure. Table 5 summarizes tentative recommendations for various pavement types.

Table 5  
Tentative Recommendations for Skid Measurement of Different Pavement Types

Measurement Method	Mode of Testing or Equipment	Highways		Airfields	
		Local Roads & Streets	Primary Highways	Runways	Taxiways
1. Trailers	Locked wheel	HA	A	P	P
	Yaw mode	A	HA	A	A
	Slip mode	P	P	HA	HA
2. Automobiles	Locking 4 wheels	P	Q	Q	Q
	Diagonal-Braked Vehicle	P	P	A	A
3. Portable & Lab. Method	California	A	P	Q	Q
	Penn State	Q	NA	NA	NA
	British Pendulum	Q	NA	NA	NA
4. Texture		Q*	Q*	Q*	Q*

HA—Highly acceptable usage

A—Acceptable usage

P—Possible but not desirable usage

Q—Questionable usage

NA—Not acceptable usage

\*Depends on the technique used for the analysis.

The U.S. Air Force is employing two indicators for its runway skid resistance survey: the wet/dry stopping distance ratio measured by the NASA DBV, and the sideways friction factor measured by the Mu-Meter (yaw mode). Figure 64 shows the correlation between DBV and Mu-Meter measurements. Figure 66 shows the correlation between DBV and C-141A measurements. After taking measurements, the Air Force uses Tables 6 and 7 to rate the skid resistance and hydroplaning potential of the runways. These tables and Figures 64 and 66, show that the measurements taken by the DBV alone are probably a sufficient indicator. However, the use of both the Mu-Meter and the DBV provides a check of the values obtained and is a measure of safety in the event of equipment malfunction.

**Table 6**  
**Mu-Meter Aircraft Pavement Rating\***

Mu	Expected Aircraft Braking Response	Response
Greater than 0.50	Good	No hydroplaning problems are expected
0.42 - 0.50	Fair	Transitional
0.25 - 0.41	Marginal	Potential for hydroplaning for some A/C exists under certain wet conditions
Less than 0.25	Unacceptable	Very high probability of hydroplaning

\*A.D. Brickman et al., *Analysis of Pavement Profile* (Pennsylvania Department of Transportation, 1969).

**Table 7**  
**Stopping Distance Ratio/Airfield Pavement Rating\***

SDR	Hydroplaning Potential
1.0 - 2.0	No hydroplaning anticipated
2.0 - 2.5	Potential not well defined
2.5 - 3.5	Potential for hydroplaning
Greater than 3.5	Very high hydroplaning potential

\*G.D. Ballentine and P.V. Compton, *Evaluation of Runway Skid Resistance Characteristics of Royal Air Force Bentwaters* (AFWL, 1973).

## 5 FUNCTIONAL PERFORMANCE AS PART OF PAVEMENT LIFE-CYCLE ANALYSIS

### Introduction

Field experience has shown that pavement design based on traffic load structural considerations alone does not provide for all functional conditions, thus unexpected maintenance and repair expenditures may occur. Such observations, in part, led to development and application of the systems life-cycle approach to pavement design.<sup>131</sup> This approach was emphasized when the Texas Highway Department in 1968 initiated a cooperative research project entitled "A Systems Approach Applied to Pavement Design and Research." The Texas cooperative research program has produced several important findings, and has demonstrated the importance of life-cycle systems analysis.<sup>132,133,134,135,136,137</sup>

### Pavement Management

The term *pavement management* includes more than pavement design; it encompasses the management of a pavement network from the time it is planned until it is salvaged. Such a process consists of pavement design, construction, maintenance, repair, and continuous performance monitoring to provide data for feedback information.

<sup>131</sup>W.R. Hudson, E.N. Finn, B.F. McCullough, K. Nair, and B.A. Vallerga, *Systems Approach to Pavement Design, Systems Formulation, Performance Definition, and Materials Characterization*, Final Report, NCHRP Project 1-10 (Materials Research and Development, Inc., 1968).

<sup>132</sup>R.C.G. Haas, *Developing a Pavement Feedback Data System*, Research Report No. 123-4 (Texas Highway Department; The University of Texas at Austin; Texas A&M University; 1971).

<sup>133</sup>W.R. Hudson, B. Frank McCullough, F.H. Scrivner, and James L. Brown, *A Systems Approach Applied to Pavement Design and Research*, Research Report 123-1 (Texas Highway Department, 1972).

<sup>134</sup>O.G. Strom, W.R. Hudson, and J.L. Brown, *A Pavement Feedback DATA System*, Research Report 123-12 (Texas Highway Department, 1970).

<sup>135</sup>M.I. Darter and W.R. Hudson, *Application of Probabilistic Concepts to Flexible Pavement System Design*, Research Report 123-18 (Texas Highway Department, 1973).

<sup>136</sup>M.Y. Shahin and B.F. McCullough, *Prediction of Low-Temperature and Thermal Fatigue Cracking in Flexible Pavements*, Research Report 123-14 (Texas Highway Department).

<sup>137</sup>R.K. Kher, W.R. Hudson, and B.F. McCullough, *A System Analysis of Rigid Pavement Design*, Research Report 123-5 (Texas Highway Department, 1970).

Before further discussion, it is important to define the terms maintenance and repair as used here. *Pavement maintenance* is the activity necessary to keep the pavement operating at its present capability. Maintenance can be minor or major. Minor maintenance consists of routine activities such as crack filling, patching of small areas, filling potholes, and joint filling. Major maintenance usually requires special consideration by the management staff and includes activities such as concrete slab-jacking and patching of larger areas.

*Pavement repair* is the activity necessary to restore the pavement to its initial operating capability rather than increasing its strength to meet new traffic demand (which is classified as construction). Typical repair processes include overlay and slab replacement. It is useful to further define the term based on the main reason for the repair. *Structural repair* is performed to restore the pavement's load-carrying capacity, while *functional repair* is performed to restore the skid and/or smoothness properties. It should be emphasized that a structural repair may also improve the functional condition of the pavement and similarly, functional repair may improve the pavement's load-carrying capacity.

Both maintenance and repair activities should be well-coordinated in order for the pavement management system to be successful in minimizing total expenditures. This coordination can be achieved only by continuous monitoring of traffic and the structural and functional conditions of the pavement, and storage of the observations in a data base in order to update the original design strategies for use in planning future maintenance and repair. Figure 68 shows how the coordination of maintenance and repair activities can be achieved within a pavement management system. Following is a brief description of the components of the figure.

**1. Monitor Performance and Evaluate Needs:** After the pavement has been constructed, its structural and functional performance should be continuously monitored and its maintenance and repair needs should be evaluated.

**2. Minor Maintenance:** The day-to-day routine maintenance work such as filling cracks and joints.

**3. Major Maintenance:** Before performing major maintenance such as patching of large areas, the

future need for functional or structural repair must be evaluated to optimize cost and traffic delay.

**4. Functional or Structural Repair:** Because of the interaction between structural and functional repair, the type of repair should be selected to optimize cost and minimize traffic delay.

**5. Updated Functional and Structural Records:** After major maintenance or repair, functional and structural records should be updated and stored in the data base for future reference.

### **Present Status of Management System Being Developed by CERL**

CERL is developing several computer programs in response to the requirements of the systems approach to pavement analysis and design. At present, these programs are applicable to certain classes of problems.

LIFE1 is a program for life-cycle costing of pavement design alternatives. It generates a set of designs based on the material properties of the subgrade and other available materials for construction of rigid and flexible pavements, and on the mission of the pavement as defined in terms of its function and expected traffic. In addition, it considers maintenance and repair strategies input by the user. At present, a maintenance or repair strategy is defined by a schedule for structural overlays and a budget level for routine maintenance. Costs based on information input by the user are computed for initial construction, overlay construction, routine maintenance, and delay of vehicle operations, as well as for aircraft maintenance related to pavement condition. The current version of LIFE1 is based largely on the design method for pavements developed and used by the Corps of Engineers. Current work includes the addition of a frost design procedure, and earthwork cost-estimation routine.

PAVER is a Management Information System for pavement facilities. It has a data base keyed to a grid system which contains information describing a set of pavements in a geographical area. This includes geometrical, condition, traffic, and environmental data; and material properties and unit costs for each section of pavement. The data base is organized in a hierarchical structure, and retrieval is facilitated by a generalized data management system called



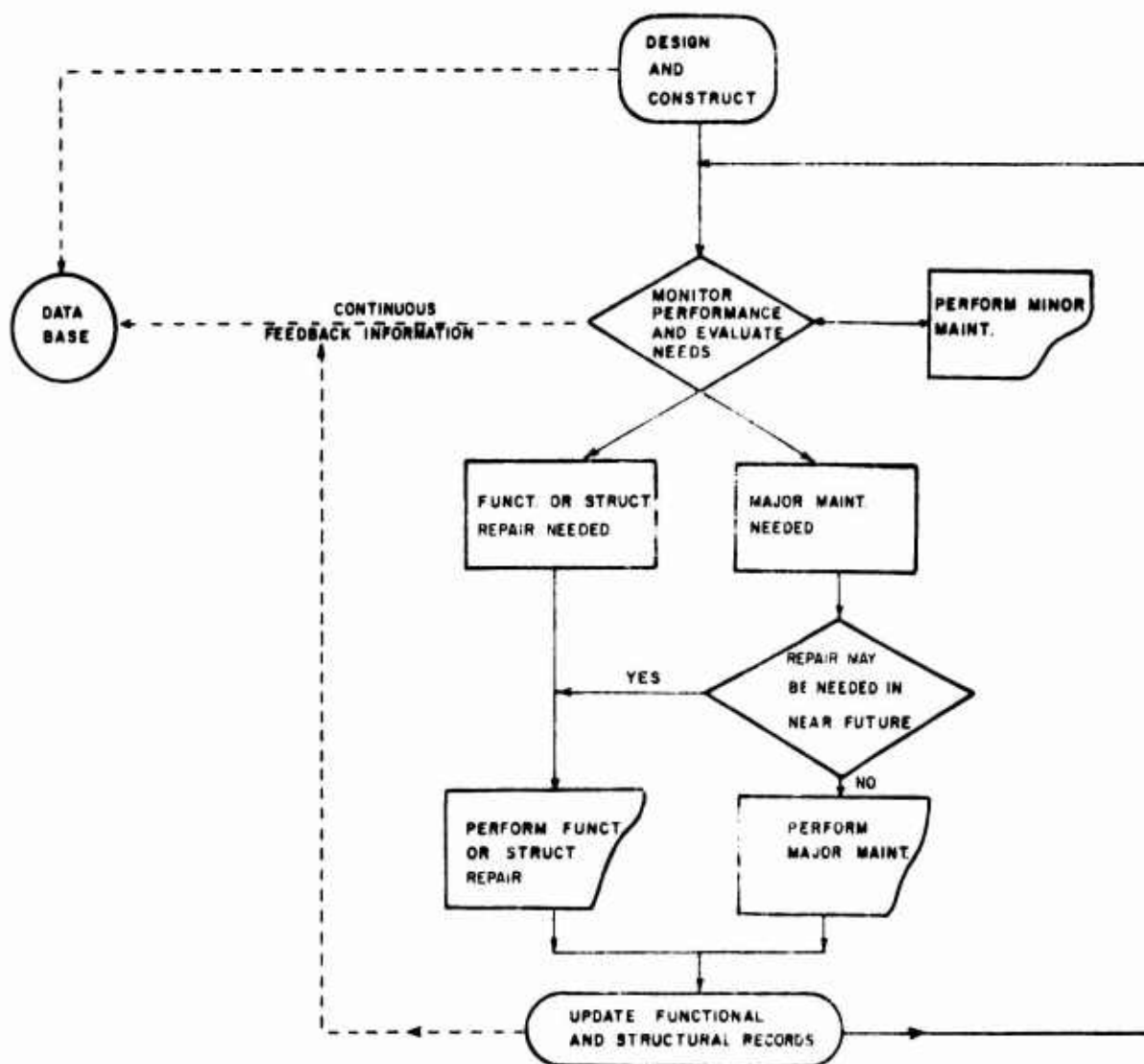


**Figure 68.** Coordination of maintenance and repair activities in pavement management system.

System 2000. A set of instructions, programmed in FORTRAN, interfaces with the data base and creates reports of interest to a variety of users. It is anticipated that the major users would be the facility engineer and his staff. Higher levels of command may desire summary information for use in comparing costs and performance at several bases or for entire commands.

LIFE1 and PAVER have been sponsored by the Corps of Engineers (the major sponsor) and the Air Force Weapons Laboratory. In response to the Air Force requirement to aid in evaluation and mainte-

nance planning for existing pavements, the PRE-FECT program is being developed to encompass the maintenance option of LIFE1. At present, LIFE1 does not consider functional performance as part of pavement life-cycle analysis.

#### **Preliminary Concepts for Incorporating Functional Performance Into Pavement Life-Cycle Analysis**

As mentioned earlier, functional requirements are primarily those of *comfort* and *safety*. The comfort of a pavement user is primarily a function of pave-

ment roughness. The level of roughness is usually low initially after construction and then increases with time and traffic until a limiting value is reached at which user comfort requirements are not satisfied.

The safety of a pavement user is affected by both the slipperiness and the roughness of the pavement. Skid resistance is usually high immediately after construction and then decreases with time and traffic until a limiting value is reached at which the probability of vehicle loss of control is higher than can be tolerated.

Corrective measures for slipperiness and roughness can vary considerably based on their objectives and on the structural condition of the pavement. For example, if the functional requirements of the users are exceeded by pavement slipperiness, the surface can be grooved or a surface treatment placed. However, if it is also determined that the pavement will soon need a structural repair, it may be more economical to apply a heavy overlay. Figure 69 shows an example of how the coordination between corrective measures for pavement slipperiness and structural deterioration can be achieved. Curve (a) shows that the skid index reached its limiting value at a time when the pavement had a high structural index; therefore only a seal coat or surface grooving would be needed to restore the surface skid resistance. Such a corrective measure may or may not affect the structural index. Curve (b) shows that the skid index reached its limiting value at a time when the structural index was close to reaching its limiting value. The most economical corrective measure in that case, as indicated in Figure 69, would be an overlay.

Similarly, if the functional requirements of the users are exceeded by pavement roughness, only major maintenance such as slabjacking could bring the roughness to an acceptable level. However, if it is also determined that the pavement needs a structural repair in the near future, it may be more economical to apply an overlay. Figure 70 is an example of how the corrective measures for pavement roughness and structural deterioration can be coordinated. Curve (c) shows that the roughness index reached its limiting value at a time when the structural index was significantly high; therefore major maintenance might be sufficient to lower the roughness index to an acceptable level. Such a corrective measure may or may not affect the structural index. Curve (d) shows the roughness index to reach its limiting value

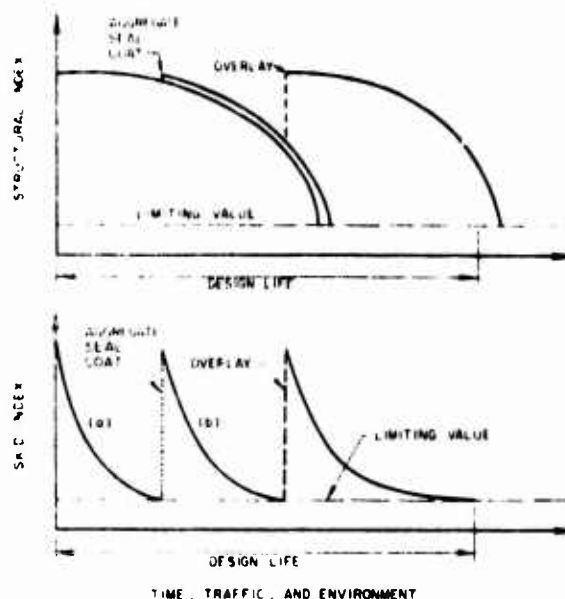


**Figure 69.** Coordination of corrective measures for pavement skid resistance and structural deterioration.

at the same time as the structural index was close to reaching its limiting value. The most economical corrective measure in that case, as indicated in Figure 70, would be an overlay.

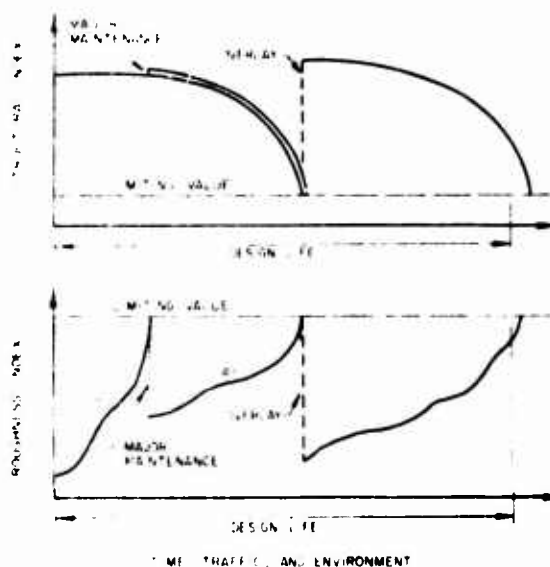


**Figure 70.** Coordination of corrective measures for pavement roughness and structural deterioration.

The examples presented in Figures 69 and 70 are extremely simplified since, in reality, optimization of



design, maintenance, and rehabilitation requires coordination among structural deterioration, slipperiness, and roughness at the same time. This coordination should be planned and optimized in the initial design stage, and also during evaluation of existing pavements for major maintenance or rehabilitation. The optimized coordinated design can be obtained only by comparing the available alternatives that can last for the desired design life in terms of time, traffic, and environment. Figure 71 shows a few of the possible alternatives that may be considered. Alternative 1 (Figure 71a) shows a pavement that is structurally designed to last about one third of the desired design life, with two overlays scheduled in the future. Alternative 2 (Figure 71b) shows a pavement that is structurally designed to last about half the design life, with an overlay and seal coat scheduled in the future. Alternative 3 (Figure 71c) shows a pavement that is structurally designed to last the entire design life, with two seal coats scheduled to keep the roughness and skid indexes from reaching their limiting values. It is to be emphasized that only a few of the possible alternatives are presented here. The number of possible alternatives will depend on the constraints specified by the designer, such as maximum number of overlays and seal coats during the design life, initial cost, and the limiting values for the structural and functional indexes.

The selection of an optimum alternative can be based on the present worth of the total cost and the average rideability during the design life of the pavement. An average rideability factor (ARF) is developed herein as follows:

$$ARF_i = (A_i/A)$$

where  $ARF_i$  = average rideability factor for design alternative  $i$ .

$A_i$  = area between roughness index curve(s) and roughness index limiting value for alternative  $i$ .

$A$  = design life in years times roughness index limiting value.

From the definition one can determine that the ARF has a minimum value of zero and a maximum value of one.

Figure 72 is a simplified example showing the calculation of the average rideability factor for two

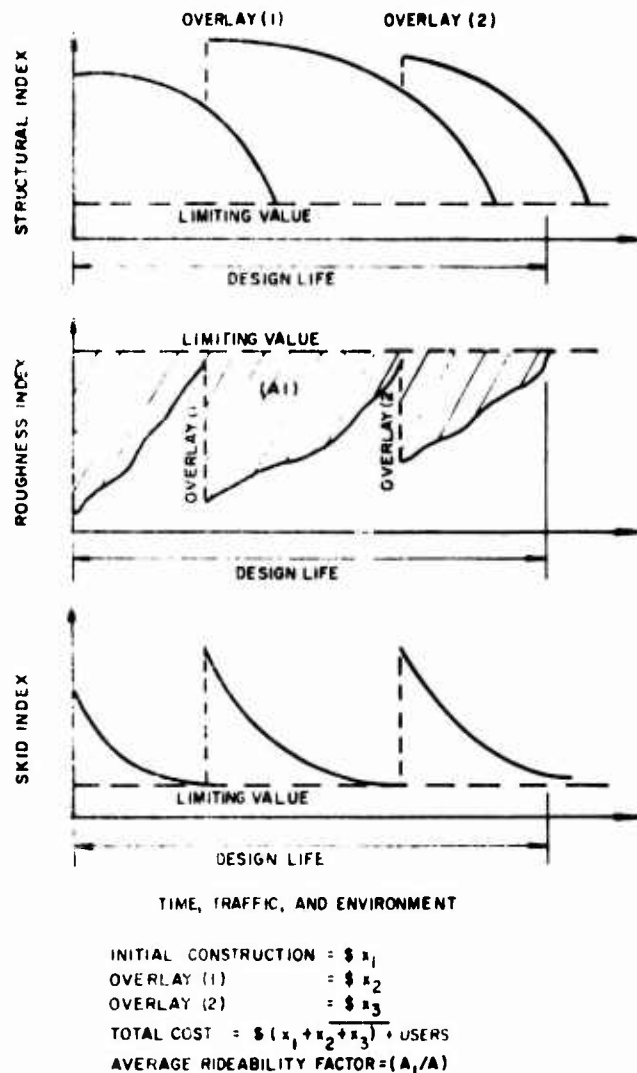


Figure 71a. Coordination of structural deterioration roughness, and slipperiness during pavement life-cycle, design alternative 1.

design alternatives. The following values were used in the example: Design Life = 20 years, Maximum Scale Value of Roughness Index = 10, Roughness Index Limiting Value = 6.

The ARF has the following merits:

1. It describes the rideability history in one number.
2. It provides the designer with a guide for selecting from design alternatives that have the same cost.
3. It allows the designer to specify a minimum average rideability value as a constraint to reduce the

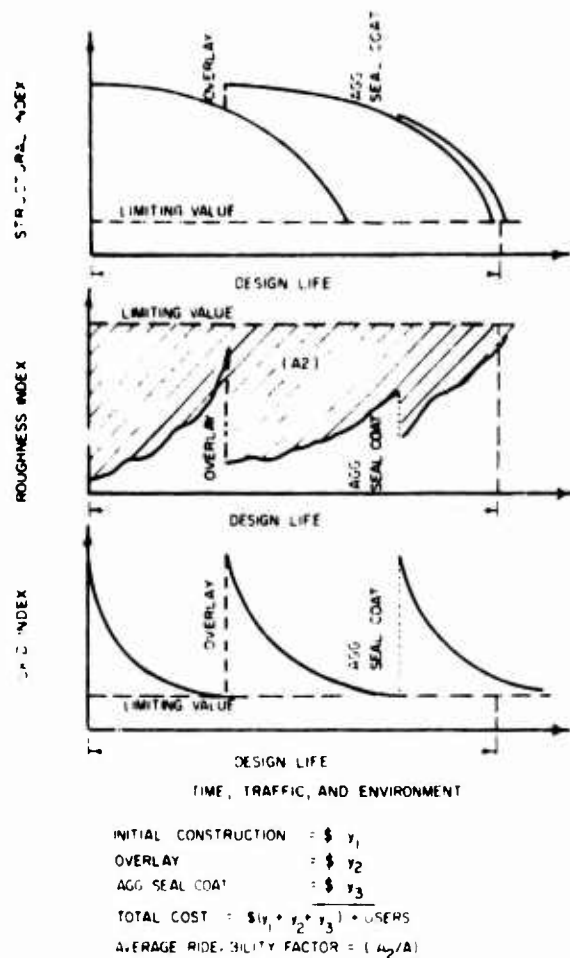


Figure 71b. Design alternative 2.

number of available design alternatives.

4. It can be used to compare the rideability history of different classes of pavements regardless of the roughness index limiting values assigned to them (Figure 73).

5. Its value does not vary when the roughness index scale is changed.

Functional performance requirements of pavements and development of models to predict their variation with traffic, time, and environment must be viewed in a system framework. Functional performance of pavements is generally related to their structural performance. Occurrence of structural distress such as cracking does not necessarily mean a functional failure; however, roughness usually occurs some time after the initial structural distress. Similarly, rutting or permanent deforma-

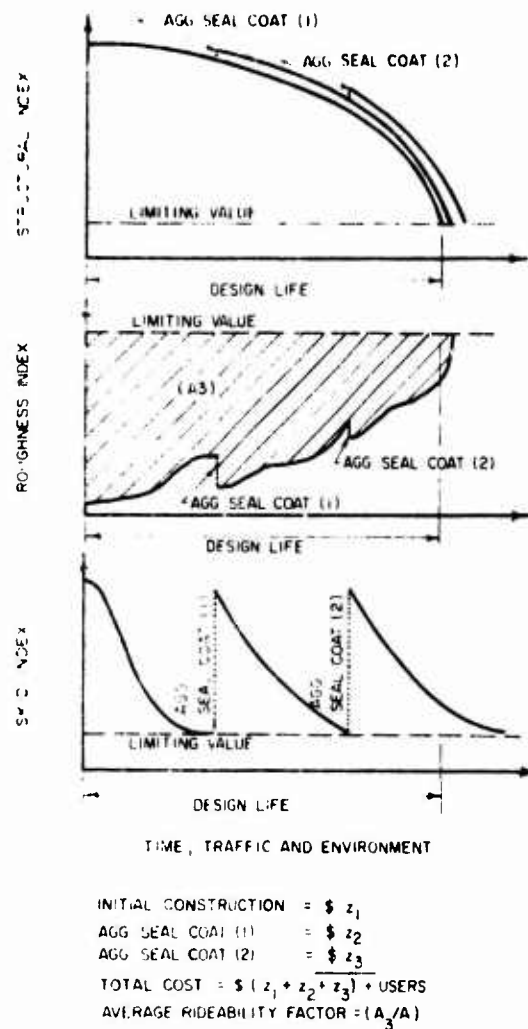
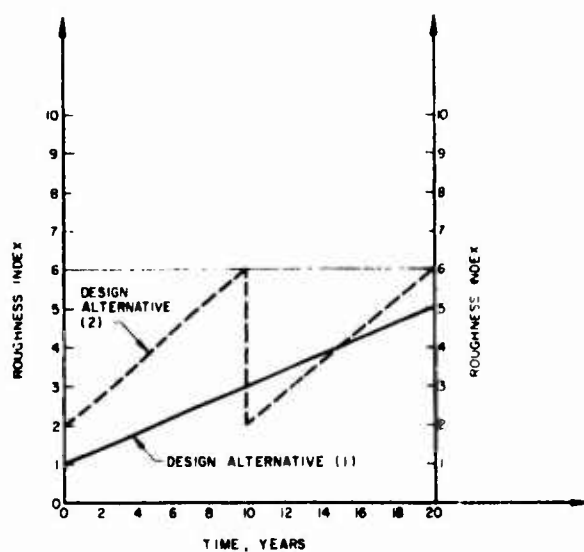


Figure 71c. Design alternative 3.

tion can increase hydroplaning potential by allowing greater water accumulation during heavy rains. Therefore, it is evident that structural distress, safety, and comfort are all related and that any adequate pavement life-cycle design system should account for all factors and their interactions.

Figure 74 summarizes the concepts mentioned above, showing only the structural/functional subsystem portion of an entire pavement system. A brief description of each component of the figure is given below.

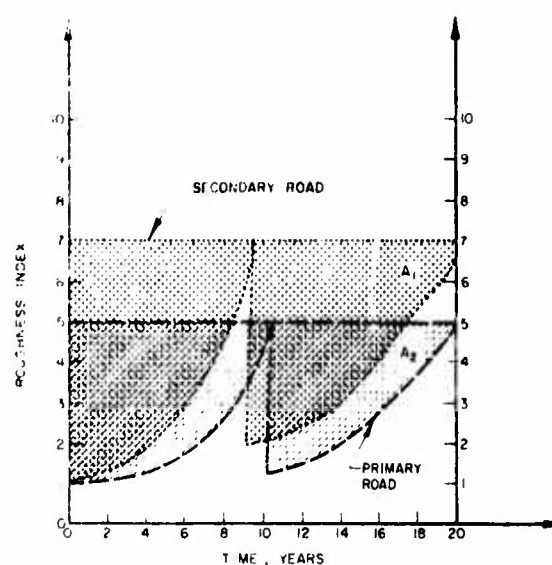
1. Inputs: All necessary data on materials, loads, environment, maintenance, costs, etc.
2. Structural Models: Models based on theory or empirically derived to predict pavement structural



$$A \cdot R \cdot F_1 = \left\{ 20 \times \left( \frac{5+1}{2} \right) \right\} / \{ 20 \times 6 \} = 0.5$$

$$A \cdot R \cdot F_2 = \left\{ 10 \times \frac{4}{2} + 10 \times \frac{4}{2} \right\} / \{ 20 \times 6 \} = 0.33$$

**Figure 72.** Example calculation of average rideability factor (ARF) for two design alternatives.



$$ARF_1 = \frac{A_1}{7 \times 20} \quad ARF_2 = \frac{A_2}{5 \times 20}$$

**Figure 73.** Primary and secondary roads that have the same rideability factor (ARF) but different roughness index limiting values.

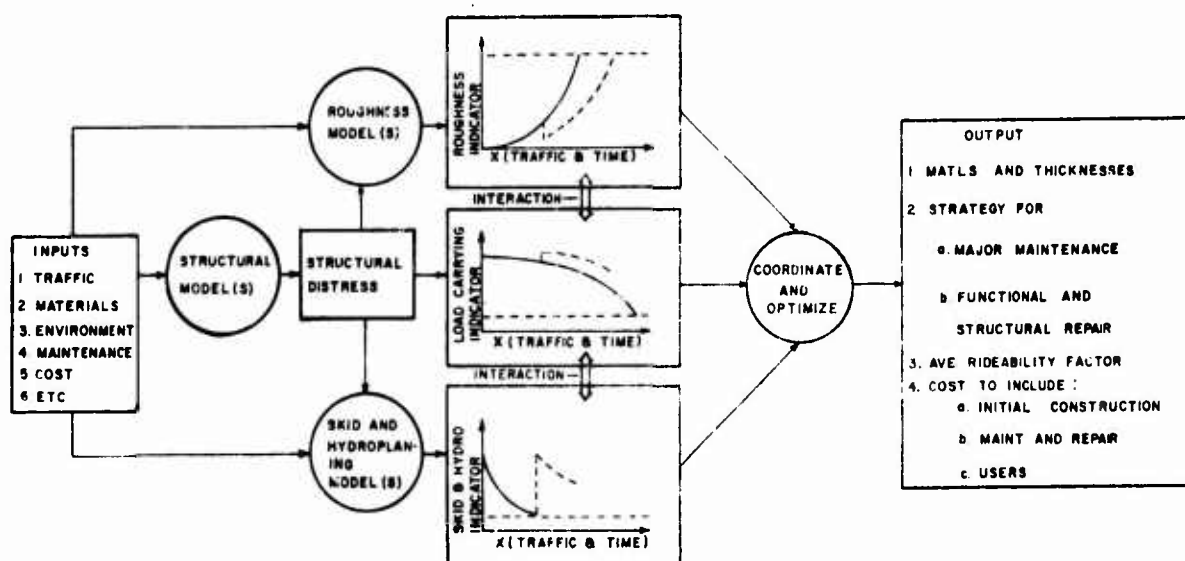


**Figure 74.** Consideration of functional performance in pavement life-cycle analysis.

distress as a function of traffic environment and time.

3. **Structural Distress:** Distress such as fracture, distortion, and disintegration.

4. **Roughness Models:** Models to predict the increase in roughness indicators as a function of traffic, environment, and time.

5. **Skid, Hydroplaning Models:** Models to predict the increase in skid and hydroplaning potential as a function of traffic, environment, and time.

6. **Coordinate and Optimize:** Based on pre-set limiting levels for structural and functional indicators, develop and optimize strategies for major maintenance, structural, and/or functional repair.

7. **Outputs:** Recommended materials and thicknesses to be used, strategies for maintenance and repair, average rideability factor, and total costs over the entire life of the pavement (including users' costs due to structural damage of vehicles or delay time), for each life-cycle design considered.

The development and implementation of accurate predictive models to incorporate functional performance considerations into life-cycle design and analysis, as shown in Figure 74, requires extensive research and long-term performance data from in-service pavements. These are not currently available. Empirical relationships, however, can be developed at present for first-order approximation. The development can be based upon available data, limited research, and engineering judgment. Methodology must be developed concurrently, to coordinate and optimize the structural and functional considerations. Once developed, these approximate predictive models and optimization techniques could be implemented into the pavement management system. The resulting feedback performance information collected from in-service pavements could be used for development of more accurate models.

## **6 SUMMARY, CONCLUSIONS, AND RECOMMENDATIONS**

### **Summary**

Chapters 1 and 2 defined pavement functional performance and identified functional condition

indicators. Functional performance was defined as the trend of the level of service provided to the pavement users throughout the initial life of the pavement and between repairs. Chapters 3 and 4 described the state of the art of measuring and evaluating the most significant functional condition indicators: roughness and skid resistance. Following is the state-of-the-art summary of indicators that can be used for measuring roughness and skid resistance.

#### *Roughness Indicators*

1. Roughness Index
2. Slope Variance
3. Wavelength, Amplitude
4. Acceleration
5. Absorbed Power
6. Subjective Evaluation

#### *Skid Resistance Indicators*

1. Friction coefficient measured with trailers with locked wheels.
2. Friction coefficient measured with trailers with unlocked wheels making a yaw angle with the direction of travel.
3. Friction coefficient measured with trailers with rolling wheels in the slip mode.
4. Reading obtained from a decelerometer installed in a vehicle.
5. The ratio between wet and dry stopping distance for an automobile applying brakes at a given speed.
6. Friction coefficient measured by portable field instruments.
7. Friction coefficient measured by laboratory equipment.
8. A code for the surface texture.

Tentative recommendations relative to appropriate roughness and skid resistance indicators for various evaluation purposes and types of pavements were presented in Tables 3, 4 (Chapter 3) and 5 (Chapter 4).

Chapter 5 presented concepts for incorporating functional consideration of roughness and skid resistance into pavement life-cycle analysis. Included were examples of how to coordinate maintenance and repair activities for structural deterioration, roughness, and slipperiness. It was suggested that selection of the optimum design alternative be based

on the present worth of the total cost and the average rideability factor (which was introduced and defined). Finally, a chart showing the structural/functional subsystem portion of an entire pavement system was presented.

## Conclusions

1. The consideration of only structural integrity in pavement life-cycle design does not adequately account for the users' functional requirements. Therefore, direct consideration of user-related functional indicators such as roughness and slipperiness is necessary for complete analysis of pavement life-cycle design.

2. Important indicators of pavement functional condition are roughness, skid resistance and hydroplaning, appearance, foreign objects on pavement surfaces, and maintenance and repair activities which cause delay or increased cost to users.

3. It is possible to measure several roughness indicators. Each of these indicators will serve some objectives better than others. One significant indicator, absorbed power, has not yet been developed sufficiently but is under investigation at Waterways Experiment Station and Air Force Weapons Laboratory. Other indicators are certainly needed to give more adequate information on vehicle structural damage and electronic equipment damage due to roughness.

4. The state of the art for measuring and evaluating skid and hydroplaning shows that while several methods are available for measuring skid resistance, there are no direct methods for measuring hydroplaning potential. Furthermore, selection of the appropriate skid resistance indicators depends primarily on the characteristics—especially speed—of vehicles using the pavement facility.

5. Although the state of the art for evaluating roughness and skid resistance does not provide adequate data to develop accurate models for predicting the variation of roughness and skid indicators with time, traffic, and environment, it does provide information for development of approximate models.

## Recommendations

Functional considerations should be included in pavement life-cycle analysis (design, maintenance, and rehabilitation). To achieve this, the following work is recommended:

1. Models should be developed to predict the variation of significant functional indicators (such as roughness and skid resistance) with time, traffic, and environment. Complete development and verification of these models requires extensive research over several years. However, approximate models can be developed from existing state-of-the-art technology and limited research. These approximate models can then be refined as more information becomes available.

2. Limiting criteria should be developed for each functional condition indicator and specific class of pavement.

3. A decision-making methodology should be developed for selecting appropriate maintenance and repair.

4. Work items 1, 2, and 3 should be implemented into pavement life-cycle analysis (design, maintenance, and repair). This will require development of a coordination and optimization technique in order to select the optimum design alternative.

## APPENDIX: INTRODUCTION TO POWER SPECTRAL DENSITY

### Definition of Sample Function and Stationary Process

A sample function of a random process is a function whose record does not have an obvious pattern; for example, the profile of a pavement surface for a given distance. A random process is an infinite ensemble of sample functions (Figure A1).

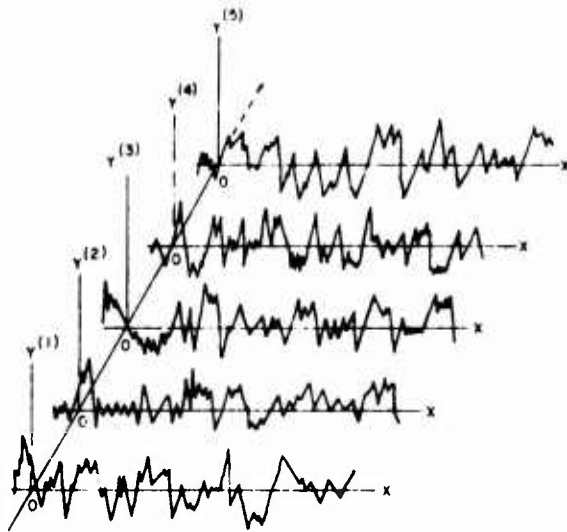


**Figure A1.** Schematic representation of a random process as an ensemble of sample functions  $y(j)(x)$ .

A random process is said to be stationary if its probability distributions are invariant from one section of a given pavement to another section of the same pavement. In particular, the first-order probability density  $p(y)$  becomes a universal distribution for a given pavement, independent of the examined section. The assumption of stationary trends is significant in the analysis of highway profiles, since only a few sections of a given highway can be examined practically. This is not necessarily true for runways, since current technology allows an entire runway profile to be examined.

### Statistical Definitions

The following definitions of statistical parameters are presented to illustrate the power spectral density concept.

- (1) The "mean" or "expected value" of a function

$y, E[y]$ , can be calculated if the first-order probability density of  $y$  is known:

$$E[y] = \int_{-\infty}^{\infty} y p(y) dy \quad [\text{Eq A1}]$$

For a sample function of length  $X$ , the mean of  $y$  can be estimated as follows:

$$M[y] = \frac{1}{X} \int_{-\frac{X}{2}}^{\frac{X}{2}} y(x) dx \quad [\text{Eq A2}]$$

Notice that  $M[y]$  will equal  $E[y]$  if the process is stationary.

- (2) Similarly, the "mean square" of a function  $y$  is defined as follows:

$$E[y^2] = \int_{-\infty}^{\infty} y^2 p(y) dy \quad [\text{Eq A3}]$$

For a sample function of length  $X$ , the mean square of  $y$  can be estimated as follows:

$$M[y^2] = \frac{1}{X} \int_{-\frac{X}{2}}^{\frac{X}{2}} y^2(x) dx \quad [\text{Eq A4}]$$

- (3) The "root mean square" of a function  $y$  is defined as the square root of the mean square of  $y$ .

$$\begin{aligned} \text{rms } [y] &= \sqrt{E[y^2]} \\ &= \sqrt{M[y^2]} \quad \text{If the process is stationary.} \dots \end{aligned} \quad [\text{Eq A5}]$$

- (4) The "variance" of a function  $y$ ,  $\sigma_y^2$ , is defined as the expected value of  $(y - E[y])^2$

$$\begin{aligned} \sigma_y^2 &= E[(y - E[y])^2] \\ &= \int_{-\infty}^{\infty} (y - E[y])^2 p(y) dy \\ &= E[y^2] - (E[y])^2 \end{aligned} \quad [\text{Eq A6}]$$

Equation A6 shows that the variance of  $y$  is equal to its "mean square" minus the square of its "mean."

(5) The "standard deviation" of a function  $y$ ,  $\sigma_y$ , is defined as the square root of its variance:

$$\sigma_y = \sqrt{\sigma_y^2} \quad [\text{Eq A7}]$$

(6) The "autocorrelation" of two functions  $y^{(1)}$  and  $y^{(2)}$ ,  $E[y^{(1)} y^{(2)}]$ , is the expected value of their products:

$$E[y^{(1)} y^{(2)}] = \int_{-\infty}^{\infty} \int_{-\infty}^{\infty} y^{(1)} y^{(2)} p(y^{(1)}, y^{(2)}) dy^{(1)} dy^{(2)}$$

In the analysis of a sample function  $y(x)$  of length  $X$ , an autocorrelation function between  $y(x)$  and another function  $y(x+\tau)$ , where  $\tau$  is a specified increment on the  $x$  scale, is referred to as  $R(\tau)$ ; where

$$R(\tau) = \lim_{X \rightarrow \infty} \frac{1}{X} \int_{-\frac{X}{2}}^{\frac{X}{2}} y(x) y(x+\tau) dx$$

However, if the function is stationary,  $R(\tau)$  can be rewritten as follows:

$$R(\tau) = \frac{1}{X} \int_{-\frac{X}{2}}^{\frac{X}{2}} y(x) y(x+\tau) dx \quad [\text{Eq A8}]$$

It should be noted that when  $\tau=0$  in Equation A8, the autocorrelation  $R(0)$  becomes:

$$R(0) = \frac{1}{X} \int_{-\frac{X}{2}}^{\frac{X}{2}} y^2(x) dx \quad [\text{Eq A9}]$$

which is the mean square of  $y$ .

Figure A2 is a schematic diagram of the variation of the normalized autocorrelation function  $R(\tau)/R(0)$  with  $\tau$  value. Note that  $R(\tau)$  is maximum at  $\tau=0$ , which represents the state of perfect correlation.

## Fourier Integrals

From the Fourier integral theorem, a function  $y(x)$  defined from  $x = -\infty$  to  $x = \infty$ , can be represented by

superposition of sinusoids as follows:

$$y(x) = \frac{1}{2\pi} \int_{-\infty}^{\infty} F(w) e^{iwx} dw \quad [\text{Eq A10}]$$

where  $F(w)$  is the Fourier transform of  $y(x)$  and is expressed as follows:

$$F(w) = \int_{-\infty}^{\infty} y(x) e^{-iwx} dx \quad [\text{Eq A11}]$$

where  $w$  is the radian frequency of the sinusoids (radian selected unit\*)

$$w = 2\pi f$$

$f$  = the frequency in cycles/selected unit.\*

Equations A10 and A11 show that  $F(w)$  is a representative of  $y(x)$ , but in the frequency domain.

Equation A11 can be rewritten as follows:

$$F(w) = \int_{-\infty}^{\infty} y(x) (\cos wx - i \sin wx) dx$$

In the case where  $y(x)$  is an even function, i.e.,  $y(x) = y(-x)$ , the complex component  $y(x) \cdot (-i \sin wx)$  is zero; therefore,

$$F(w) = \int_{-\infty}^{\infty} y(x) \cos wx dx \quad [\text{Eq A12}]$$

if  $y(x)$  is an even function.

## The Power Spectral Density Theorem

The previous section demonstrated that a function can be represented in terms of sinusoids of continuously varying frequencies. The same concept can be applied to the autocorrelation function  $R(\tau)$  of a sample function  $y(x)$ . The resulting Fourier transform of  $R(\tau)$  is also the power spectral density of  $y(x)$ :

$$R(\tau) = \frac{1}{2\pi} \int_{-\infty}^{\infty} p(w) e^{i\tau w} dw \quad [\text{Eq A13a}]$$

\*The unit selected in the analysis of highway profile is usually "feet."

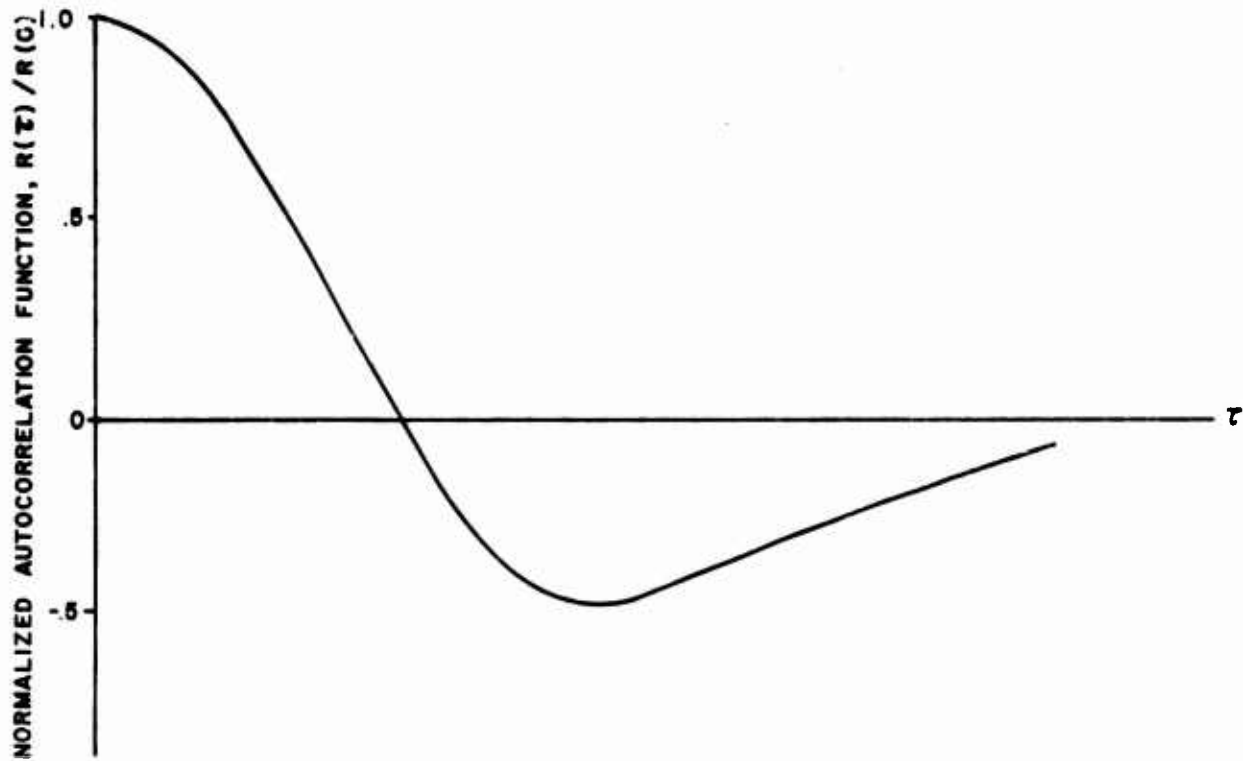


**Figure A2.** A schematic diagram of the normalized autocorrelation function for different  $\tau$  values.

and 
$$P(w)^* = \int_{-\infty}^{\infty} R(\tau) \cos w\tau d\tau \quad [\text{Eq A13b}]$$

where  $P(w)$  is the Fourier transform of  $R(\tau)$  and the power spectral density of  $y(x)$ .

To illustrate the physical meaning of the power spectral density, consider the limiting case where  $\tau=0$ :

$$\begin{aligned} R(0) &= \text{mean square of } y(x) = \frac{1}{X} \int_{-\frac{X}{2}}^{\frac{X}{2}} y^2(x) dx \quad \text{from Eq A9} \\ &= \frac{1}{2\pi} \int_{-\infty}^{\infty} P(w) dw \quad \text{from Eq A13} \end{aligned}$$

This may be interpreted such that  $P(w)dw$  represents the contribution to the mean square of  $y(x)$  from frequencies between  $w$  and  $w+dw$ . From this interpretation one may find that the units of the power spectral density are the mean square of function considered/unit frequency.

Since the type frequency often used is cycles/selected unit,  $f$ , rather than radians/selected unit,  $w$ , Equations A13 and A14 for calculation of the power spectral density can be rewritten in terms of  $f$  as follows:

$$R(\tau) = \int_{-\infty}^{\infty} P(f) e^{i2\pi f\tau} df \quad [\text{Eq A14a}]$$

and

$$P(f) = \int_{-\infty}^{\infty} R(\tau) e^{-i2\pi f\tau} d\tau \quad [\text{Eq A14b}]$$

---

\*Note that  $R(\tau)$  is an even function, i.e.,  $R(\tau) = R(-\tau)$ .

Equations A14a and A14b can be written as a summation over the positive frequency and lag



values respectively:

$$R(\tau) = 2 \int_0^{\infty} P(f) e^{i2\pi f \tau} df \quad [\text{Eq A15a}]$$

and

$$P(f) = 2 \int_0^{\infty} R(\tau) e^{-i2\pi f \tau} d\tau \quad [\text{Eq A15b}]$$

The power spectral density  $P(f)$  of a sample function  $y(x)$  can be determined experimentally or computed digitally. Both methods are briefly presented in the next two sections.

### Experimental Determination

The power spectral density of a sample function  $y(x)$  can be determined experimentally by using the special case when the lag value  $\tau = 0$  in Equation A15a.

$$R(0) = \text{mean square value of } y = 2 \int_0^{\infty} P(f) df \quad [\text{Eq A16}]$$

From Equation A16 it is clear that the power spectral density describes the frequency composition of the sample function in terms of its mean square value.

If the sample record is passed through a bandpass filter and then the average of the squared value of the filter output is computed, an estimate is obtained of the mean square value of the sample record's content in the frequency band for which the filter is set.<sup>118</sup>

The output of the filter is then the mean square of all sinusoidal constituents of the original sample function,  $y(x)$ , having frequencies between  $f$  and  $(f + \Delta f)$ . The power spectral density can be estimated as  $^{119}$  (mean square value/unit frequency):

$$P(f) \cong \frac{1}{2} \{R_{L+1} - R_L\} / \Delta f \quad [\text{Eq A17}]$$

<sup>118</sup>A.D. Brickman et al., *Analysis of Pavement Profile* (Pennsylvania Transportation and Traffic Safety Center, 1969).

Figure A3 shows a summary of the experimental procedure for estimating  $P(f)$ . It should be noted that this method is only accurate when  $\Delta f$  approaches zero.

### Digital Computation

The power spectral density  $P(f)$  of a sample function  $y(x)$  can be computed digitally by first computing the autocorrelation function  $R(\tau)$  of  $y(x)$  using the following equations:

$$R^*(\tau) = \frac{1}{X} \int_{-\frac{X}{2}}^{\frac{X}{2}} y(x) y(x + \tau) dx \quad \text{from Eq A8}$$

$$= \frac{1}{X} \int_0^X y(x) y(x + \tau) dx \quad [\text{Eq A18}]$$

$$P^*(f) = 2 \int_0^{\infty} R(\tau) e^{-i2\pi f \tau} d\tau \quad \text{from Eq A15b}$$

$$= 2 \int_0^{\infty} R(\tau) \cos 2\pi f \tau d\tau \quad [\text{Eq A19}]$$

The algorithms and computer program for calculating  $R(\tau)$  and  $P(f)$  from the above equations are given in Hutchinson.<sup>119</sup>

### Average Amplitude Corresponding to Each Power Value

As shown in Equation A16, the mean square value of a sample function  $y(x)$  can be expressed in terms of the power spectral density as follows:

$$\text{mean square value of } y \cong R(0) = 2 \int_0^{\infty} P(f) df$$

\* $y(x)$  is assumed to be stationary and  $R(\tau)$  is an even function.

<sup>119</sup>B.G. Hutchinson, *Analysis of Road Roughness Records by Power Spectral Density Techniques*, Final Report No. 101 (Department of Highways, Ontario, Canada, 1965).

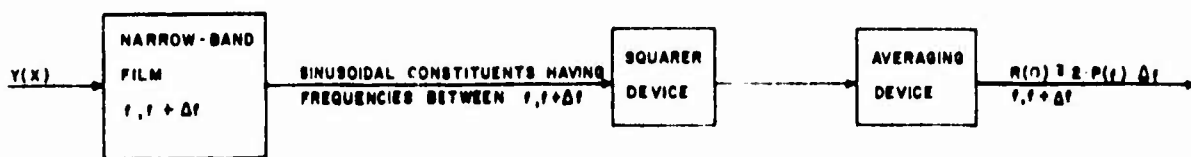


Figure A3. Experimental determination of power spectral density of a sample function  $y(x)$ .

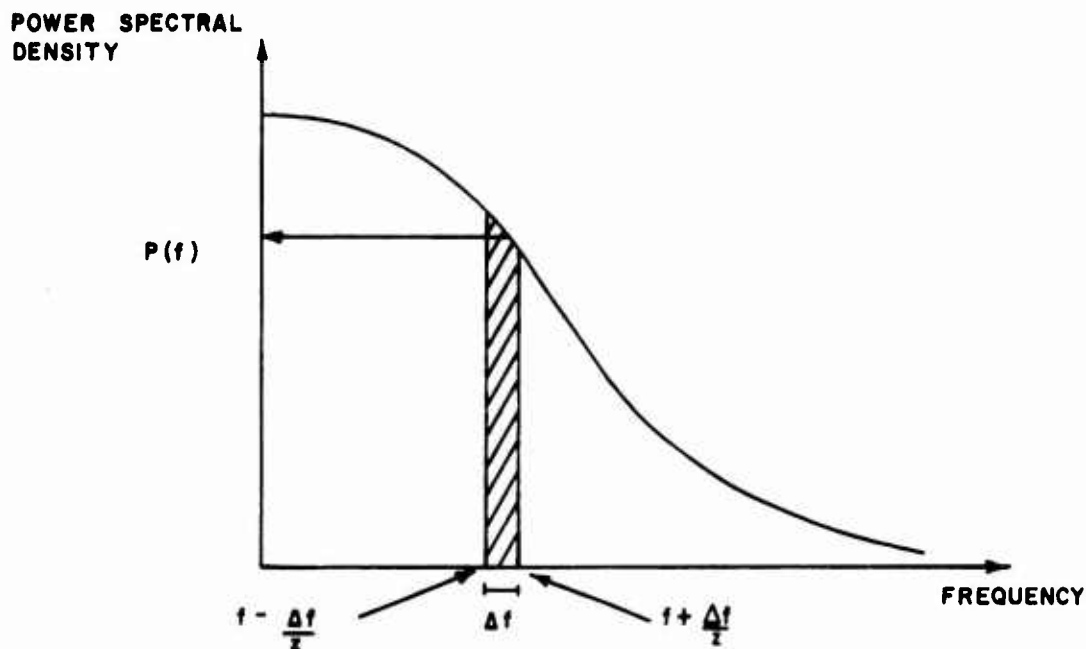


Figure A4. A schematic diagram of power spectral density vs frequency.

This relationship is expressed graphically in Figure A4, which indicates that the mean square value of the sinusoidal constituents of  $y$  having frequencies between  $(f - \Delta f/2)$  and  $(f + \Delta f/2)$  is equal to twice the hatched area, i.e.:

mean square value of  $y$

$$\text{between } (f - \frac{\Delta f}{2}), (f + \frac{\Delta f}{2}) = 2 P(f) \cdot \Delta f \quad [\text{Eq A20}]$$

By assuming a sine function whose amplitude is  $A$ , one can show that the mean square of the function is equal to  $A^2/2$  (Figure A5).

Substituting this relationship into Equation A20:

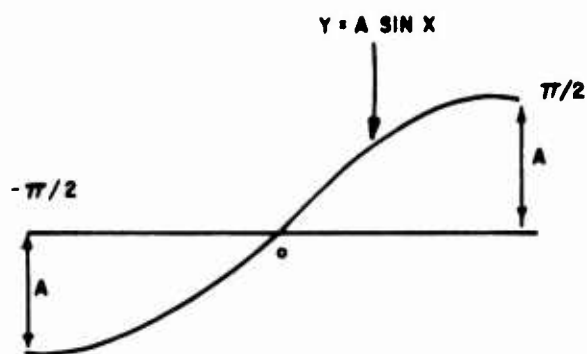
$$\frac{A^2}{2} = 2P(f) \Delta f$$

or

$$A = 2 \sqrt{P(f) \Delta f} \quad [\text{Eq A21}]$$

It should be emphasized that  $A$  is the *average* amplitude of the sinusoidal constituents of  $y(x)$  in the frequency range  $(f - \Delta f/2)$  and  $(f + \Delta f/2)$ . Therefore, it will be more appropriate to write Equation A21 as follows:

$$\bar{A} = 2 \sqrt{P(f) \Delta f} \quad [\text{Eq A22}]$$



$$E[y^2] = \frac{1}{\pi} \int_{-\pi/2}^{\pi/2} (A \sin x)^2 dx$$

$$= \frac{A^2}{2}$$

**Figure A5.** Mean square of a sine function  $y(x)$  in terms of its amplitude.

## CITED REFERENCES

- A Comparison of Aircraft and Ground Vehicle Stopping Performance on Dry, Wet, Flooded, Slush, Snow, and Ice Covered Runways*, NASA Technical Note D-6098 (1970).
- AASHTO Road Test: Report 5—Pavement Research*, Special Report 61-E (Highway Research Board [HRB], 1962).
- Argue, G.H., *A Canadian Evaluation Study of Road Meters*, Special Report 133 (HRB, 1973).
- Ballentine, G.D. and P.V. Compton, *Procedures for Conducting the Air Force Weapons Laboratory Standard Skid Resistance Test* (Air Force Weapons Laboratory [AFWL], 1973).
- Ballentine, G.D. and P.V. Compton, *Evaluation of Runway Skid Resistance Characteristics of Royal Air Force Bentwaters* (AFWL, 1973).
- Brickman, A.D. et al., *Analysis of Pavement Profile* (Pennsylvania Department of Transportation, 1969).
- Brickman, A.D., J.C. Wambold, and J.R. Zimmerman, *An Amplitude-Frequency Description of Road Roughness*, Special Report 116 (HRB, 1974).
- Brokaw, M.P., *Development of an Automatic Electromechanical Null-Seeking Device for the PCA Road Meter*, Special Report 133 (HRB, 1973).
- Burns, J.C. and R.J. Peters, *Surface Friction Study of Arizona Highways*, Highway Research Record [HRR] 471 (HRB, 1973).
- Butterworth, C.K. and D.E. Boozer, *C-141A Computer Code for Runway Roughness Studies*, AFWL-TR-70-71 (AFWL, 1970).
- Canadian Good Roads Association, Pavement Design and Evaluation Committee, *A Guide to the Structural Design of Flexible and Rigid Pavements in Canada* (Canadian Good Roads Association [CGRA], 1965).
- Canadian Good Roads Association, Pavement Design and Evaluation Committee, "Field Performance Studies of Flexible Pavements in Canada," *Proceedings, Second International Conference on Structural Design of Asphalt Pavements* (University of Michigan, 1967).
- Canadian Good Roads Association, *Manual on Pavement Investigations*, Technical Publication No. 11 (CGRA, 1959).
- Canadian Good Roads Association, Pavement Design and Evaluation Committee, "Pavement Evaluation Studies in Canada," *Proceedings, International Conference on Structural Design of Asphalt Pavements* (University of Michigan, 1962).
- Carey, W.N. and P.E. Irick, *The Pavement Serviceability—Performance Concept*, Bulletin 250 (HRB, 1960).
- Chong, G.J., *Measurement of Road Rideability in Ontario*, Report 1R 29 (Department of Transportation and Communications of Ontario, 1969).
- Chong, G.J. and W.A. Phang, *PCA Road Meter Measuring Road Roughness at 50 mph*, Special Report No. 133 (HRB, 1973).

- Coleman, T.L. and A.W. Hall, *Implications of Recent Investigations on Runway Roughness Criteria*, paper presented to AGARD, NATO, Paris (1963).
- Culley, R.W., *Roughness Index Standards for Saskatchewan Pavements*, Technical Report 1 (Saskatchewan Department of Highways, 1966).
- Darlington, J.R., *Evaluation and Application Study of the General Motors Corporation Rapid Travel Profilometer*, Research Report No. R-731 (State of Michigan, Department of State Highways, 1970).
- Darter, M.I., *Probabilistic Application to Rigid Pavement Structures*, paper presented at ASCE Specialty Conference on Probabilistic Applications to Engineering (Stanford University, 1974).
- Darter, M.I. and W.R. Hudson, *Application of Probabilistic Concepts to Flexible Pavement System Design*, Research Report 123-18 (Texas Highway Department, 1973).
- Gallaway, B.M. and J.G. Rose, *Comparison of Highway Pavement Friction Measurements Taken in the Cornering-Slip and Skid Modes*, HRR 376 (HRB, 1971).
- Gerardi, A. G. and A. K. Lohwasser, *Computer Program for the Prediction of Aircraft Response to Runway Roughness*, AFWL-TR 73-109, Vol 1 (AFWL, 1973).
- Gerardi, A.G. and A.K. Lohwasser, "A Digital Computer Program for Aircraft Runway Roughness Studies," *The Shock and Vibration Bulletin*, No. 43 [Part 2] (Naval Research Laboratory, 1973).
- Gillespie, T.D., W.E. Meyer, and R.R. Hegmon, *Skid Resistance Testing from a Statistical Viewpoint*, HRR 471 (HRB, 1973).
- Gregg, L.E. and W.S. Foy, "Triaxial Acceleration Analyses Applied to the Evaluation of Pavement Riding Qualities," *HRB Proceedings*, Vol 34 (HRB, 1955).
- Haas, R.C.G., *Developing a Pavement Feedback Data System*, Research Report No. 123-4 (Texas Highway Department: The University of Texas at Austin; Texas A&M University, 1971).
- Harris, C.M. and C.E. Crede, *Shock and Vibration Handbook*, 3 Vols (McGraw-Hill Book Company, Inc., 1961).
- Hudson, W.R., *High-Speed Road Profile Equipment Evaluation*, Research Report No. 73-1 (Center for Highway Research, The University of Texas at Austin, 1968).
- Hudson, W.R., B. Frank McCullough, F.H. Scrivner, and James L. Brown, *A Systems Approach Applied to Pavement Design and Research*, Research Report 123-1 (Texas Highway Department, 1970).
- Hudson, W.R., F.N. Finn, B.F. McCullough, K. Nair, and B.A. Vallerger, *Systems Approach to Pavement Design, Systems Formulation, Performance Definition, and Materials Characterization*, Final Report, NCHRP Project 1-10 (Materials Research and Development, Inc., 1968).
- Hudson, W.R., W.E. Teske, Karl H. Dunn, and E.B. Spangler, *State of the Art of Pavement Condition Evaluation*, Special Report 95 (HRB, 1968).
- Hughes, Patrick C., *Evaluation of the PCA Road Meter*, Special Report 133 (HRB, 1973).
- Hutchinson, B.G., *Analysis of Road Roughness Records by Power Spectral Density Techniques*, Final Report No. 101 (Department of Highways, Ontario, Canada, 1965).
- Hutchinson, B.G., *Principles of Subjective Rating Scale Construction*, HRR 46 (HRB, 1964).
- Hutton, G.B., *Uneven Runways Encountered by Subsonic Jet Transport Aircraft During Scheduled Airline Operations*, Technical Report 72095 (Royal Aircraft Establishment, 1972).
- Hveem, F.N., *Devices for Recording and Evaluating Pavement Roughness*, Bulletin 264 (HRB, 1960).

- Kher, R.K. and M.I. Darter, *Probabilistic Applications to AASHO Interim Guide for Design of Rigid Pavement Structures*, HRR 466 (HRB, 1973).
- Kher, R.K., W.R. Hudson, and B.F. McCullough, *A System Analysis of Rigid Pavement Design*, Research Report 123-5 (Texas Highway Department, 1970).
- Lander, I.I.W. and I. Williams, *The Skidding Resistance of Wet Runway Surfaces with Reference to Surface Texture and Tyre Conditions*, Road Research Laboratory, RRL Report LR 184 (Ministry of Transport, England, 1968).
- Law, S.M. and W.T. Burt, III, *Road Roughness Correlation Study*, Research Report No. 48 (Research and Development Section, Louisiana Department of Highways, 1970).
- Lee, R.A. and F. Pradko, "Analytical Analysis of Human Vibration," *SAE Transactions*, Vol 77, Paper 680091 (1968).
- Liddle, W.J. et al., *Evaluation of Pavement Serviceability on Utah Highways*, Interim Report 1969 (Utah Highway Department, 1969).
- Lins, W.F., *Human Vibration Response Measurement*, Technical Report No. 11551 (U.S. Army Tank—Automotive Command, 1972).
- Mahone, D.C. and S.N. Runkle, *Pavement Friction Needs*, HRR 396 (HRB, 1972).
- Marvin, E.L. and P. McManus, *Life Cycle Analysis of an Airfield Pavement Facility*, Unpublished Report (Construction Engineering Research Laboratory [CERL], 1973).
- Mays' Ride Meter Booklet* (Rainhart Co., 1972).
- Measurement of Runway Friction Characteristics on Wet, Icy, or Snow Covered Runways*, Report No. FS-160-65-68-1 (Department of Transportation, Federal Aviation Administration, 1971).
- Phillips, M.B. and G. Swift, *A Comparison of Four Roughness Measuring Systems*, HRR 291 (HRB, 1969).
- Quade, D.A., *Location of Rough Areas of Runways for a B-52 Aircraft*, AFFDL-TR-67-175 (The Boeing Company, 1968).
- Rayner, W.H. and M.O. Schmidt, *Surveying Elementary and Advanced* (D. Van Nostrand Co., 1960).
- Rizenbergs, R.L., *Accelerometer Method of Riding—Quality Testing*, Interim Report KYHPR-64-25 (Kentucky Department of Highways, 1965).
- Rizenbergs, R.L. et al., *Pavement Roughness, Measurement and Evaluation*, HRR 471 (HRB, 1973).
- Roberts, Freddy L. and W. Ronald Hudson, *Pavement Serviceability Equations Using the Surface Dynamics Profilometer*, Research Report 73-3 (Center for Highway Research, The University of Texas at Austin, 1970).
- Runway Skid Resistance Survey Reports* (Air Force Civil Engineering Center, Tyndall AFB, 1974).
- Schonfeld, R., *Photo Interpretation of Skid Resistance*, HRR 311 (HRB, 1970).
- Scrivner, F.H., *A Modification of the AASHO Road Test Serviceability Index Formula*, Technical Report No. 1 (Texas Transportation Institute, 1963).
- Shahin, M.Y. and B.F. McCullough, *Prediction of Low-Temperature and Thermal Fatigue Cracking in Flexible Pavements*, Research Report 123-14 (Texas Highway Department, 1972).
- Sherman, G.B., *In Situ Materials Variability*, Special Report 126 (HRB, 1971).
- Skid Resistance*, NCHRP Synthesis of Highway Practice No. 14 (1972).
- Sonneburg, P.N., *Determination of Runway Roughness Criteria*, Interim Report to AFWL (1974).
- Spangler, E.B. et al., *Evaluation of the Surface Dynamics Profilometer for Runway Profile Measurement*, Technical Report No. AFWL-TR-68-43 (AFWL, 1968).

- Spangler, F.B. and W.J. Kelley, *GMR Road Profilometer - A Method for Measuring Road Profile* (General Motors Corp., 1964).
- Spangler, F.B. and W.J. Kelley, *GMR Road Profilometer - A Method for Measuring Road Profile*, HRR 121 (HRB, 1965).
- Spangler, F.B. and W.J. Kelley, *Servo Seismic Method of Measuring the Road Profile*, Bulletin 328 (HRB, 1962).
- Steitle, David C., *Development of Criteria for Airport Runway Roughness Evaluation*, MS Thesis (The University of Texas at Austin, 1972).
- Strom, O.G., W.R. Hudson, and J.L. Brown, *A Pavement Feedback DATA System*, Research Report 123-12 (Texas Highway Department, 1974).
- Territa, M., *Friction Coefficients Between Tires and Pavement Surfaces*, Technical Report R303 (U.S. Naval Civil Engineering Laboratory, 1964).
- Wagner, H.L. and B.P. Shields, *Development of a Modified PCA Road Meter for Pavement Roughness Testing* (Research Council of Alberta Highway Research Division, 1969).
- Walker, Roger S. and W. Ronald Hudson, *A Correlation Study of Mays' Road Meter with the Surface Dynamics Profilometer*, Research Report 156-1 (Center for Highway Research, The University of Texas at Austin, 1973).
- Walker, Roger S., Freddy L. Roberts, and W. Ronald Hudson, *A Profile Measuring, Recording, and Processing System*, Research Report 73-2 (Center for Highway Research, The University of Texas at Austin, 1970).
- Walker, R.S. and W.R. Hudson, *A Road Profile Data Gathering and Analysis System*, paper presented at the 40th Annual Meeting of the Highway Research Board, Washington, D.C. (1970).
- Walker, Roger S. and W. Ronald Hudson, *Analog-to-Digital System*, Research Report 73-4 (Center for Highway Research, The University of Texas at Austin, 1970).
- Walker, R.S. and W.R. Hudson, *Method for Measuring Serviceability Index with Mays' Road Meter*, Special Report 133 (HRB, 1973).
- Walker, R.S. and W.R. Hudson, *The Use of Spectral Estimates for Pavement Characterization*, Research Report 156-2 (Center for Highway Research, University of Texas at Austin, 1973).
- Walker, Roger S., W. Ronald Hudson, and Freddy L. Roberts, *Development of a System for High-Speed Measurement of Pavement Roughness, Final Report*, Research Report 73-5F (Center for Highway Research, The University of Texas at Austin, 1971).
- Willmer, J., P. McManus, and E. Marvin, *User Manual for LIFE1 Computer Program*, Technical Report S-28 (CERL, 1974).
- W.D.M. Limited, *SCRIM, Information Brochure* (Western Works, Staple Hill, Bristol BS16, 4NX, Great Britain, 1972).
- Yoder, E.J. and R.T. Milhous, *Comparison of Different Methods of Measuring Pavement Condition*, NCHRP Report No. 7 (HRB, 1964).
- Zube, E. and J. Skog, *A Study of the Pennsylvania State Drag Tester for Measuring the Skid Resistance of Pavement Surfaces*, Report M&R 633251 (Material and Research Department, California Division of Highways, 1967).

## UNCITED REFERENCES

- Airfield Pavement Evaluation and Condition Survey Report, Bitburg Air Base, Germany* (Air Force Civil Engineering Center, Tyndall AFB, 1974).
- Brokaw, M.P., *A 5-Year Report on Evaluation of Pavement Serviceability With Several Road Meters*, Special Report 116 (HRB, 1970).
- Crandall, S.H. and W.D. Mark, *Random Vibration in Mechanical Systems* (Academic Press, Inc., 1963).
- Gillespie, T.D., W.E. Meyer, and R.R. Hegmon, *Skid Resistance Testing from a Statistical Viewpoint*, HRR 471 (HRB, 1973).

- Haas, R.C.G. and W.R. Hudson, *The Importance of Rational and Compatible Pavement Performance Evaluation*, Special Report 116 (HRB, 1971).
- Hanson, D.L., *Special Problems with Airfield Pavement Maintenance*, Florida (CEC).
- Hearst, R.M., "Photographic Inventory," Special Report 133 (HRB, 1973).
- Ivey, D.L. and B.M. Gallaway, *Tire-Pavement Friction: A Vital Design Objective*, HRR 471 (HRB, 1973).
- Roads and Transportation Association of Canada, Pavement Management Committee, "Output Measurements for Pavement Management Studies in Canada," *Proceedings, Third International Conference on the Structural Design of Asphalt Pavements* (London, 1972).
- Standard Nomenclature and Definitions for Pavement Components and Deficiencies*, Special Report 113 (HRB, 1970).
- "Symposium—Skid Resistance," *Proceedings, Association of Asphalt Paving Technologists*, Vol 42 (1973).
- Tomita, M. and HISAO, *Tire Pavement Friction Coefficients*, NCEI-TR-672 (Naval Civil Engineering Laboratory, 1970).
- Watson, J.R. and L.M. Cook, "A National Program to Standardize Skid Resistance Measurements," *Public Roads*, 32(3) (1972).